



This is to certify that the

dissertation entitled

FLOW INJECTION IN MICROBORE CAPILLARIES

presented by

Dana M. Spence

has been accepted towards fulfillment of the requirements for

PhD _____degree in _____Chemistry_

Date 6-20-97

0.12771

Stenl A bouch

FLOW INJECTION IN MICROBORE CAPILLARIES

By

Dana M. Spence

A DISSERTATION

Submitted to
Michigan State University
in partial fulfillment of the requirements
for the degree of

DOCTOR OF PHILOSOPHY

Department of Chemistry

1997

ABSTRACT

FLOW INJECTION IN MICROBORE CAPILLARIES

By

Dana M. Spence

Flow injection (FI) employing capillary tubing with inside diameters of 75 μm or less is described. Capillary flow injection combines many of the advantages found in conventional FI and air-segmented continuous flow analysis (ASCFA). Capillary FI maintains the simplicity, speed of analysis, and the ease of automations of conventional FI. However, it also reduces the amount of dispersion due to convective forces due to the small inside diameter, not unlike the minimized dispersion due to air-segmentation in ASCFA. In addition, Capillary FI also reduces the amount of sample volume needed, reagent consumption, and waste generation by two orders of magnitude in selected cases. Design considerations, fundamental dispersion studies, stopped-flow methods, mixing efficiencies and a new method of simulating FI are reported.

Design considerations are reported since much of the system components had to be modified such that the miniaturized instrumentation could be used in conjunction with conventional detectors, injectors and pumping mechanisms. The fundamental dispersion studies indicated that there was still a need for proper mixing techniques within a CFI system thus, studies involving mixing in capillary FI were performed. Stopped-flow methods are reported not only to show some of the benefits of performing such a technique in a miniaturized format, but also to reveal some of the possible pitfalls that one

may encounter only in a CFI format. Finally, a FI simulation is performed which uses a non-linear partial least squares regression algorithm to predict response signals and peak shape in a capillary FI system.

To Diane ~

I honestly do not know where I would be, let alone who I would be, without you.

ACKNOWLEDGMENTS

By far this is the part of my thesis that I have been waiting to compose since there have been so many people, not always in the academic ranks, who have affected my life in one form or another. In addition, since these acknowledgments are directed at *all* of the people who have contributed to my thesis being finished, you may find some references to those who helped me get to graduate school in the first place.

I would first and foremost like to express my sincerest gratitude to Dr. Stan

Crouch. I could not, and still can not, picture myself working with anyone else. To me,

Stan is what every professor should be. An excellent researcher and teacher who learns

with the students. I have often told many that I learned more from Stan in passing

conversations in the laboratory or his office, than I did in any classes. If I end up being

half the professor he is, my career will be fine.

In addition to gaining some knowledge in the past five years at Michigan State, I have also made numerous friends who have made my stay all the more enjoyable. Of course it must start with the Ledford group, my group away from my group. The camaraderie of Ed Townsend (who got me started in the TAC program), Mike Thelen, Kathy Severin, Per Askeland, and Greg Noonan will always be remembered. I would also like to recognize Dave Karpovich in the Blanchard lab. Dave was my classmate colleague who made the first year easier to swallow and was always available for a good beagle discussion or two (or three).

There have also been many Crouch group members who have helped along the way. Dave Binder, who received a coursework Master's degree under Stan, is someone that every person should have a conversation with at some point in their life because he will force you to open your mind. I would also like to thank Brett Quencer. I may not have graduated from the Crouch group if not for some words of wisdom from BQ in my first year. I'd like to thank YunSheng (Tony) Hsieh for introducing me to continuous flow analysis. I would like to recognize all of the undergraduates who I have had the privilege to work with: Andy Sekelsky, John Hybl, Susan Dornseifer, Brad Hogan, Dan Morris, and Amy Cox. Finally, the current group also deserves some recognition; Chunhong Peng, Shi Yi, and especially Tom Cullen for his friendship in the lab, courage to join the group, and also his excellence in grammar skills and computing facilities.

There are so many others; Lamont T., Al S., Asara (you never did get those shoes, huh guy?), all of the Drew students, and support staff (Lisa D., Beth T., B. McGaw, G. Hebert and the departmental machine shop) who have made my years here very enjoyable. A special thanks goes to Dr. Vicki McGuffin for serving as my second reader and providing excellent advice in the writing of my dissertation. Also thanks to the rest of my committee (Drs. Berglund, McCracken, and Mantica) for their support and suggestions. The Havicans (Craig and Amy) also deserve a special spot for making so many of the weekends fun.

TABLE OF CONTENTS

CHAPTER		PAGE
	LIST OF TABLES	хi
	LIST OF FIGURES	xii
1.	Continuous Flow Analysis: History, Current Status and Miniaturization	1
	1.1 DEFINING A CONTINUOUS FLOW ANALYZER	1
	1.2 COMPARISON OF ASCF TECHNIQUES AND FI	2
	1.3 FLOW INJECTION AS AN ANALYTICAL TOOL	7
	1.4 ENHANCEMENT OF FI THROUGH MINIATURIZATION	9
	LIST OF REFERENCES	14
2.	Design Considerations for Capillary Flow Injection Systems	16
	2.1 EXPERIMENTAL	17 17 17 20 23 24
	2.2 RESULTS AND DISCUSSION	25 25 28 29

CHAPTER		PAGE
2.	2.3 CONCLUSIONS	35
	LIST OF REFERENCES	36
3.	An Investigation of Pressure in Capillary	27
	Flow Injection Systems.	37
	3.1 EXPERIMENTAL	38
	3.1.1 Reagents	38
	3.1.2 Apparatus	39
	3.1.3 Procedure for Pressure Drop Measurements	40
3.	3.2 RESULTS	42
	3.2.1 Maximum Attainable Pressures	42
	3.2.2 A Comparison of Baseline Noise Levels	45
	3.2.3 Considerations for Manifold Design	50
	3.2.4 Reproducibility of Pumping Mechanisms	54
	3.3 CONCLUSIONS	57
	LIST OF REFERENCES	60
4.	Factors Affecting Zone Variance in a	
	Capillary Flow Injection System	61
	4.1 EXPERIMENTAL SECTION	62
	4.1.1 Pumping Mechanism	. 62
	4.1.2 Injection Process	. 62
	4.1.3 Tubing	64
	4.1.4 Flow Cells	64
	4.1.5 Reagents	. 64
	4.1.6 Procedures for Dispersion Studies	64
	4.2 RESULTS AND DISCUSSION	65
	4.2.1 Studies of Dispersion	65
	4.2.2 Determination of the zone variance	67
	4.3 CONCLUSIONS	. 77
	LIST OF REFERENCES	78

CHAPTER		PAGE
5.	Mixing Efficiencies in Capillary Flow Injection Systems	80
	5.1 INTRODUCTION TO MIXING IN	
	FLOW INJECTION	80
	5.2 EXPERIMENTAL	83
	5.2.1 Reagents	83 83
	5.3 RESULTS	
	5.3.1 Dye Dispersion Studies5.3.2 Investigating the Completeness of Mixing	85
	with the Fe(SCN) ₃ Reaction	89
	5.4 CONCLUSIONS	92
	LIST OF REFERENCES	94
6.	Capillary Flow Injection for Stopped Flow	
	Kinetic Determinations	95
	6.1 EXPERIMENTAL	96
	6.1.1 Instrumentation	96
	6.1.2 Reagents	96
	6.1.3 Procedure	97
	6.2 RESULTS AND DISCUSSION	97
	6.2.1 Stopped Flow Considerations	97
	6.2.2 Benefits of a Capillary FI System	102
	6.3 CONCLUSIONS	105
	LIST OF REFERENCES	107

CHAPTER PAGE

7.	Simulating Flow Injection Response Signals Using a Non-Linear Partial Least Squares Regression Algorithm	108
	7.1 EXPERIMENTAL	109
	7.1.1 Apparatus	109
	7.1.2 Reagents	109
	7.1.3 Programs used for Data Acquisition and Simulation	110
	7.1.4 Procedures for Obtaining Calibration Data	110
	7.1.5 Performing the NLPLS Regression	112
	7.2 RESULTS AND DISCUSSION	
	7.2.1 Comparison of Simulated vs.	
	Experimentally Obtained Data	114
	7.2.2 Errors in the Simulation	123
	7.3 CONCLUSIONS	125
	LIST OF REFERENCES	126
8.	Future Prospects of Capillary	
	Flow Injection	127
	8.1 INSTRUMENTATION IMPROVEMENTS	128
	8.1.1 Pumping Mechanism	128
	8.1.2 Injection Methods	129
	8.1.3 Improved Detection Methods	130
	8.2 IMPROVED KINETIC METHODS OF ANALYSIS	131
	8.2.1 Flow Reversal Enhancements	131
	8.2.2 Determinations Involving Immobilized Media	132
	8.3 AUTOMATED CALIBRATION IN STOPPED	
	FLOW CAPILLARY FLOW INJECTION USING	
	ON-COLUMN DETECTION	132
	LIST OF REFERENCES	135

LIST OF TABLES

TABL	E	PAGE
3.1	Effect of syringe size on maximum attainable pressure	46
3.2	Reproducibility of the pressure output using the peristaltic and syringe pumps at varying pressures	55
4.1	Regression analyses for the capillary and the conventional FI system	74
4.2	Major contributors to peak variance in a conventional and a capillary FI system	75
5.1	Dispersion coefficients for the capillary FI system as a function of varying reactor lengths. The linear flow rates were held constant for each reactor at 2.0 ± 0.1 cm s ⁻¹	90

LIST OF FIGURES

FIG	URE	PAGE
1.1	A typical air-segmented continuous flow system. The bubble gate may be replaced by a debubbler to physically gate the bubbles, rather than electronically, from the detector. The reaction shown, the Griess reaction for nitrite, is described in more detail in chapter 2. SAN, sulfanilamide; NNED, N-(1-naphthyl)ethylenediamine	4
1.2	View of the bolus flow profile that develops between the segments of an air segmented continuous flow system. The air bubbles act as barriers, breaking up the laminar flow profile. This leads to minimized dispersion and enhanced mixing of reagents	. 5
1.3	A typical flow injection system. Note the presence of the injection valve and the absence of the bubble gate and the air-segmentation as was found in an air-segmented continuous flow system. This reaction, the Trinder reaction for the determination of glucose, is described in more detail in chapter 3	6
1.4	Development of the parabolic flow profile in an unsegmented, open tube used in flow injection	8
2.1	Schematic of capillary flow injection manifold. Capillary inside diameters measured 75 μ m. The inside diameter of the flow rated tubing was 190 μ m. The solid and dashed lines on the injection valve represent the non-inject and inject mode, respectively	18
2.2	Fused silica capillary adaptation to conventional switching valve. The fused silica capillary is surrounded by the adapter sleeve (380 µm i.d.), ferrule, and nut. This assembly is then set into the valve and ready for use.	19
2.3	Cross sectional view of fixed volume flow cell. The path length is 3 mm with a volume of approximately 0.67 µL. The capillaries are adapted to the cell in the same manner as when set in the switching valve	

2.4	Cross sectional view of variable volume flow cell with a PEEK sleeve constituting the flow path. The rubber O-ring creates a tight fit around the sleeve to prevent leaking. Parts A and B are then brought together and tightened with Allen screws.	22
2.5	Principle behind timed injections. Figure 2.5a shows the valve in the non-inject mode. In figure 2.5b the actuator has switched the valve to the injecting position. Here, sample is being pumped into the reaction coil for a specified amount of time. In figure 2.5c, the valve is returned to the non-inject mode. The sample plug is now being carried to the detector	26
2.6	Response signals for repetitive injections of phenol red into a borate buffered stream. The RSD of the peak heights is 1.2%	27
2.7	Calibration curve for Fe^{2+} using the fixed volume flow cell. The volume of the flow cell was approximately 0.67 μL while the path length was 3 mm. The volume injected was 1.75 μL	30
2.8	Calibration curve for Fe^{2+} using the variable volume flow cell. The volume of the flow cell was approximately 0.9 μ L while the path length was 8 mm. The volume injected was 1.35 μ L	31
2.9	Schematic of capillary flow injection manifold when multiple streams are involved. The Y coupler allows for multiple reagent streams to be employe in a CFI system. Again, the solid and dashed lines on the injection valve represent the non-inject and inject mode, respectively	d 33
2.10	Response signal for the determination of nitrite by the Griess reaction. The RSD in peak height is 2.1%	34
3.1	Schematic of the system used to measure the pressure gradient in a capillary. L1 represents a portion of fused silica capillary that was kept as short as possible, typically about 15 cm, whereas L2 is the capillary that was varied when the pressure gradient was investigated as a function of reactor length. Procedural details are contained within the text	41
3.2	Calculated and measured pressure gradients as a function of increasing flow rate using the manifold shown in figure 3.1. The measured values were obtained with the peristaltic pump	43

FIGURE PAGE

3.3	Calculated and measured pressure gradients as a function of increasing reactor length using the manifold shown in figure 3.1 and the peristaltic pump. The observed values deviate from predicted values because of the pump's pressure output limitations.	44
3.4	Measured baseline noise levels for two peristaltic pumps, one containing 8 rollers and the other containing 16 rollers. The four signals are offset for ease of reading. Each tick mark on the absorbance axis = 5 mAU	48
3.5	Investigation of pump pulsations by measuring the absorbance of the phenol red dye at steady state under various pumping conditions. The bottom trace used 190 mm i.d. flow rated tubing to introduce the reagents into the capillary, while the middle trace was obtained using flow rated tubing of 250 mm i.d. The upper trace used the 190 mm i.d. flow rated tubing but the pump was idle during the measured portion shown.	49
3.6a	Calculated maximum linear velocity plotted as a function of reactor length using both the peristaltic pump and the syringe pump with various syringe sizes. The maximum change in pressure employed for the calculations involving the peristaltic pump (●) was 7.9 bar. The pressure changes employed for the 10cm³ (●), 5 cm³ (■), and 3 cm³ (●) syringes were 7.9, 10.1, and 19.2 bar respectively	51
3.6b	Calculated maximum linear velocity plotted as a function of tubing radius using both the peristaltic pump and the syringe pump with various syringe sizes. The maximum change in pressure employed for the calculations involving the peristaltic pump (●) was 7.9 bar. The pressure changes employed for the 10cm³ (●), 5 cm³ (■), and 3 cm³ (●) syringes were 7.9, 10.1, and 19.2 bar respectively	52
3.6c	Calculated maximum linear velocity plotted as a function of solution viscosity using both the peristaltic pump and the syringe pump with various syringe sizes. The maximum change in pressure employed for the calculations involving the peristaltic pump (●) was 7.9 bar. The pressure changes employed for the 10cm³ (●), 5 cm³ (■), and 3 cm³ (●) syringes were 7.9, 10.1, and 19.2 bar respectively	53

FIGURE PAGE

3.7	Schematic of manifold employed for the enzyme-catalyzed determination of glucose. The distance of the fused silica capillary from the flow rated tubing to the switching valve is about 15-20 cm. The length of the reactor was 400 cm. EC = enzyme composite reagent, G = glucose sample.	56
3.8	Absorbance measurements as a function of glucose concentration. The measurements were made at a wavelength of 540 nm. The correlation coefficient between the peak height and the glucose concentration is 0.996	58
4.1	Manifold used for capillary FI. The PEEK reactor is used since it is easier to adapt to the valve and flow cell. Fused silica tubing is used at the pump since it can be inserted into the small bore flow rated tubing	63
4.2	Response signals obtained with the capillary FI system by injecting 5 x 10 ⁻⁵ M solutions of phenol red into buffer flowing at 2 cm s ⁻¹ with various lengths (in cm) of 0.064 mm i.d. reactors	66
4.3	Response signals obtained with the conventional FI system by injecting 5 x 10 ⁻⁵ M solutions of phenol red into buffer flowing at 2 cm s ⁻¹ with various lengths (in cm) of 0.50 mm i.d. reactors	68
4.4	Response signals obtained with 400 cm reactors of capillary tubing and conventional tubing. The maximum absorbance obtained with the capillary FI system is nearly twice that with the conventional FI system	69
4.5	Response signals obtained with the capillary FI system as a function of the volume of sample injected (proportional to peak area). The sample volumes represented by the three curves are 720 nL (area = 6), 1.0 μ L (area = 9), and 1.25 μ L (area = 12)	71
4.6	Response signals obtained with the capillary FI system as a function of flow cell volume. The flow cell volume was varied by inserting PEEK sleeves of varying i.d., thus, the path length for each volume studied was identical (1 cm). The areas under each curve are equal (± 1%)	72
5.1	Calibration curves for the enzyme-catalyzed determination of glucose. Note the increased slope of the curve using the conventional FI system due to more efficient mixing within the reactor	82

FIGU	J RE	PAGE
5.2	Manifold employed for the investigation of mixing using the Fe(SCN) ₃ reaction	84
5.3	Drawing of the 0.029 μL mixing tee	. 86
5.4	Steady state absorbances of phenol red. The upper trace is for the capillary system with no mixing tee. The bottom trace is the response signal after the phenol red was mixed with buffer in the $0.029~\mu L$ mixing tee.	88
5.5	Examination of the extent of mixing of a conventional FI system, a capillary FI system and a capillary FI system with a mixing tee. The linear velocities in all three manifolds were held constant at 2.1 ± 0.1 cm s ⁻¹	. 91
6.1	Manifolds used for stopped-flow kinetic determination of ascorbic acid. In figure 6.1a, the pump delivers the sample (ascorbic acid, AA) and reagents (water and toluidine blue, TB) through the flow cell. When the 4-port valve is switched for a pre-selected amount of time, a zone of toluidine blue is introduced into the reaction tubing. In figure 6.1b, the 6-port injection valve is switched, thus disconnecting the pump from the reagent and sample coils	
6.2	Stopped-flow kinetic determination of 230 μ M ascorbic acid using a conventional FI manifold. The inside diameter of the reaction tubing was 0.5 mm. In order to stop the flow, the peristaltic pump is simply turned off near the toluidine blue peak maximum.	99
6.3	Stopped-flow kinetic determination of ascorbic acid using a capillary FI manifold. The inside diameter of the reaction tubing was 0.064 mm. Again, the flow is stopped by turning off the peristaltic pump. However, the sample zone continues to flow through the cell	100
6.4	Stopped-flow kinetic determination of ascorbic acid using the same system used to collect the data in figure 6.3. Now the flow is being stopped by switching the 6-port valve as shown in figure 6.1b	. 101
6.5	Calibration curve obtained by running ascorbic acid samples ranging in concentration from 30-230 μ M. The correlation coefficient for the determination is 0.9957. The non-zero intercept is most likely caused by some slight continued movement of the sample zone through the cell after stopping the flow	103
	the cell after stopping the flow	103

FIGU	RE	PAGE
7.1	Response signal in the form of an exponentially modified Gaussian (EMG). The EMG is described using the area, centroid, width and distortion. The a terms are shown in equation 7.1 and described in section 7.1.4.	111
7.2	Multivariate calibration as a "black box". The calibration model is generated from the data matrix and system properties matrix. The regression is then performed and the unknown system properties matrix (the simulated data) is returned	113
7.3a	Predicted areas from the NLPLS algorithm versus the actual areas used in the calibration model. The correlation coefficient is 0.473 . The lines within the plot represent \pm 10% error	115
7.3b	Predicted centroids from the NLPLS algorithm versus the actual centroids used in the calibration model. The correlation coefficient is 0.983. The lines within the plot represent \pm 10% error	116
7.3c	Predicted widths from the NLPLS algorithm versus the actual widths used in the calibration model. The correlation coefficient is 0.770. The lines within the plot represent \pm 10% error	117
7.3d	Predicted distortions from the NLPLS algorithm versus the actual distortions used in the calibration model. The correlation coefficient is 0.786. The lines within the plot represent \pm 10% error	118
7.4	Simulated response signals as a function of increasing reactor length. The reactor lengths were varied from 100 cm to 350 cm; concentration of the dye = 5×10^{-4} ; volume injected = $2.0 \mu L$; flow rate = 3 cm s^{-1}	120
7.5	Response signals as a function of dye concentration. Reactor length = 125 cm; concentrations ranged from 1 x 10^{-5} M to 6 x 10^{-4} M; volume injected = 1.8 μ L; flow rate = 2.4 cm min ⁻¹ . The linear regression statistics are discussed within the text	. 121
7.6	Simulated response signals as a function of increasing sample volume . Reactor length = 150 cm; concentration of the dye = 5×10^{-4} M. sample volumes were varied from $0.5 \mu L$ to $2.0 \mu L$; flow rate = 2 cm s^{-1} . The correlation coefficient between peak height and sample volume was 0.978	
	was v.7/0	122

FIGURE		PAGE
7.7	Simulated response signals as a function of increasing flow rate. Reactor length = 100 cm ; concentration of the dye = 5×10^4 . sample volume injected = $2.0 \mu \text{L}$; flow rates were varied from 1 cm s^{-1} up to 4 cm s^{-1}	124

,

Chapter 1

Continuous Flow Analysis: History, Current Status, and Miniaturization

1.1 DEFINING A CONTINUOUS FLOW ANALYZER

Automated analyses in the laboratory have become routine over the past few decades. Many of the techniques that have benefited from automation are those which employ some form of a continuous flowing stream of reagent, be it a gas, liquid, or supercritical fluid. This continuous flow allows for the reagent(s) to be carried to a point in the instrument manifold where typically an optical or electrochemical measurement is made. Although there are numerous techniques which employ a continuous flow, the definition of continuous flow analysis (CFA) which will be used throughout this work will only refer to air-segmented continuous flow analysis (ASCFA) or flow injection analysis (FIA). There are some forms of chromatography, for example, that could definitely be considered as continuous flow techniques. However, there are some forms, such as paper chromatography, that require an "off-line" detection scheme and capillary migration as the pumping mechanism. Most users of ASCFA or FIA will agree that some form of constant flow pumping mechanism and on-line detection scheme are requirements worthy of the title, continuous flow analysis. In addition, from this point forward, based on discussions by Pardue¹ and Mottola² regarding the steps in a complete analysis, we will refer to the non-segmented form of CFA as flow injection (FI) rather than FIA.

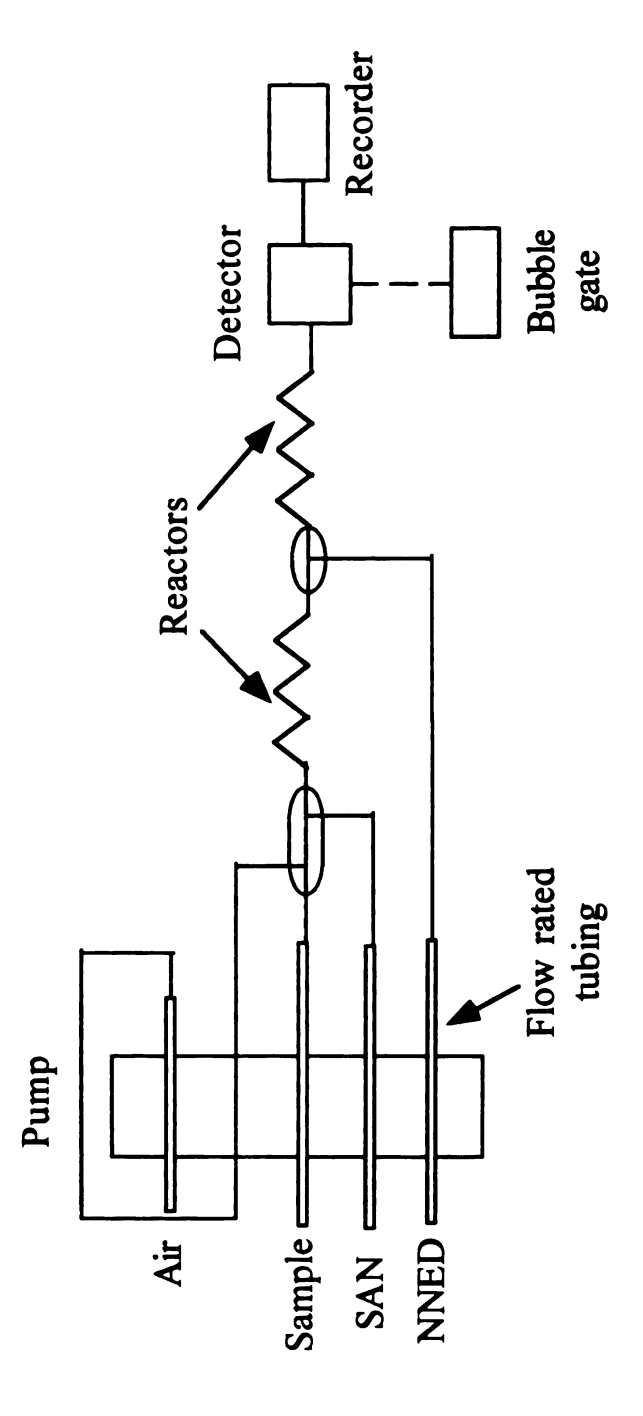
Adhering to the above definition, CFA was first developed in the 1950's by Leonard Skeggs.³ This system, later developed by the Technicon Corporation as the Autoanalyzer, used air-segmentation within the reaction tubes in order to avoid intermixing between samples as they traversed towards the detector. For the next twenty years or so the Autoanalyzer, although going through a few minor improvements and upgrades, was the method of choice for continuous flow and automated analyses. However, in the mid-1970's simultaneous experiments on non-segmented CFA were reported by Kent Stewart and co-workers⁴ and by Elo H. Hansen and Jaromir Ruzicka⁵. It was Ruzicka and Hansen who would name this technique flow injection analysis. After the reports by Stewart and Ruzicka and Hansen, CFA was essentially divided into segmented vs. non-segmented modes. Since this split of continuous flow methods, both ASCFA and FI have matured and improved in their efficiencies and in the scope of their applications. It is therefore worthwhile to compare and contrast these two techniques with regard to advantages, disadvantages, simplicity, applicability, and potential for the future.

1.2 COMPARISON OF ASCF TECHNIQUES AND FI

Since the inception of FI in 1975, proponents of ASCFA and FI have argued as to which method is more appropriate for determinations involving continuous flow. It is not difficult to understand why each side believes that one method is advantageous over the other since both methods are powerful in different ways. For example, consider the

typical air-segmented manifold depicted in figure 1.1. The manifold is comprised of a pump, typically a peristaltic pump, flow-rated polyvinyl chloride (PVC) tubing to introduce the reagents and sample, some sort of reaction tubing, any required mixing aids, a debubbler or electronic bubble gate, and of course a detector. The debubbler or electronic bubble gate is needed so the detector does not record the constant fluctuations brought about by successive zones of air and liquid passing through the flow cell. If the detector had to measure both the liquid portion of the stream and the air portion, one can imagine the unsteady baseline that would result. Thus, the bubbles must either be physically removed using the debubbler or electronically gated using the bubble gate. A more detailed description of both of these methods is described elsewhere⁶. The important feature of ASCFA is that the air bubbles introduced do not allow for excessive sample dispersion due to convective forces since they actually behave as barriers. In addition, any dispersion that does occur within the liquid solution between two bubbles results in a secondary flow which promotes excellent mixing. This bolus flow pattern is shown in figure 1.2. This reduced dispersion makes ASCFA the system of choice when complex chemical procedures are involved or when long reaction periods are necessary.

A typical FI system is shown in figure 1.3. An examination of this manifold reveals some differences between it and the ASCFA system shown in figure 1.1. For example, a valve capable of introducing reproducible amounts of sample is necessary in the FI system. Also, there are no air bubbles being introduced into the flowing streams and therefore, no requirement of removing the air bubbles prior to detection with either a debubbler or an electronic bubble gate. In addition to its simple instrumentation, FI is often the system of



A typical air-segmented continuous flow system. The bubble gate may be replaced by a debubbler to physically gate the bubbles, rather than electronically, from the detector. The reaction shown, the Griess reaction for nitrite, is described in more detail in chapter 2. SAN, sulfanilamide; NNED, N-(1naphthyl)ethylenediamine. Figure 1.1.



Figure 1.2. View of the bolus flow profile that develops between the segments of an air-segmented continuous flow system. The air bubbles act as barriers, breaking up the laminar flow profile. This leads to minimized dispersion and enhanced mixing of reagents.

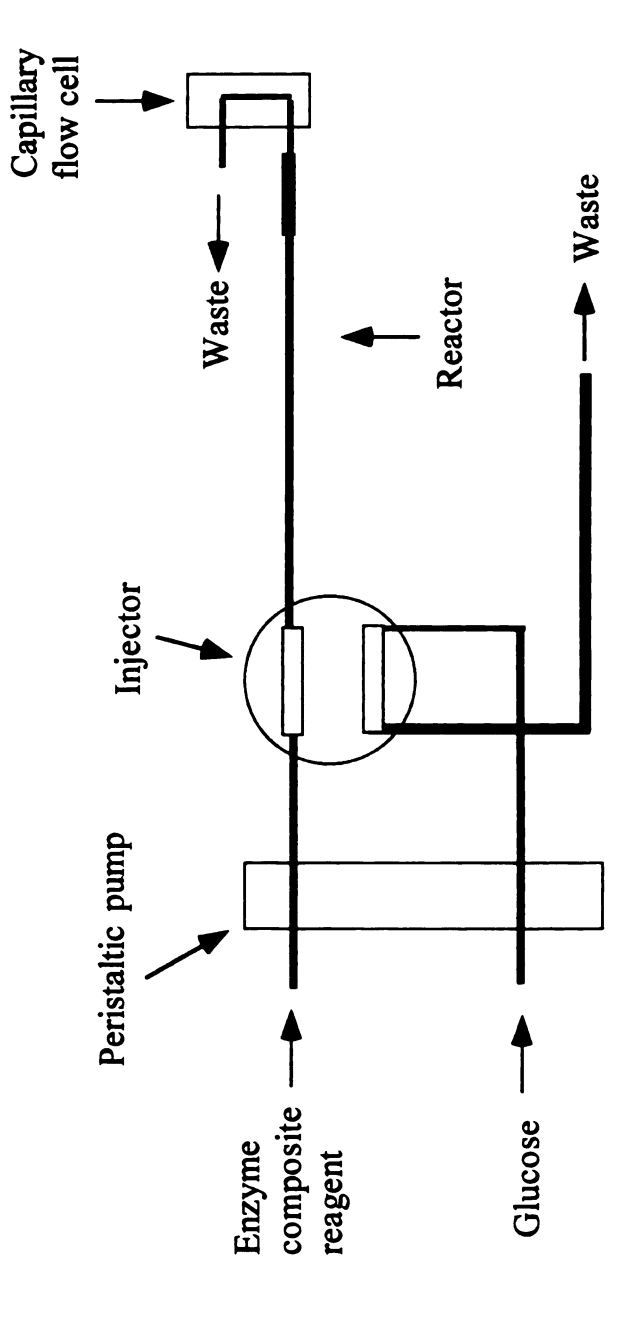


Figure 1.3. A typical flow injection system. Note the presence of the injection valve and the absence of the bubble gate and the air-segmentation as was found in an air-segmented continuous flow system. This reaction, the Trinder reaction for the determination of glucose, is described in more detail in chapter 3.

choice due to its high degree of automation, high sample throughput, and reproducible sample handling capabilities. As commonly practiced, FI depends upon precise timing, reproducible injection of samples, and a controlled amount of dispersion of the sample and reagent zones involved. The parabolic flow profile, shown in figure 1.4, is the result of the laminar flow in FI streams. Of course, there will be some contribution to the overall dispersive process from diffusion and this is also depicted in figure 1.4. However, it is usually the convective forces which dominate the dispersive processes in conventional FI tubing.

1.3 FLOW INJECTION AS AN ANALYTICAL TOOL

The FI technique is fast approaching its silver anniversary and the numbers of papers, conferences and applications dealing with FI continue to grow⁷. No longer is FI simply a means of automating a simple reaction, or used to carry a plug of sample from point "a" to point "b" in a process stream. On the contrary, FI is finding increased use in such techniques as kinetic methods of analysis⁸⁻¹¹, extractions^{12,13}, preconcentrations¹⁴, and immunoassays^{15,16}. FI has recently been used as a source of renewable surfaces in chemical microscopy techniques¹⁷.

Despite its widespread acceptance in analytical and process control laboratories, there are some tasks for which FI is not ideally suited. Patton and Crouch¹⁸ have compared FI with ASCF methods and concluded that FI has advantages where the chemistry and sample manipulations are relatively simple and the reactions are fairly rapid. In other situations, the dispersion that occurs in FI methods can lead to a lack of sensitivity or an inability to detect a product at all. Dispersion and the resulting zone

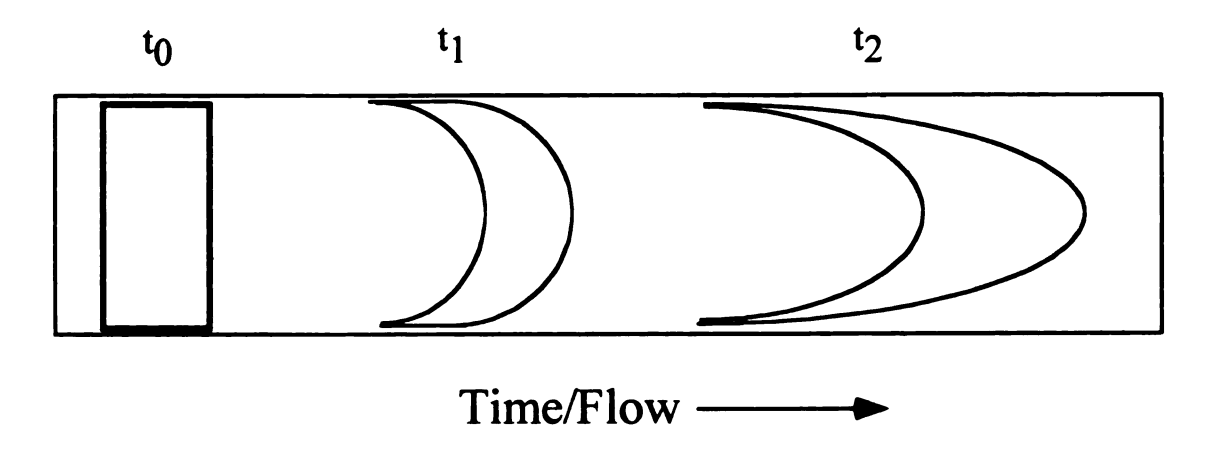


Figure 1.4. Development of the parabolic flow profile in an unsegmented, open tube used in flow injection.

broadening can also severely limit the sampling frequency of FI methods involving complicated chemistries, extractions, or slow reactions. These same authors concluded that no one system was the total answer to all of the necessary problems in continuous flow analyses. However, it does seem logical that the ideal continuous flow analyzer would simply combine the low dispersion associated with ASCF and the simplicity and efficiency associated with FI systems.

1.4 ENHANCEMENT OF FI THROUGH MINIATURIZATION

As previously discussed, the ability to reduce the amount of dispersion in a non-segmented stream would definitely enhance the efficiency of a FI system. It is thus noteworthy to point out that there are other methods one can employ (in addition to air-segmentation) to reduce the amount of dispersion in a system involving flowing streams. For example, the laminar flow profiles can be disrupted in FI by incorporating solid particles such as beads¹⁹ or by simply tightly coiling the reactors^{20,21}. In a determination of chloride using a simple displacement reaction, Patton showed that both methods improved the signal to noise ratio. However, the improvement in signal to noise ratio was only about 10% and the peak widths were roughly the same. Thus, it would seem that other instrumental changes need to be considered if FI is to be raised to a new level of usefulness and practicality.

The Aris-Taylor theory of dispersion, embodied in equation 1.1 states that the dispersion (zone variance) is directly proportional to the square of the tubing radius. In equation 1.1, the overall variance σ^2 due to flow contributions is described by the residence time \overline{T} , the tubing radius r, and the molecular diffusion coefficient D_m . Thus,

by using tubing of smaller diameter, the amount of dispersion due to convective forces should be decreased. This lowering of dispersion would then allow for systems

$$(\sigma^2)_{\text{flow}} = \frac{\overline{T}r^2}{24D_m} \tag{1.1}$$

requiring complex chemistries or long reaction periods to be employed in a FI setup rather than having to resort to ASCF. Also, since zones from one injection to the next should be less broadened inside the reactor, more samples per unit time could be introduced, thus improving the efficiency of the technique. Reagent and sample consumption should also be decreased substantially in such miniaturized systems. There have already been several excellent articles describing the advantages of miniaturized instrumentation. ^{22,23}

Despite the advantages of operating on a microscale, FI has only recently found success in a miniaturized form. In 1983, Ruzicka and Hansen^{24,25} were performing FI in micromachined conduits on substrates not much larger than a thick credit card. The cross sectional area of the channels was approximately 0.8 mm² however, the authors did not indicate the depth of the etched channels. The reagent consumption in such cases was on the order of 200 μL to 1 mL per run. However, in the second edition of their book on FI²⁶, these same authors list some caveats to those who want to attempt further miniaturization of the reaction conduits to the low μm regime. First, with such tubing diameters, the resistance to flow is high which may make conventional pressure-induced flow difficult. The major advantages of narrow bore tubes should be observed at low flow rates (ca. 1-10 μL min⁻¹), where the authors have reported difficulties in achieving stable

flow rates. Some researchers²⁷⁻³¹ have overcome this problem through the use of electroosmosis as the pumping mechanism. In other recent work, though FI was not the main focus nor even mentioned in the reports, syringe pumps using microliter-volume syringes were able to deliver steady flow rates needed to introduce reagents either into a mass spectromenter³² or a second capillary³³ for further separation. The work presented in this dissertation is the first that employs a simple peristaltic pump to drive the necessary reagents in a capillary-based FI system.

A second caveat given by Ruzicka and Hansen is that narrow bore tubes may be easily clogged by particulates, which could limit the utility of the method. Finally, typical spectrophotometric flow cells are of much larger volume than is optimal with narrow bore tubes leading to nonuniformity of the detected solution and dispersion (dilution) within the detector. In chapter 2, the fabrication of a flow cell with an internal volume below 1µL that has a path length of 1 cm is described.

Despite these obstacles, we felt that many of the problems associated with a FI system in the capillary format were no longer insurmountable. Thus, the remainder of this dissertation describes the steps taken in order to develop and characterize capillary flow injection or CFI. The second chapter describes many of the initial design considerations with regards to the method of sample injection, flow cell design, and methods for adapting the micrometer-sized capillaries to conventional 1/16" plumbing. The reproducibility of the capillary system is reported as well as data obtained from a multi-reagent CFI system.

Chapter 3 describes an investigation of various pumping mechanisms, namely peristalsis, positive displacement (a syringe pump), and a dual piston pump. The pressure

output capability of each pump was investigated as well as baseline noise levels. This study showed that the dual piston pump was not capable of delivering the necessary low volumetric flow rates needed in CFI. The results from this study then allowed for some practical considerations for designing more complex system manifolds in the capillary format.

Attempting to understand the forces controlling zone dispersion is the focus of chapter 4. The second moment, or variance, about the mean was determined for a series of determinations involving a dye injected into a buffered stream. Solving three equations simultaneously allowed for the zone variance to be expressed as a function of reactor length, flow cell volume, and injection volume. Implications of these findings towards the development of second generation CFI systems are presented.

Chapter 5 is, in many ways, an extension of chapter 4. In chapter 4, the amount of dispersion that occurs within a conventional FI system is compared to a CFI system. It was found that the amount of dispersion occurring within the reactor in a capillary system is greatly reduced. Though at first thought this may seem to be a definite advantage for the capillary system over its conventional counterpart, it does have its drawbacks. For example, it was previously noted earlier in this chapter that FI methods depend on a controlled amount of dispersion for mixing to occur within the reactor tubing. Thus, if there is too little mixing there will be no resultant reaction. Therefore, chapter 5 is an investigation of the extent of mixing that is occurring within the capillary system and a description of when the mixing is complete. The fast reaction between Fe³⁺ and SCN⁻ was

investigated in order to characterize the extent of mixing in both a CFI and a conventional FI system. Studies involving a mixing tee of nanoliter volume is also reported.

The work presented in chapter 6 demonstrates the instrumental differences between conventional and capillary FI methods. In this chapter, results from an initial investigation of stopped flow injection in the capillary format are presented. A determination of ascorbic acid is made based on its reduction of toluidine blue. It was found that a more complex manifold was required in the capillary format in order to operate in the stopped flow mode.

Finally, chapter 7 contains results from a simulation to demonstrate the benefits and caveats of a CFI system. This simulation uses a non-linear partial least squares (NLPLS) regression algorithm to generate a calibration set that is subsequently employed to give four parameters (area, width, centroid, and distortion) that describe the simulated peak. The program sends these parameters into an equation describing an exponentially modified Gaussian (EMG) peak and calculates the expected absorbance versus time.

The final chapter of this dissertation attempts to take the reader into the near future and describes some possible techniques and applications that may benefit from CFI. In addition, some insight as to improvements that need or should be made for second generation CFI systems is presented.

List of References

- 1. Pardue, H.L. Abstracts of Papers, 182nd National Meeting of the American Chemical Society, New York, NY, August, 1981.
- 2. Mottola, H. Anal. Chem. 1981, 53, 1312A.
- 3. Skeggs, L.T. Amer. J. Clin. Path. 1957, 28, 311.
- 4. Stewart, K.K.; Beecher, G.R.; Hare, P.E. Anal. Biochem. 1976, 70, 167.
- 5. Hansen, E.H.; Ruzicka, J. Anal. Chim. Acta 1975, 78, 145.
- 6. Patton, C.J. Ph.D. Thesis, Michigan State University, East Lansing, MI, 1982.
- 7. Proceedings from the Sixth International Conference on Flow Analysis, *Anal. Chim. Acta* 1995, 308, 1.
- 8. Fernandez, A.; Luque de Castro, M.D.; Valcarcel, M. Anal. Chem. 1984, 56, 1146.
- 9. Romero-Saldana, M.; Rios, A.; Valcarcel, M. Fresenius Z. Anal. Chem. 1992, 342, 547.
- 10. Christian, G.D.; Ruzicka, J. Anal. Chim. Acta 1992, 261, 11.
- 11. Mottola, H.A.; Perez-Bendito, D. Anal. Chem. 1996, 68, 257R.
- 12. Kuban, V.; Ingman, F. CRC Crit. Rev. Anal. Chem. 1991, 22(1,2), 37.
- 13. Kuban, V. CRC Crit. Rev. Anal. Chem., 1991, 22(6), 477.
- 14. Clark, G.D.; Whitman, D.A.; Christian, G.D.; Ruzicka, J. CRC Crit. Rev. Anal. Chem. 1990, 21(5), 357.
- 15. Gubitz, G.; Shellum, C. Anal. Chim. Acta 1993, 283, 421.

- 16. Puchades, R.; Maquieira, A.; Atienza, J.; Montoya, A. CRC Crit. Rev. Anal. Chem. 1992, 23, 301.
- 17. Pollema, C.H.; Ruzicka, J. Anal. Chem. 1994, 66, 1825.
- 18. Patton, C.J.; Crouch, S.R. Anal. Chim. Acta 1986, 179, 189.
- 19. Reijn, J.M.; Van Der Linden, W.E.; Poppe, H. Anal. Chim. Acta 1981, 123, 229.
- 20. Snyder, L.R. Anal. Chim. Acta 1980, 114, 3.
- 21. Tijssen, R. Anal. Chim. Acta 1980, 114, 71.
- 22. Manz, A.; Fettinger, J.C.; Verpoorte, E.; Ludi, H.; Widmer, H.M.; Harrison, D.J. *Trends Anal. Chem.* 1991, 10, 144.
- 23. Manz, A.; Miyahara, Y.; Miura, J.; Watanabe, Y.; Miyagi, H.; Sato, K. Sensors and Actuators, B1 1990, 249.
- 24. Ruzicka, J.; Hansen, E.H. Anal. Chim. Acta 1984, 161, 1.
- 25. Ruzicka, J. Anal. Chem. 1983, 55, 1040A.
- 26. Ruzicka, J.; Hansen, E.H. Flow Injection Analysis, Wiley, NY, 1988.
- 27. Liu, S.; Dasgupta, P.K. Anal. Chim. Acta 1992, 268, 1.
- 28. Liu, S.; Dasgupta, P.K. Anal. Chim. Acta 1993, 283, 747.
- 29. Dasgupta, P.K.; Liu, S. Anal. Chem. 1994, 66, 1792.
- 30. Daykin, R.N.C.; Haswell, S.J. Anal. Chim. Acta 1995, 313, 155.
- 31. Olson-Cosford, R.J.; Kuhr, W.G. Anal. Chem. 1996, 68, 2164.
- 32. Pergantis, S.A.; Heithmar, E.M.; Hinners, T.A. Anal. Chem. 1995, 67, 4530.
- 33. Lada, M.W.; Kennedy, R.T. Anal. Chem. 1996, 68, 2790.

Chapter 2

Design Considerations for Capillary Flow Injection Systems

The use of fused silica capillaries has greatly enhanced such techniques as gas and liquid chromatography, and of course separations based on electrophoresis¹⁻³. Although there have been numerous discussions about capillary flow injection (CFI), Liu and Dasgupta were the first to report on CFI with 75 μ m inside diameter capillaries as the tubing and electroosmotic flow (EOF) as the pumping mechanism⁴⁻⁶. EOF was used in order to overcome what was thought to be a major obstacle to CFI, namely a stable and reproducible flow rate at the μ L min⁻¹ level.

This chapter describes some of the initial designs used for the CFI systems. In addition to a simple single-line manifold, this chapter also describes some initial work performed with multi-reagent systems. In these CFI systems, fused silica capillaries with inside diameters of 75 µm have been used as the reactor tubing. In order to benefit from such a system operating on a micro-scale, much of the equipment used in conventional FI had to be modified. Thus, fused silica capillaries were adapted to a regular 4-port switching valve, while a flow cell was designed and constructed to allow UV-visible absorption measurements on sample volumes in the nL range. In addition, Y-shaped

connectors were employed, to allow multiple reagent systems to be used in a capillary manifold.

2.1 EXPERIMENTAL

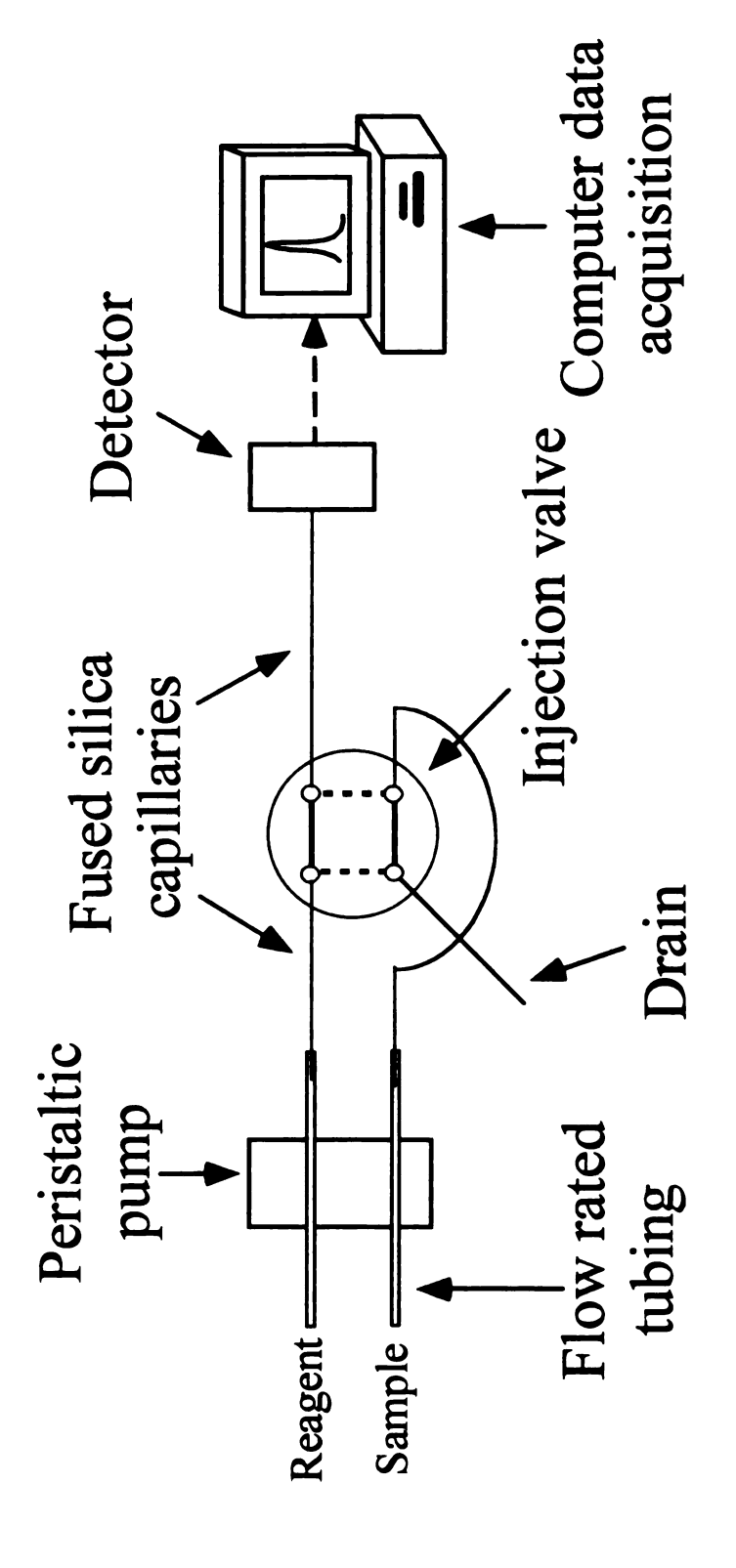
2.1.1 Pumping Mechanism

Figure 2.1 shows a typical single-line manifold employed in this work. A peristaltic pump (Ismatec, model IP-12) was used to induce flow. In order to reduce pump pulsations encountered in air-segmented applications, the pump had been previously modified in our laboratory⁷ by doubling the number of rollers from 8 to 16. The reagents were introduced into the capillaries using typical flow-rated tubes (Cole Parmer) with inside diameters of 0.19 mm. The capillaries are simply inserted into the flow rated tubing. No leaking was experienced except at pressure drops exceeding 110 psi (7.6 bar).

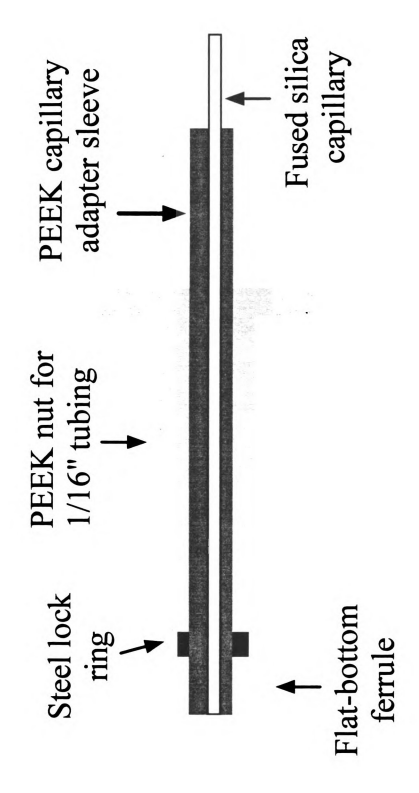
2.1.2 Injector

The injector used was a 4-port switching valve (Upchurch Scientific, model V•101D) with a non-metallic rotor. The non-metallic rotor was used so that future CFI studies using electroosmotic flow (EOF) could be performed with the same injector. Coupling the capillaries to the injector presents a small obstacle.

An adapter sleeve (Upchurch Scientific, model F•230), Polyetheretherketone (PEEK) nut, is slid over the fused silica capillary. Next, a steel lock ring and ferrule (Upchurch Scientific, model P•250X) are slid over the adapter sleeve. When screwed into a threaded hole, the lock ring and ferrule clamp down on the sleeve holding the capillary. The adapted capillary resembles that shown in figure 2.2.



Schematic of capillary flow injection manifold. Capillary inside diameters measured 75 µm. The inside diameter of the flow rated tubing was 190 µm. The solid and dashed lines on the injection valve represent the non-inject and inject mode, respectively. Figure 2.1.



Fused silica capillary adaptation to conventional switching valve. The fused silica capillary is surrounded by the adapter sleeve (380 mm i.d.), ferrule, and nut. This assembly is then set into the valve and ready for Figure 2.2.

2.1.3 Photometric Flow Cell Designs

Figures 2.3 and 2.4 show the flow cells designed for the photometric detector used with the CFI system. The flow cell in figure 2.3 is made from black Delrin and, save for the various nuts used in the design, is all one unit. The design consists of two threaded holes for nuts which hold the adapted capillary tubing (prepared as described previously). These serve to introduce the flowing stream and carry it to waste, respectively. At the bottom of each of these threaded holes is a channel with an inside diameter of 0.020 inches and length of 0.025 inches. This channel then intersects the flow path, which has an optical path length of ≈3 mm. The ball lenses (Edmund Scientific, model SF-8, 4 mm) serve a dual purpose. First, they are used to block the flow from leaking out each end of the flow cell. Secondly, one lens focuses the light from the source into the cell and the second focuses it onto the detector. Two large screws are used to hold the spherical ball lenses in place so they will form a tight seal against the flow path. One of the larger screws contains a channel in which a fiber optic can be inserted in order to bring the light into the flow cell. The second screw was constructed in such a way that it has a cylindrical extension which carries the light to the detector after having passed through the flow cell. The entire flow cell is about 3 inches x 3 inches.

The flow cell shown in figure 2.4 is very similar to that shown in figure 2.3. However, this flow cell is much more versatile since the internal volume can be varied. It is also constructed of black Delrin and utilizes the ball lenses in the same manner as previously described. However, it differs in that it is comprised of two identical units each with a hole (1/16 inch i.d.) drilled to a length of 0.48 cm. Within this drilled hole, one can

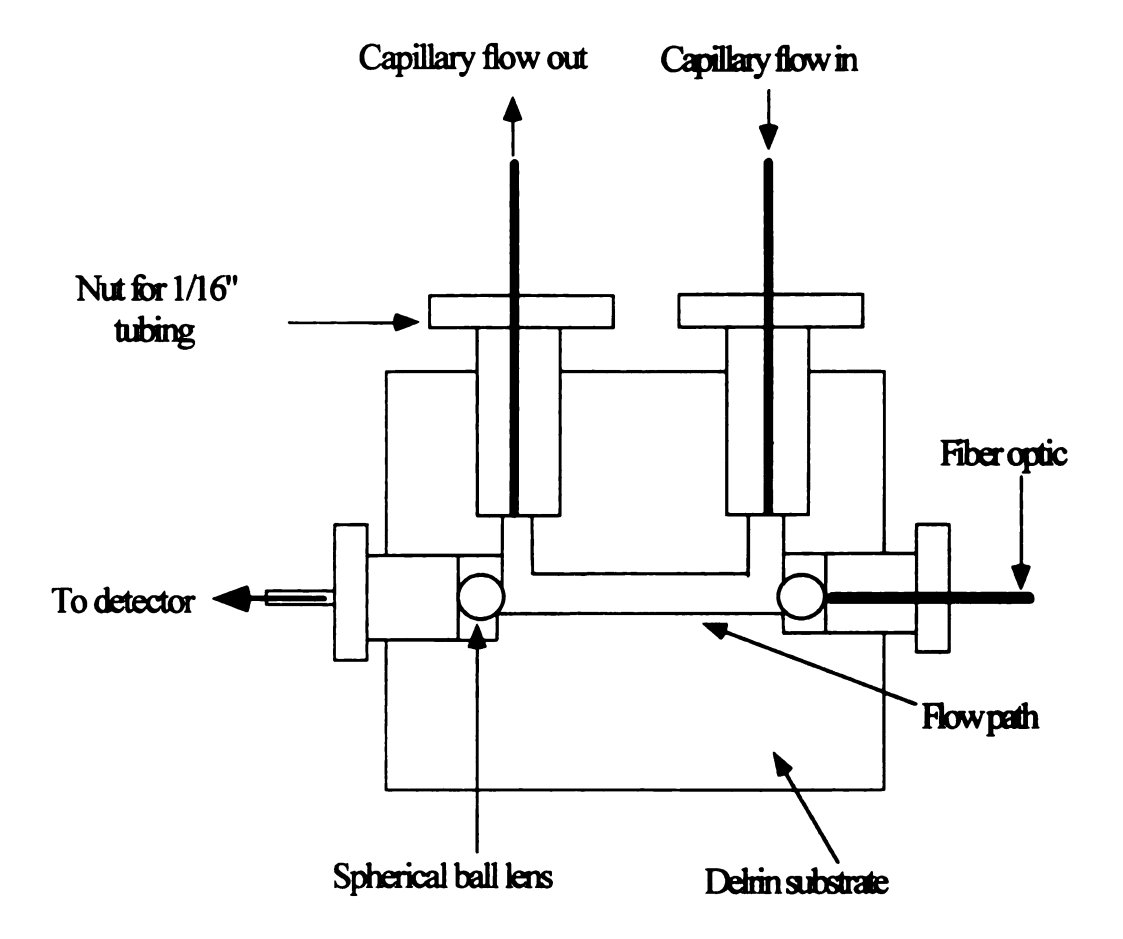
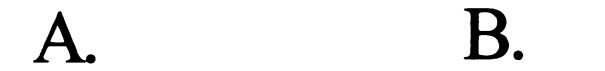


Figure 2.3 Cross sectional view of fixed volume flow cell. The path length is 3 mm with a volume of approximately 0.67 μ L. The capillaries are adapted to the cell in the same manner as when set in the switching valve.



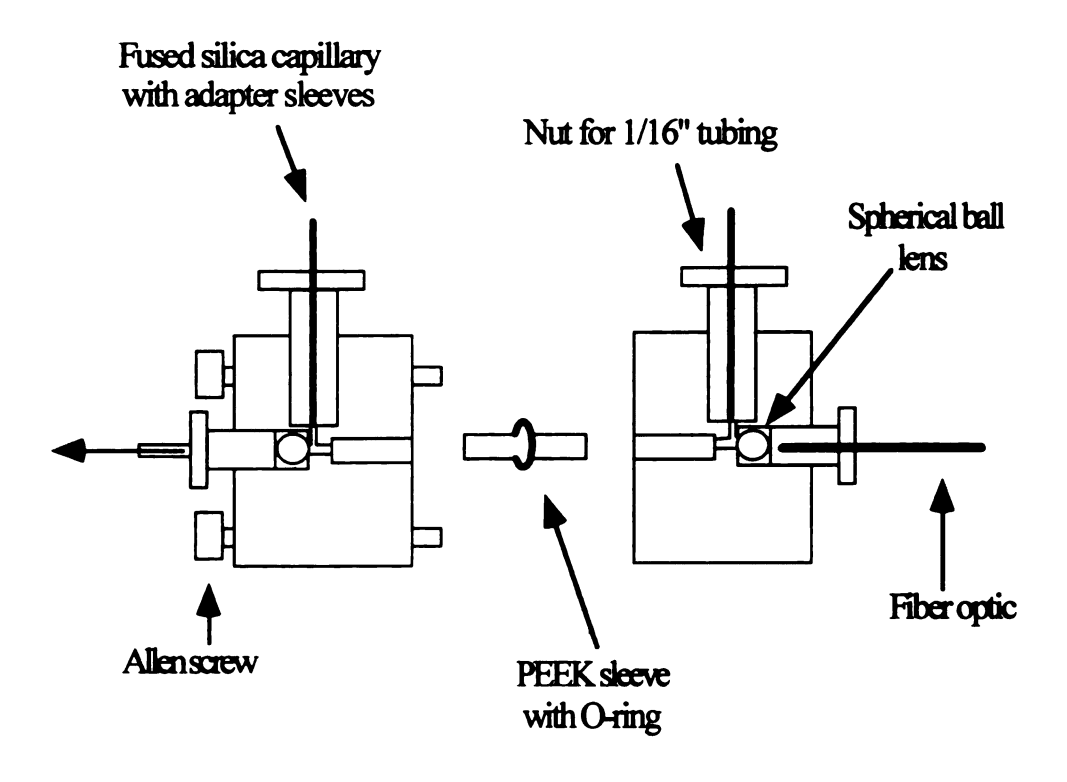


Figure 2.4 Cross sectional view of variable volume flow cell with a PEEK sleeve constituting the flow path. The rubber O-ring creates a tight fit around the sleeve to prevent leaking. Parts A and B are then brought together and tightened with Allen screws.

insert a sleeve (1/16 inch o.d.) made of PEEK with inside diameters ranging from 0.008 inches to 0.020 inches or greater if necessary. The two units are attached by means of four Allen screws and threaded holes. A rubber O-ring is used so that no leaking occurs when the two pieces are joined together. With this flow cell, the internal volume can be changed from 320 nL to $2.2~\mu$ L while still maintaining a path length of 1 cm.

2.1.4 Mixing Aids and Connectors in CFI

We have also investigated the use of multiple line manifolds for CFI determinations. There are several commercially available Y-shaped connectors for capillary tubing. The Y connectors chosen for this study (FTF International) are prepared by using a heat gun for about 45 seconds on the capillary after sliding it into the Y connector. The intense heat melts the polyimide coating on the capillary. Upon cooling, the capillary becomes set in the Y connector. In addition, the Y connector can be reheated and the capillary pulled out if replacement is necessary. Other mixers were studied and these are presented in more detail in chapter 5.

The mixers described in chapter 5 are more advantageous in terms of simplicity. For example, the Y connectors described in the previous paragraph can be difficult to prepare and once set, are not easy to reuse. The mixing tee employs standard 10-32 threading and allows for easy adaptation of the fused silica capillary tubing through the use of the special PEEK adapter sleeves mentioned earlier. In addition, the nuts, sleeves, and tubing can be easily interchanged when using this tee.

2.1.5 Reagents

All solutions were prepared with distilled water (DW). No special filtering of the solutions was needed.

Iron Determination Solutions. A 1.3 mM FeSO₄ (Baker) stock solution was made by transferring 0.202 g FeSO₄ to a 1-L volumetric flask and diluting to the mark with DW. Iron standards with concentrations ranging from 0.270 mM up to 1.10 mM were prepared by appropriate dilution of the stock solution with DW. The 1,10-phenanthroline (G.Frederick Smith) was prepared by dissolving approximately 0.2 grams in about 5 mL of methanol. This solution was then transferred to a 200 mL volumetric flask and diluted with DW.

Nitrite Determination Solutions. All of the solutions for this determination should be stored in amber glass bottles to minimize photodecomposition effects. A 50 mM nitrite (Baker) stock solution was made by transferring 0.863 g of NaNO₂ to a 250 mL volumetric flask and diluting to the mark with DW. The working solution of nitrite (500 μM) was made by a 1:100 dilution with DW. A 58 mM solution of sulfanilamide (Baker) was made by combining 10 g sulfanilamide with 100 mL of concentrated HCl in a 1-L volumetric flask followed by dilution to the mark with DW. A 3.8 mM solution of N-(1-naphthyl)ethylenediamine dihydrochloride reagent (Baker) was made by transferring 1.0 g of the N-(1-naphthyl)ethylenediamine dihydrochloride to a 1-L volumetric flask and diluting with DW.

Phenol Red Solutions. Borate buffer (pH 9.5) was prepared as described elsewhere⁷. The 1 mM stock solution of phenol red (Baker) was prepared by adding 0.1 g

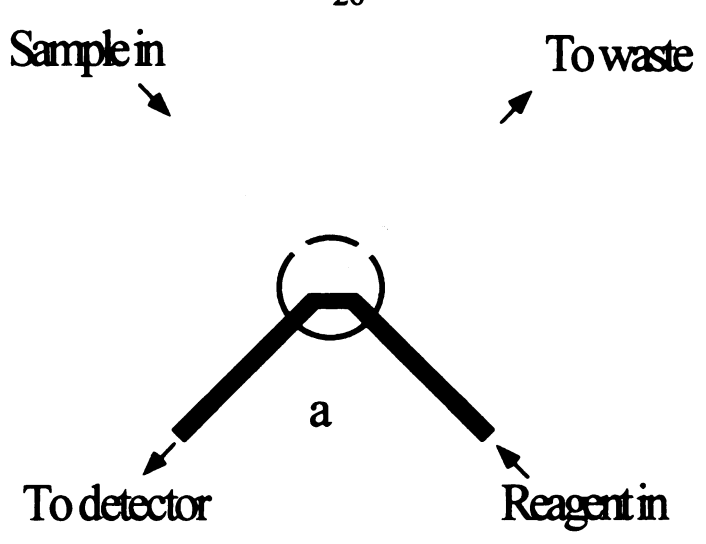
of the dye to a 500 mL volumetric flask and diluting to the mark with 0.001 M NaOH. The working phenol red solution used in the sample throughput and reproducibility studies was composed of 25 mL of the stock solution diluted to 500 mL with the borate buffer.

2.2 RESULTS AND DISCUSSION

2.2.1 Reproducibility of Injections

Although injection valves are available with sample sizes as low as 20 nL, most of these are fixed volume injectors because they contain internal sample loops. Thus, in order to vary the sample size, the rotor must be changed. With other injectors, an external loop may be changed rather easily. However, the swept volume alone associated with these valves (on the order of a few µL) is often too large for our studies. Therefore, we decided to base our injections on time rather than on an injection loop. Figure 2.5 demonstrates the principle behind timed injections. In figure 2.5a, the sample and reagent streams are flowing to waste and to the detector, respectively. The valve is then switched using a computer-controlled pneumatic actuator for a period of time as shown in figure 2.5b. When the valve is switched back to its original position in figure 2.5c, the reaction coil contains a sample zone which is carried to the detector.

Figure 2.6 demonstrates the reproducibility of injections made with our valve. The reproducibility, reported as the RSD of the peak height for repetitive injections of the phenol red into the borate buffered stream, is $\approx 1\%$. The construction of such a valve is also advantageous since any volume of sample can be injected. The user can either vary the time the valve is in the injection mode or simply have a different flow rate in the sample stream. Changing the flow rate can be accomplished by using different types of



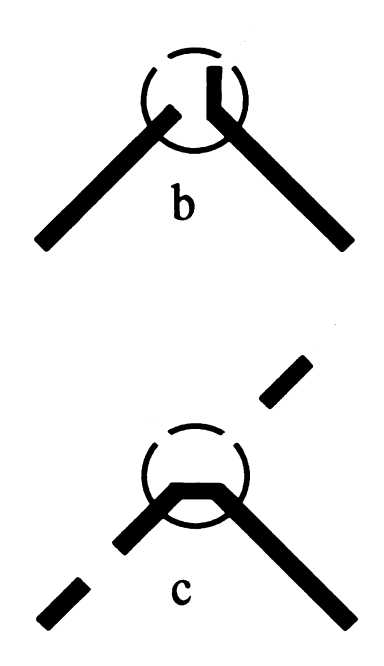


Figure 2.5 Principle behind timed injections. Figure 2.5a shows the valve in the non-inject mode. In figure 2.5b the actuator has switched the valve to the injecting position. Here, sample is being pumped into the reaction coil for a specified amount of time. In figure 2.5c, the valve is returned to the non-inject mode. The sample plug is now being carried to the detector.

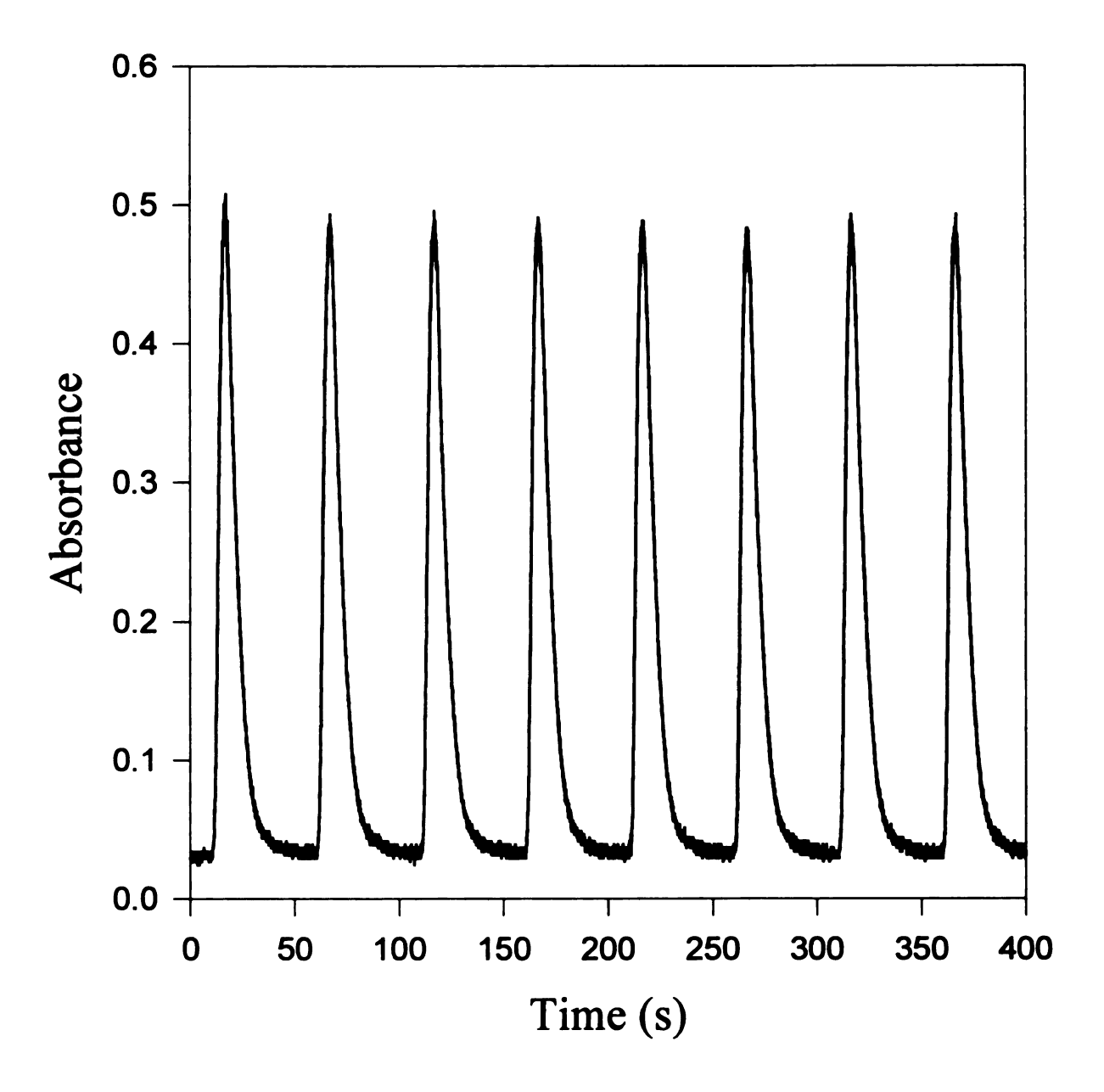


Figure 2.6. Response signals for repetitive injections of phenol red into a borate buffered stream. The RSD of the peak heights is 1.2%.

flow rated tubing typically used in conventional FI. A drawback to such a technique is that sample must continually be pumped through the valve. However, most conventional flow injection systems utilizing an injection loop continuously pump sample in order to maximize sample throughput. The exception to this occurs when a syringe is used to fill the sample injection loop. However, since the capillary volume is minimal, even continuous pumping at relatively high linear flow rates does not result in high sample consumption. For example, the total amount of sample used to obtain the eight FI peaks in figure 2.6 was approximately 80 µL even though sample was being continuously pumped through the valve. A single injection using conventional sized tubing is on the order of 30 µL. Thus, if one were to obtain the same data using conventional flow injection, 240 µL of sample would be consumed at an absolute minimum, three times that of the CFI system. If the sample were continuously pumped in a conventional FI system (as with an external injection loop) with tubing diameters of 1 mm, the amount of sample consumed would be >10 mL. Thus, sample consumption is greatly reduced in a CFI system.

2.2.2. Absorbance Linearity of Fabricated Flow Cells

Detection has been one of the few shortcomings of capillary zone electrophoresis (CZE). Quite often, analysts are forced to use on-column detection methods since any sort of additional plumbing will lead to band broadening and thus lower resolution. Other methods⁸ have been used in CZE such as the use of multireflection throughout the inside of the capillary, rectangular capillaries to help minimize stray light and end-column detection. Recently, a capillary bent into a "Z" has been used to increase the effective path

length⁹. These Z-cells are commercially available and, with low volume, are excellent for techniques using capillaries and small volumes of reagents. However, these Z-cells are expensive, and since resolution is not a large concern in FI methods, the two different flow cells described earlier were designed with volumes slightly larger than the capillary Z-cell, but smaller than those typically used in FI applications.

Figures 2.7 and 2.8 show the results of the iron determinations using the flow cells in figures 2.3 and 2.4, respectively. Each data point is the average of three replicate injections. In this determination, the 1,10-phenanthroline complexation of the ferrous ion results in the Fe(1,10-phenanthroline)²⁺ product that absorbs at a wavelength of 508 nm. Both flow cells show good linearity with r² values of 0.997 and 0.998 for the curves in figures 2.7 and 2.8, respectively. The Student t test shows that both intercepts (-2.0 x 10⁻² for the flow cell shown in figure 2.3 and -9.0 x 10⁻³ for the variable volume cell shown in figure 2.4, respectively) are not significantly different from zero at the 99% confidence level.

2.2.3 Multiple Reagent Manifolds in CFI

A final aspect of this study was to determine whether or not manifolds requiring multiple reagent streams could be implemented in the capillary format. Thus, a determination of nitrite was performed using the Griess reaction^{10,11}.

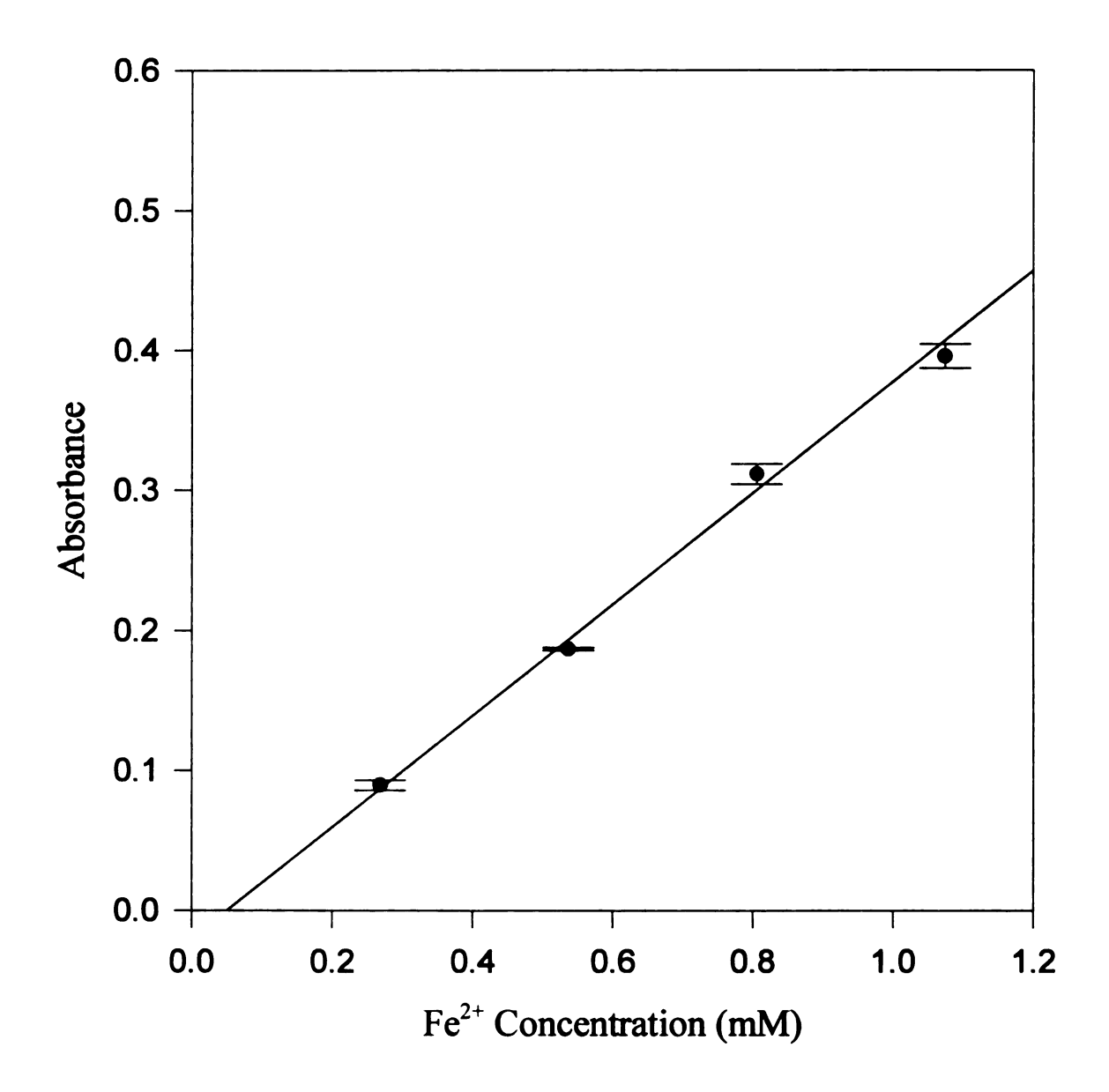


Figure 2.7. Calibration curve for Fe^{2+} using the variable volume flow cell. The volume of the flow cell was approximately 0.67 μ L while the path length was 3 mm. The volume injected was 1.75 μ L.

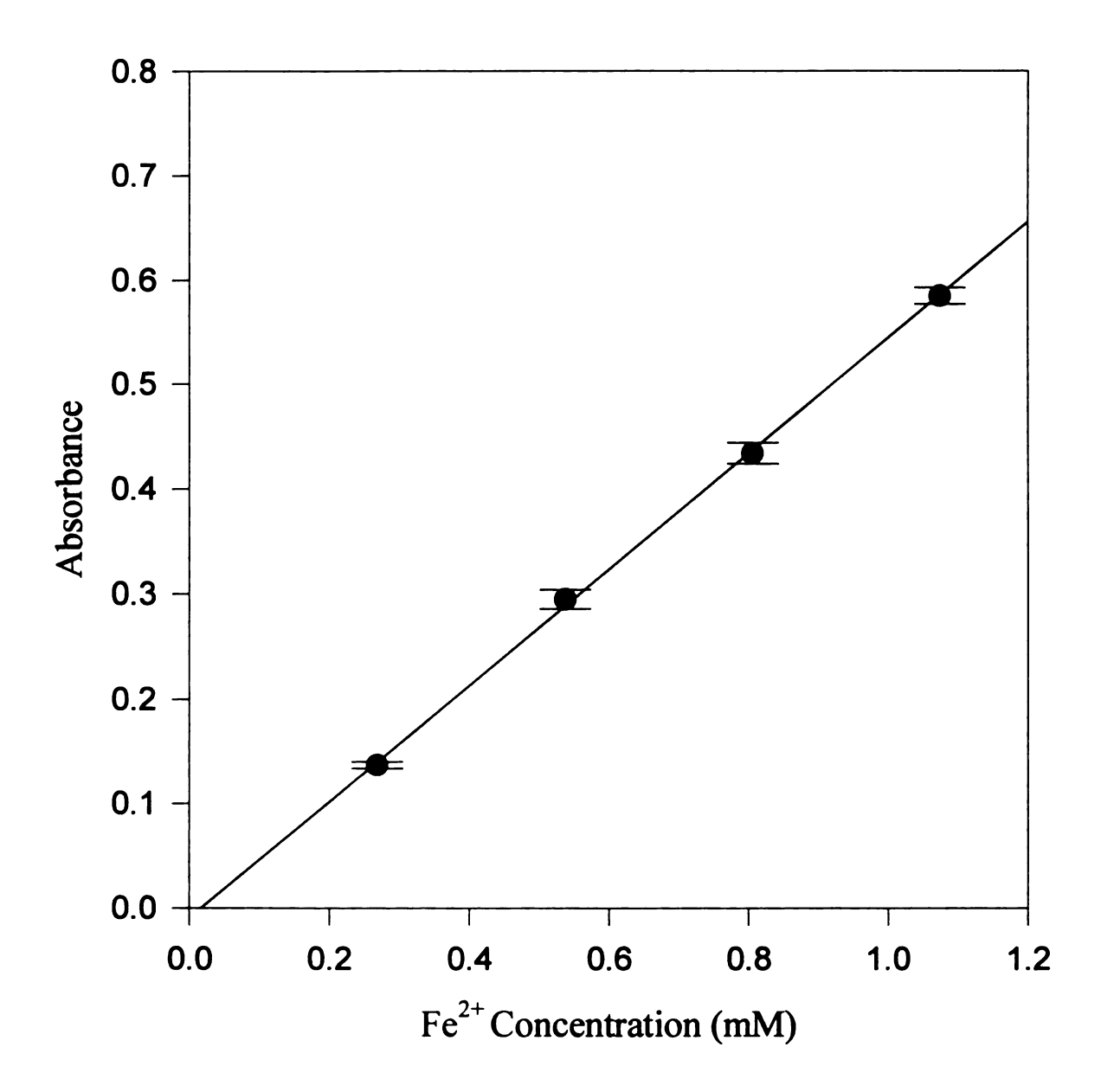
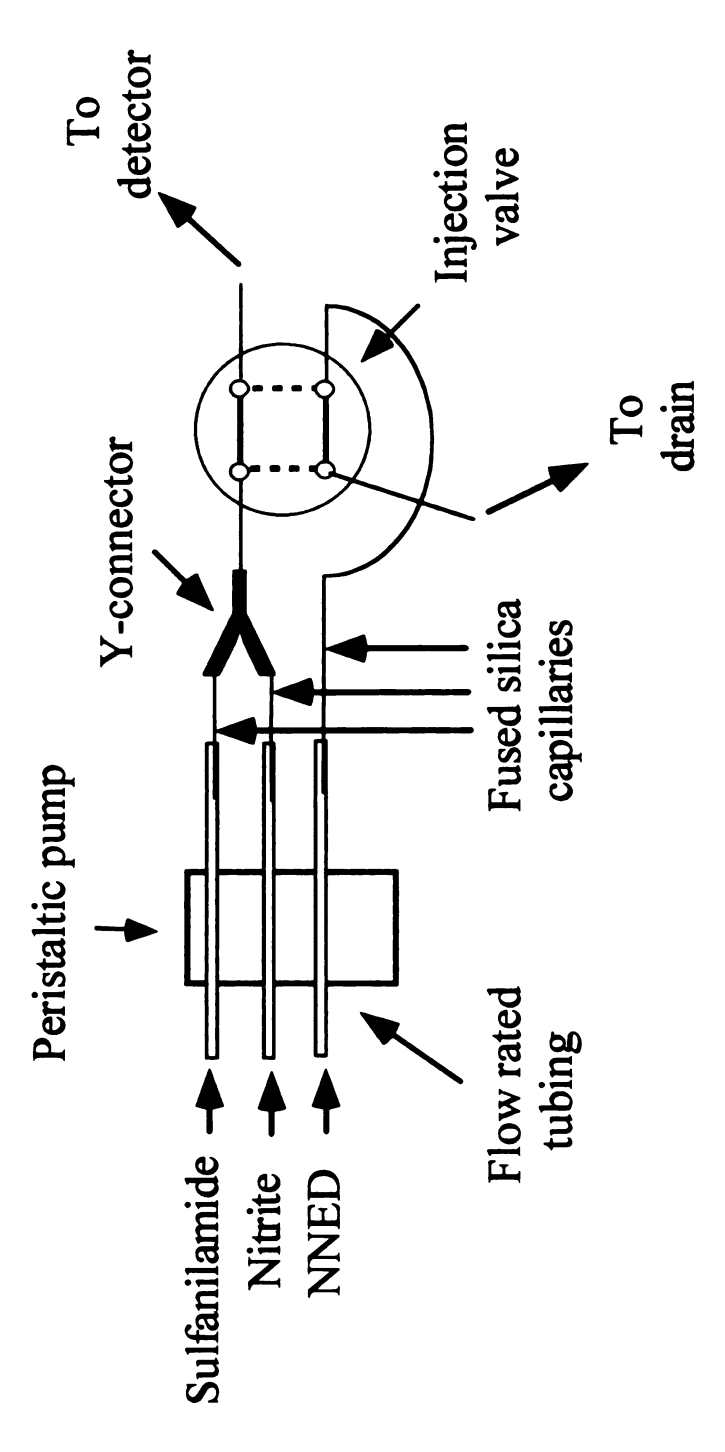


Figure 2.8. Calibration curve for Fe^{2+} using the variable volume flow cell. The volume of the flow cell was approximately 0.9 μ L while while the path length was 8 mm. The volume injected was 1.35 μ L.

This reaction, shown below, produces a product detectable at 550 nm. The manifold used

for this study is that shown in figure 2.9. The RSD of the peaks obtained by this study, shown in figure 2.10, was 2.1%. Another aspect of this particular experiment is that a sleeve with an inside diameter of 0.008 inches was used, thus effectively reducing the flow cell volume to approximately 260 nL. This study indicates that multiple reagent flow injection systems may be implemented with success in the capillary format. More detailed studies involving pressure drops and mixing in multiple line capillary flow injection systems are described in chapters 3,5, and 6, respectively.



involved. The Y coupler allows for multiple reagent streams to be employed Schematic of capillary flow injection manifold when multiple streams are in a CFI system. Again, the solid and dashed lines on the injection valve represent the non-inject and inject mode, respectively. Figure 2.9.

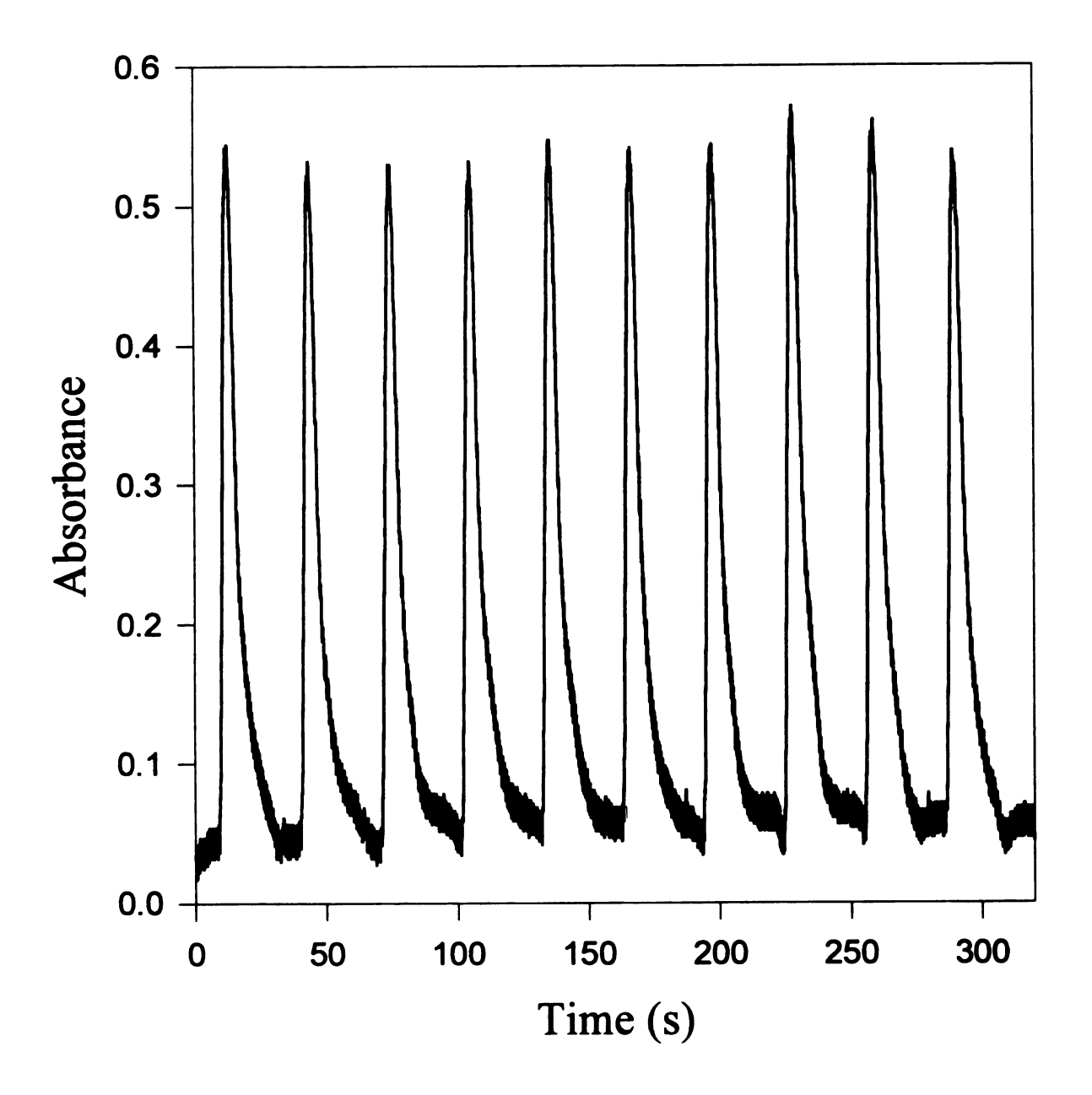


Figure 2.10. Response signals for the determination of nitrite by the Griess reaction. The RSD in peak height is 2.1%.

2.3 CONCLUSIONS

The use of fused silica capillaries as the reagent vessels for flow injection analysis has been described. In addition, special pumping, injection, and detection schemes have been presented and proven beneficial. The flow cell volume has been effectively decreased in order to allow for detection of sub-µL sample volumes. The use of Y-shaped connectors allows for multiple line manifolds to be implemented, enabling complex reactions to be studied.

List of References

- 1. Lee, M.L; Yang, F.J.; Bartle, K.D. Open Tubular Column Gas Chromatography, Wiley, New York, 1984.
- 2. Novotny, M.; Ishii, D. (eds.) *Microcolumn Separation Methods*, Elsevier, Amsterdam, 1985.
- 3. Camilleri, P. (ed.) Capillary Electrophoresis: Theory and Practice, CRC Press, Boca Raton, FL, 1993.
- 4. Liu, S.; Dasgupta, P.K. Anal. Chim. Acta 1992, 268, 1.
- 5. Liu, S.; Dasgupta, P.K. Anal. Chim. Acta 1993, 283, 747.
- 6. Dasgupta, P.K.; Liu, S. Anal. Chem. 1994, 66, 1792.
- 7. CRC Handbook of Chemistry and Physics, CRC Press, Boca Raton, FL, 1988.
- 8. Albin, M; Grossman, P.D.; Moring, S.E. Anal. Chem. 1993, 65, 489A.
- 9. Moring, S.E.; Reel, R.T.; van Soest, R.E.J. Anal. Chem. 1993, 65, 3454-3459.
- 10. Fox, J.B., Jr. Anal. Chem. 1979, 51, 1493.
- 11. Patton, C.J. Ph.D. Thesis, Michigan State University, East Lansing, MI, 1982.

Chapter 3

An Investigation of Pressure in Capillary Flow Injection Systems

Ruzicka and Hansen^{1,2} discussed flow injection (FI) miniaturization via microconduit technology over a decade ago. In their monograph³, these same authors point out several possible pitfalls in miniaturizing FI. Liu and Dasgupta^{4,5}, reported FI in the capillary format with 75 µm fused silica capillaries as the reaction conduit. Although fused silica capillary and on-column detectors became available in the 1980's along with valve-based injection techniques⁶, capillary flow injection (CFI) has developed rather slowly. The major reason for this has been the need for a reliable pumping system that can deliver steady flow rates in the µL min⁻¹ range.

Dasgupta and Liu⁷ have also reported on various pumping schemes commonly employed in FI systems and have described the use of electroosmotic flow (EOF) as a reliable and steady pumping technique. We⁸ have previously reported on a CFI system employing capillary tubing with inside diameters of 75 µm as the reaction tubing and a modified peristaltic pump to propel the necessary reagents. In addition, this system showed no apparent pulsations from the pump used to propel the reagents and samples. Although we have shown in work performed to date that peristaltic pumps can provide the

necessary reproducibility in both continuous and stopped-flow CFI regimes⁹, the limitations of such pumps for CFI have not been reported. For example, most manufacturers of peristaltic pumps guarantee pressures up to approximately 2.8 bar. However, performance characteristics at higher pressures have not been reported. Likewise, there is a need to investigate pressure drops and flow stability with syringe pumps, especially when tubing of capillary dimensions is considered.

This work reports on internal pressures, pumping stability and baseline noise levels for a CFI system using two different peristaltic pumps, a syringe pump, and a typical dual-piston HPLC pump. Our goal is to show the limitations of each type of pump investigated since it is anticipated that peristaltic, syringe, and HPLC pumps will have importance in different applications. Because of its completely different operating mechanism, EOF is not considered here with the pressure-induced flow systems.

3.1 EXPERIMENTAL

3.1.1 Reagents

Phenol Red Solutions. The preparation of the phenol red dye and the borate buffer were described in chapter 2.

Reagents for Glucose Determination. All reagents for glucose determinations were used as received. The glucose (Sigma) standards were made from a 1 g/L stock solution in DW. The glucose oxidase enzyme solution was prepared by dissolving 0.12 g of glucose oxidase (Sigma, Type II, from Aspergillus niger) in 50 mL of DW. The composite reagent solution consisted of 10 mL of glucose oxidase solution, 5 mL of 10 mM 4-aminoantipyrine (Sigma), 5 mL of 10 mM 3,5-dichloro-2-hydroxphenyl sulfonic

acid (Sigma), 12 mg of horseradish peroxidase (Sigma, Type II) and 20 mL of 0.05 M phosphate buffer mixed together in an amber bottle before use.

3.1.2 Apparatus

Fused silica capillaries (75 µm i.d. x 365 µm o.d., Polymicro Technologies) were used as the manifold tubing for all studies. The pressure measurements were made using a pressure gauge with a maximum pressure of 200 psi. These pressures were subsequently converted to bar (1 psi \approx 0.069 bar) A tee adapter (Upchurch Scientific) allowed for the pressure gauge to be implemented on line. This adapter is constructed with a 1/4" thread common to most pressure gauges on the top and standard 1/16" threads on each side of the adapter. These 1/16" threads then can hold a standard 1/16" nut which houses the PEEK sleeves which in turn allow the fused silica capillaries to be adapted to standard Three different types of pumping mechanisms were investigated. A typical 8fittings. roller peristaltic pump (Ismatec, model IP-12) was investigated as well as a modified version of this pump with 16 rollers¹⁰. The adaptation of the fused silica capillaries to the flow rated tubing used in conjunction with the peristaltic pumps has been described elsewhere⁸. The syringe pump used in this study was a dual channel model (Harvard Apparatus, model 22). Various disposable syringes (Becton Dickinson), ranging in size from 5.0 to 20.0 mL, were coupled to a 25 gauge syringe needle. The fused silica capillaries were then adapted to the needle using flow rated tubing (Cole Parmer) with an inside diameter of 250 µm. The final pump investigated was a dual piston HPLC pump (Hitachi L6200 Intelligent Pump). The fused silica capillaries were adapted to the HPLC pump using PEEK adapter sleeves (Upchurch Scientific) of 0.015" inside diamter and 1/16" outside diameter coupled to stainless steel nuts (Upchurch Scientific).

3.1.3 Procedure for Pressure Measurements

The pressures were measured using the pressure gauge in-line with the manifold. The basic schematic for all pressure measurements is shown in figure 3.1. The solution pumped through the system for all measurements was distilled water at room temperature, typically 22 ± 1° C. In order to measure the flow rates, the amount of water pumped through the system per unit time (the amount of time was approximately 1 h, therefore evaporation of the water was negligible) was collected and weighed. From the density of water at 22 °C, the volumetric amount of water per unit time was calculated. Since the amount of solution pumped through the fused silica capillaries is very small, equilibration of the pressure gauge sometimes required more than one hour. The exact equilibration time depends on the flow rate.

The procedure for the determination of the glucose standards was very simple. The enzyme composite reagent and the glucose standards were both pumped continuously at $4.4 \, \mu L \, min^{-1}$ using the peristaltic pump. Injections of the glucose sample into the enzyme reagent stream were performed with a four-port switching valve¹² that was switched for a period of 15 seconds resulting in a sample injection volume of approximately $1 \, \mu L$. The response signal was then measured at a wavelength of 510 nm using a colorimeter with a 1 cm path length flow cell⁸.

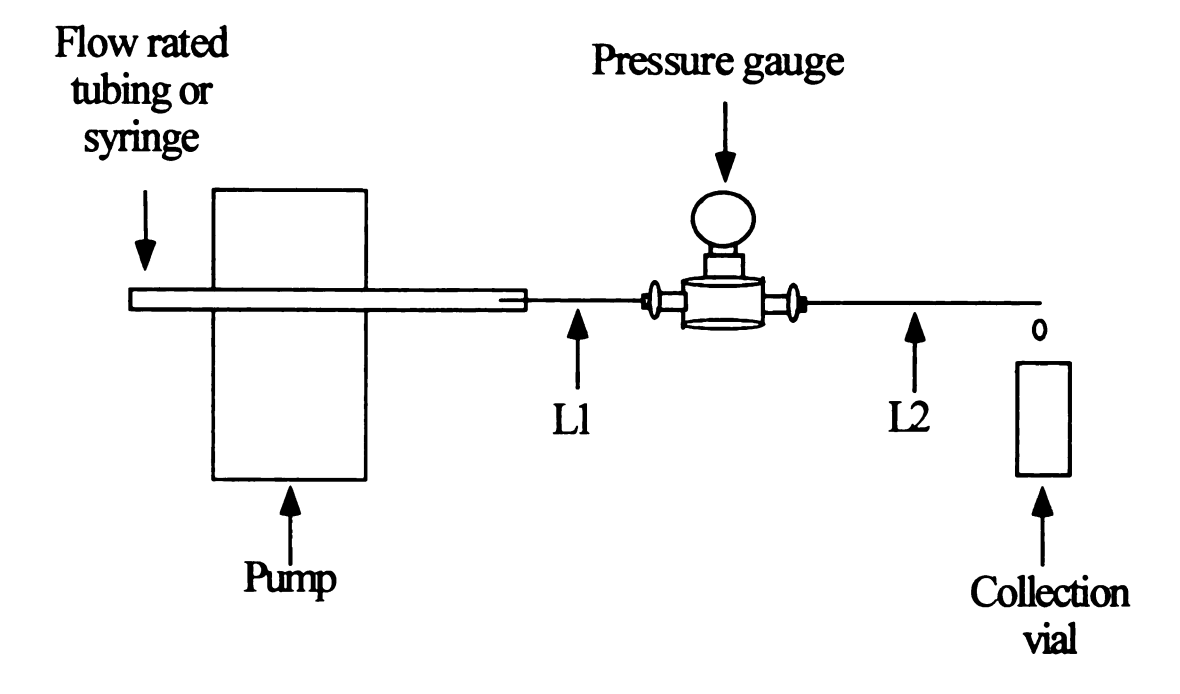


Figure 3.1. Schematic of the system used to measure the pressure gradient in a capillary. L1 represents a portion of fused silica capillary that was kept as short as possible, typically about 15 cm, whereas L2 is the capillary that was varied when the pressure gradient was investigated as a function of reactor length. Procedural details are contained within the text.

3.2 RESULTS

3.2.1 Maximum Attainable Pressures

Peristaltic Pumps. Experiments were performed to determine the back pressure limitations of the three types of pumps. The Hagen-Poiseuille equation shown below describes the pressure drop, ΔP , along an open tubular column of length L with radius

$$\Delta P = \frac{8L\eta v}{r^2}$$
 (3.1)

r containing a solution of viscosity η traveling at a linear flow rate of ν . In order to assure that the manifold with the pressure gauge in-line was operating properly, a plot of ΔP versus linear velocity was made with values of ΔP calculated from equation 1 compared to those measured experimentally with the 16-roller peristaltic pump. The viscosity was assumed to be 1 cp. This comparison, shown in figure 3.2, indicates that the system is behaving according to theory. In figure 3.2, the maximum measured pressure was 3.96 \pm 0.03 bar at a linear velocity of 11.4 ±0.1 cm s⁻¹. However, it may be necessary at times to use a column longer than the 62 cm reactor used to obtain the data shown in figure 3.2. Therefore a plot of ΔP versus capillary length was constructed and is shown in figure 3.3. Notice that at a column length of 200 cm, the observed ΔP is much less than the predicted value given by equation 3.1. It is important to note that in this particular figure, the pump was not adjusted to compensate for the increased capillary length. When the combs over the flow rated tubing were tightened or the pump rollers increased, we were able to achieve pressures of greater than 10.3 bar. However, these pressures could not be

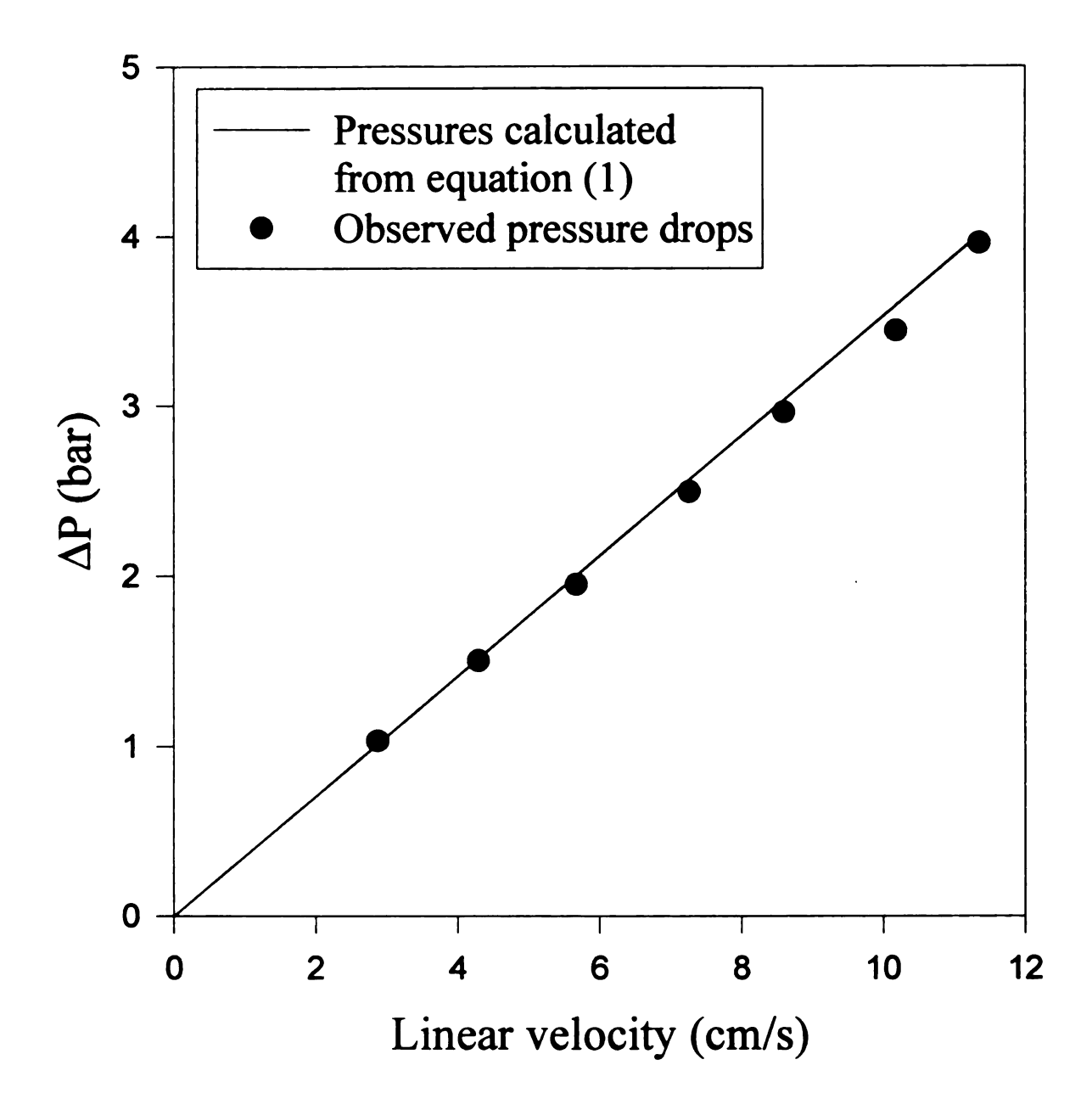


Figure 3.2. Calculated and measured pressure gradients as a function of increasing flow rate using the manifold shown in figure 3.1. The measured values were obtained with the peristaltic pump.

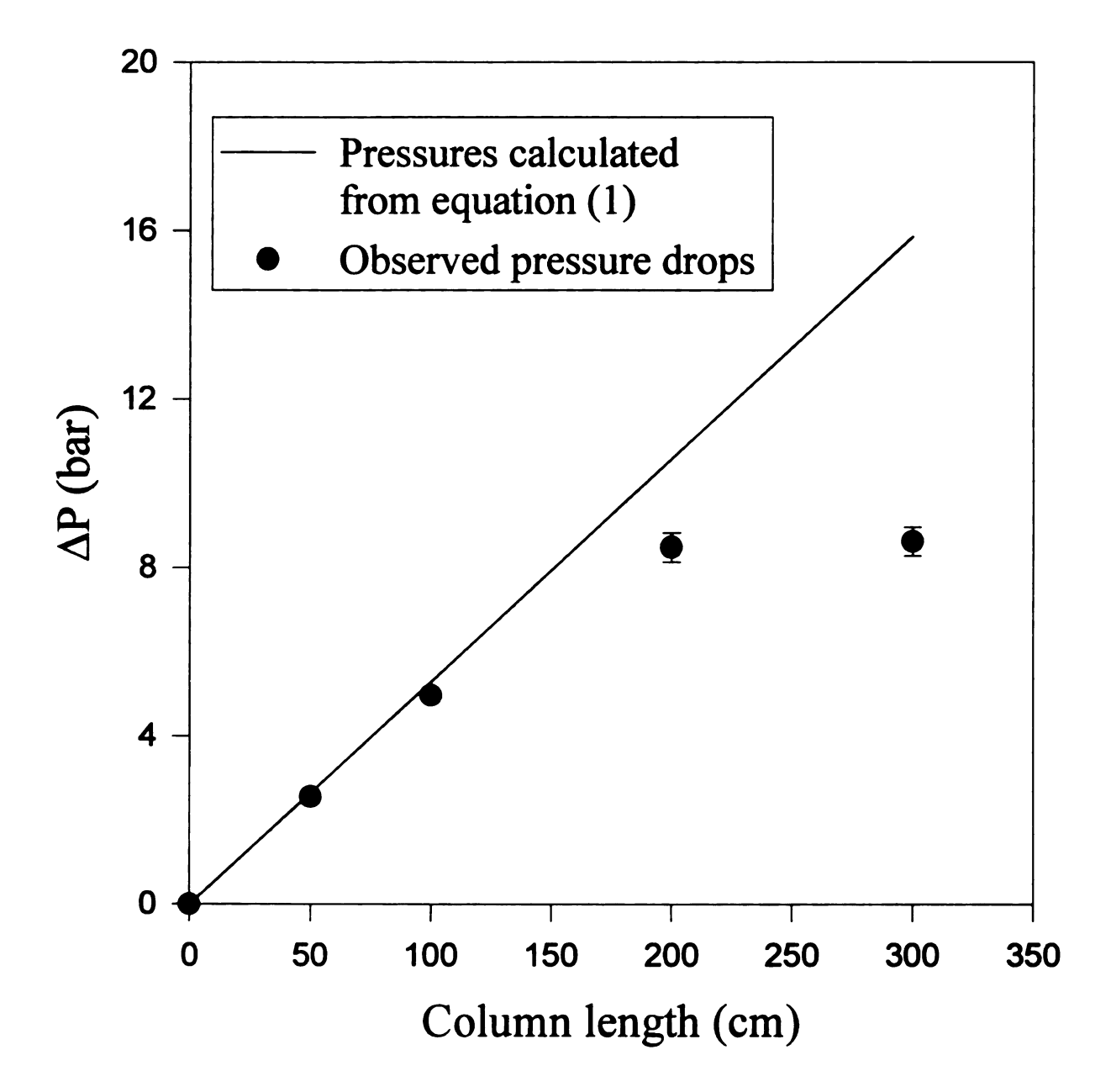


Figure 3.3. Calculated and measured pressure gradients as a function of increasing reactor length using the manifold shown in figure 3.1 and the peristaltic pump. The observed values deviate from predicted values because of the pump's pressure output limitations.

sustained for a long time because flow rated tubing becomes worn much faster under such conditions. In fact, at times, the flow rated tubing would burst, thus losing all pressure. From our studies we believe that the maximum operable pressure using this peristaltic pump is approximately 7.6 bar. Any pressures greater than this value were unstable.

Syringe Pump. It was noticed during the studies with the syringe pump that the maximum attainable pressure was inversely dependent upon the radius of the syringe barrel containing the reagents. The syringe pump used in this study will shut off if the backpressure becomes too high since the motor-driven turnscrew used to push the syringe ends could be ruined. Thus, the pump was monitored with the pressure gauge until pump shut-down, at which point the pressure was immediately measured. Table 3.1 shows the maximum attainable pressures for three different syringe sizes.

Dual Piston HPLC Pump. The dual piston HPLC pump shows the most promise for determinations that require long capillary lengths and/or extremely high flow rates since these pumps can easily exceed pressures of 140 bar. In contrast to a peristaltic pump, dual piston pumps should maintain constant flow rates despite changes in capillary length.

3.2.2 A Comparison of Baseline Noise Levels

The baseline noise levels were measured using a UV-vis absorbance detector for the various types of pumps. We were unable to obtain a steady baseline with the dual piston pump employed during this study. From this we concluded that the pump was simply not able to deliver the necessary low volume flow rates needed in CFI. However, there are various syringe pumps (Isco, Eldex) that can now exceed pressures of 340 bar at

 Table 3.1. Effect of syringe radius on maximum attainable pressure.

Syringe volume (cm ³)	Syringe radius (mm)	Pressure (± 0.3 bar) ^a
3	4.33	19.2
5	6.03	10.1
10	7.25	7.9

^aPressure was measured the moment the syringe pump turnscrew automatically shut down.

flow rates as low as 0.01 µL min⁻¹. Figure 3.4 shows that there are no differences in baseline noise for the two types of peristaltic pumps between the pressures of 0 and 7.6 The noise in the absence of flow is probably a combination of dark current or flucuations in the light source. This was not the anticipated result since the 16-roller pump was modified in order to decrease pump pulsations. However, these modifications were originally performed for use in an air-segmented continuous flow (ASCF) system since air bubbles used for segmentation are more compressible than liquids. Thus, in ASCF pulsations may be more noticeable than in homogeneous FI systems with no airsegmentation. In addition, pump pulsations are probably not detected since the inside diameters of the flow rated tubing and the flow cell employed in this CFI system are so small (190 µm and 365 µm, respectively). In order to verify the absence of pump-induced measurable pulsations, the noise levels were also observed while the flow cell was filled with the absorbing dye. As shown in figure 3.5, there is very little difference in the observed signals whether the pump is running or is idle. There is also not much of an increase in pulsations when flow rated tubing with a larger inside diameter (250 µm) is employed and this effect is also shown in figure 3.5. The two different sizes of flow rated tubing were also employed at a linear velocity of 1 cm s⁻¹ (≈ 2.65 µL min⁻¹) and showed no definite increase of pulsations in the measured response signals.

The noise levels measured with the syringe pump were very similar to those of the peristaltic pump. The baseline noise level was roughly 5 milliabsorbance units. By measuring the same baseline noise levels whether the pump was running or idle, we concluded that the noise levels (when employing the syringe pump) were also independent

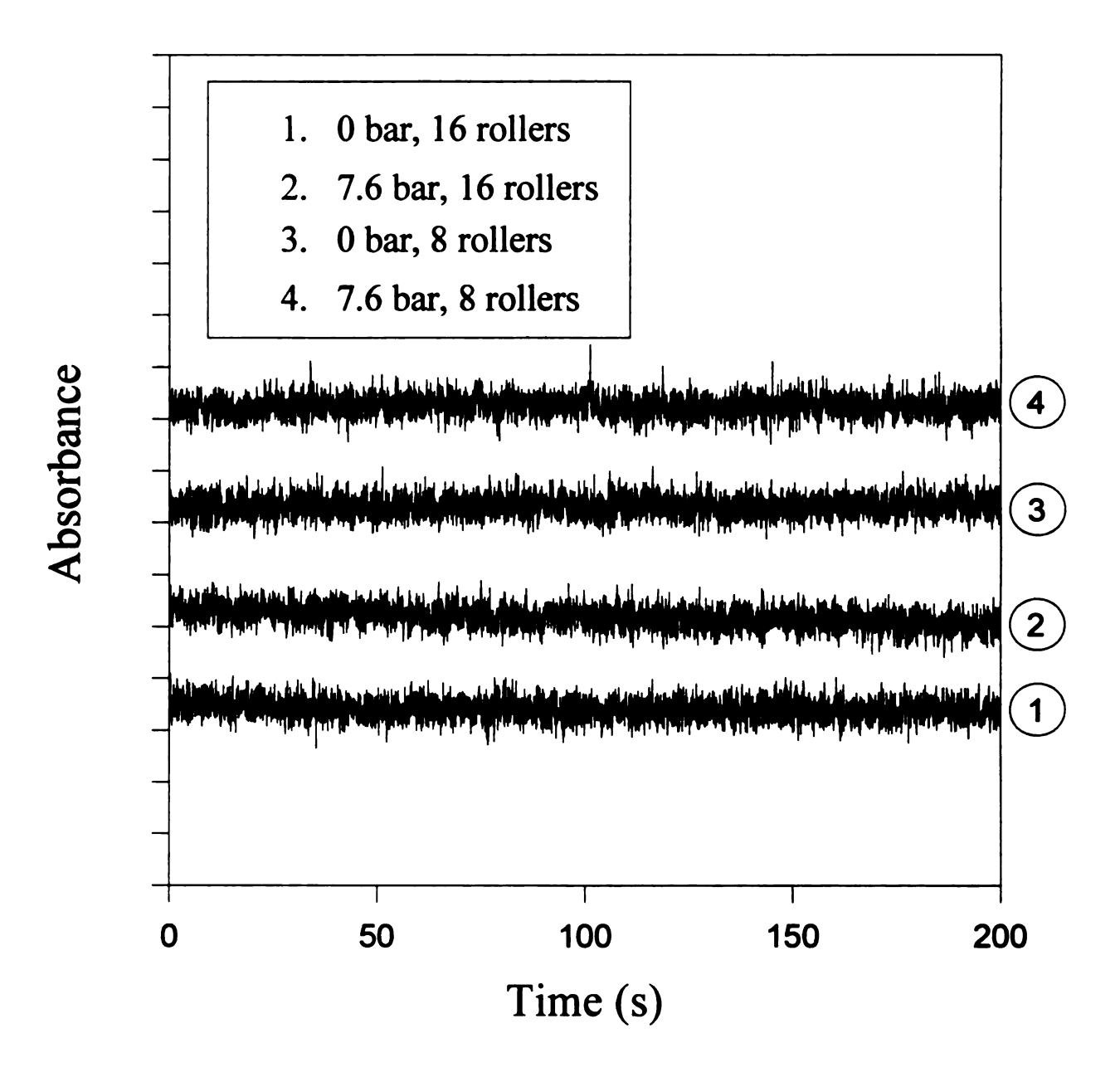


Figure 3.4. Measured baseline noise levels for two peristaltic pumps, one containing 8 rollers and the other containing 16 rollers. The four signals are offset for ease of reading. Each tick mark on the absorbance axis = 5 mAU.

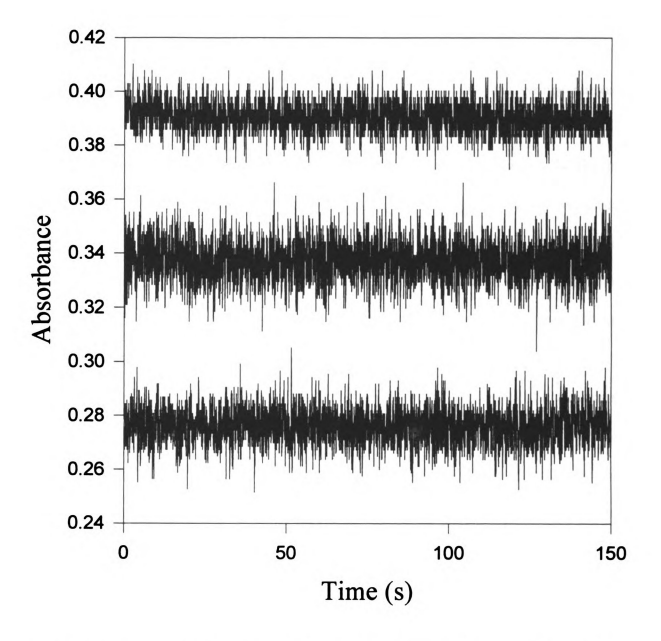


Figure 3.5 Investigation of pump pulsations by measuring the absorbance of the phenol red dye at steady state under various pumping conditions. The bottom trace used 190 mm i.d. flow rated tubing to introduce the reagents into the capillary, while the middle trace was obtained using flow rated tubing of 250 mm i.d. The upper trace used the 190 mm i.d. flow rated tubing but the pump was idle during the measured portion shown.

of flow rate. Baseline noise levels for the dual piston pump were not investigated since a steady baseline could not be achieved, as mentioned earlier.

3.2.3 Considerations for Manifold Design

Due to the pressure output capabilities of typical peristaltic and syringe pumps, capillary FI manifolds will have limits on available flow rates, inside diameters, and reactor lengths. For example, figure 3.6a shows the maximum attainable linear velocities at various capillary reactor lengths for the different pumps investigated. These velocities were calculated from equation 1 using the maximum pressure output from each pump as ΔP , 37.5 μ m as the radius, r, and a viscosity of 1 cp. From this plot one can see it is not feasible to obtain a flow rate greater than 3 cm s⁻¹ at capillary lengths greater than 350 cm unless an HPLC-type pump capable of high pressure output is employed.

In addition, the use of smaller bore capillary tubing will decrease the maximum attainable linear velocities. Figure 3.6b shows these velocities as a function of varying radii for the peristaltic pump and the syringe pump, again using the highest observed pressure for each as ΔP . The reactor length was 100 cm and the viscosity used in the caluculation was 1 cp.

Finally, more attention will be needed concerning viscous solutions. Calculated in the same manner as figures 3.6a and 3.6b, figure 3.6c shows the maximum solution viscosity that can be pumped at various viscosities for the pumps investigated. Again the reactor length was 100 cm while the tubing radius was 37.5 µm. This particular parameter is one of great importance since many samples requiring filtration and other preparative steps before the measurement step are often viscous, in a suspension or even in a slurry.

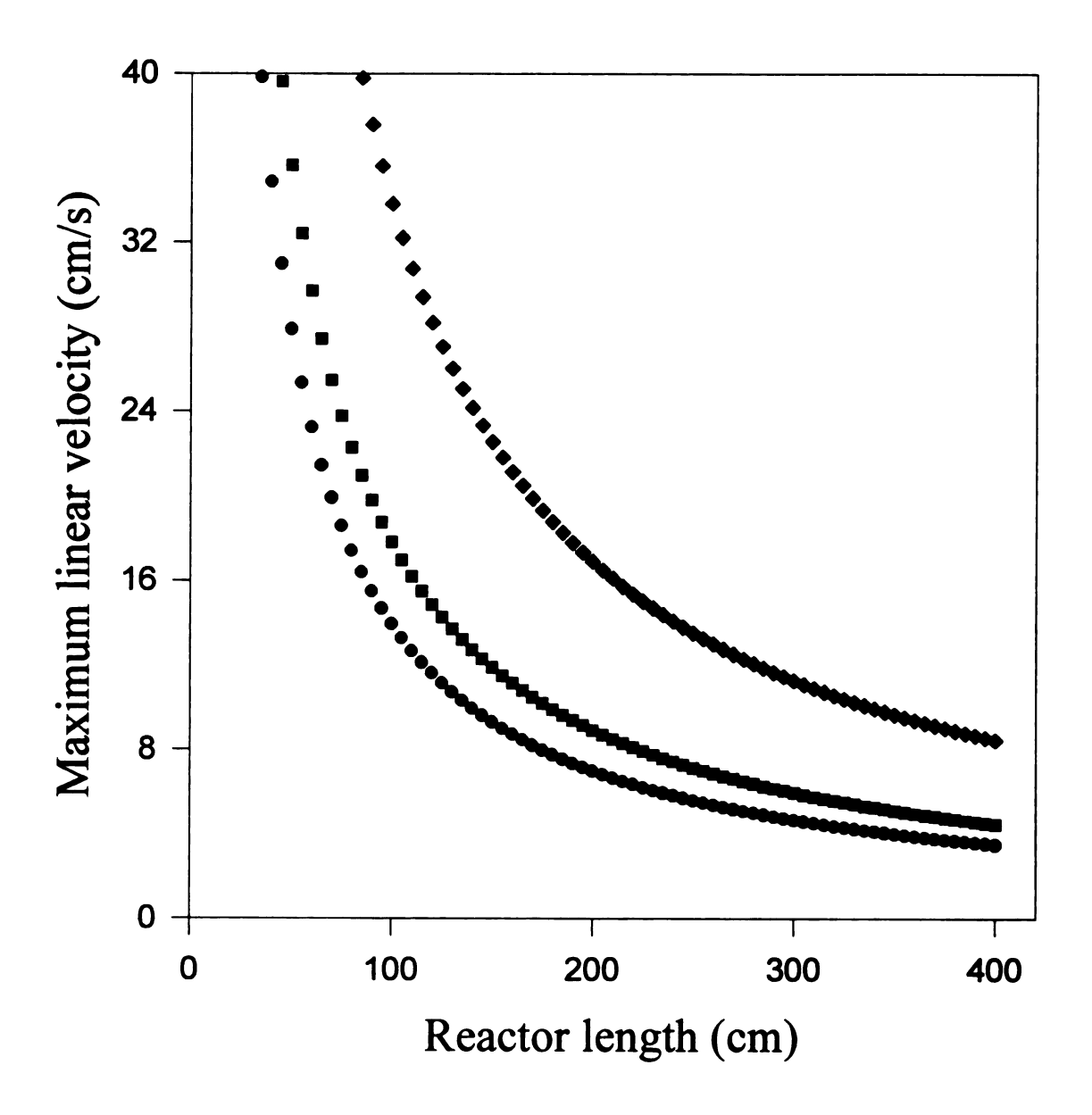


Figure 3.6a. Calculated maximum linear velocity plotted as a function of reactor length using both the peristaltic pump and the syringe pump with various syringe sizes. The maximum change in pressure employed for the calculations involving the peristaltic pump (•) was 7.9 bar. The pressure changes employed for the 10cm³ (•), 5 cm³ (•), and 3 cm³ (•) syringes were 7.9, 10.1, and 19.2 bar respectively.

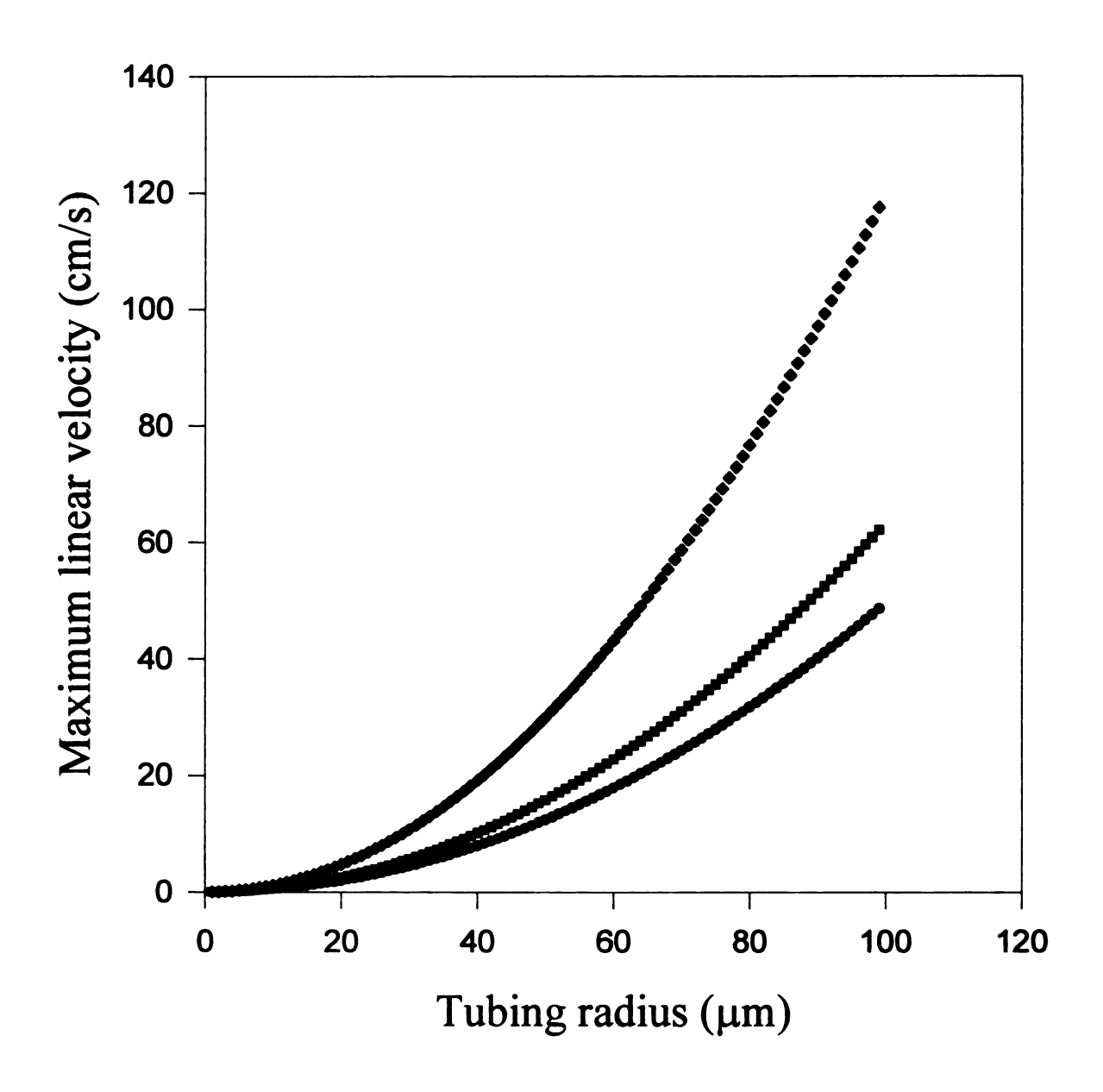


Figure 3.6b. Calculated maximum linear velocity plotted as a function of tubing radius using both the peristaltic pump and the syringe pump with various syringe sizes. The maximum change in pressure employed for the calculations involving the peristaltic pump (•) was 7.9 bar. The pressure changes employed for the 10cm^3 (•), 5 cm^3 (•), and 3 cm^3 (•) syringes were 7.9, 10.1, and 19.2 bar respectively.

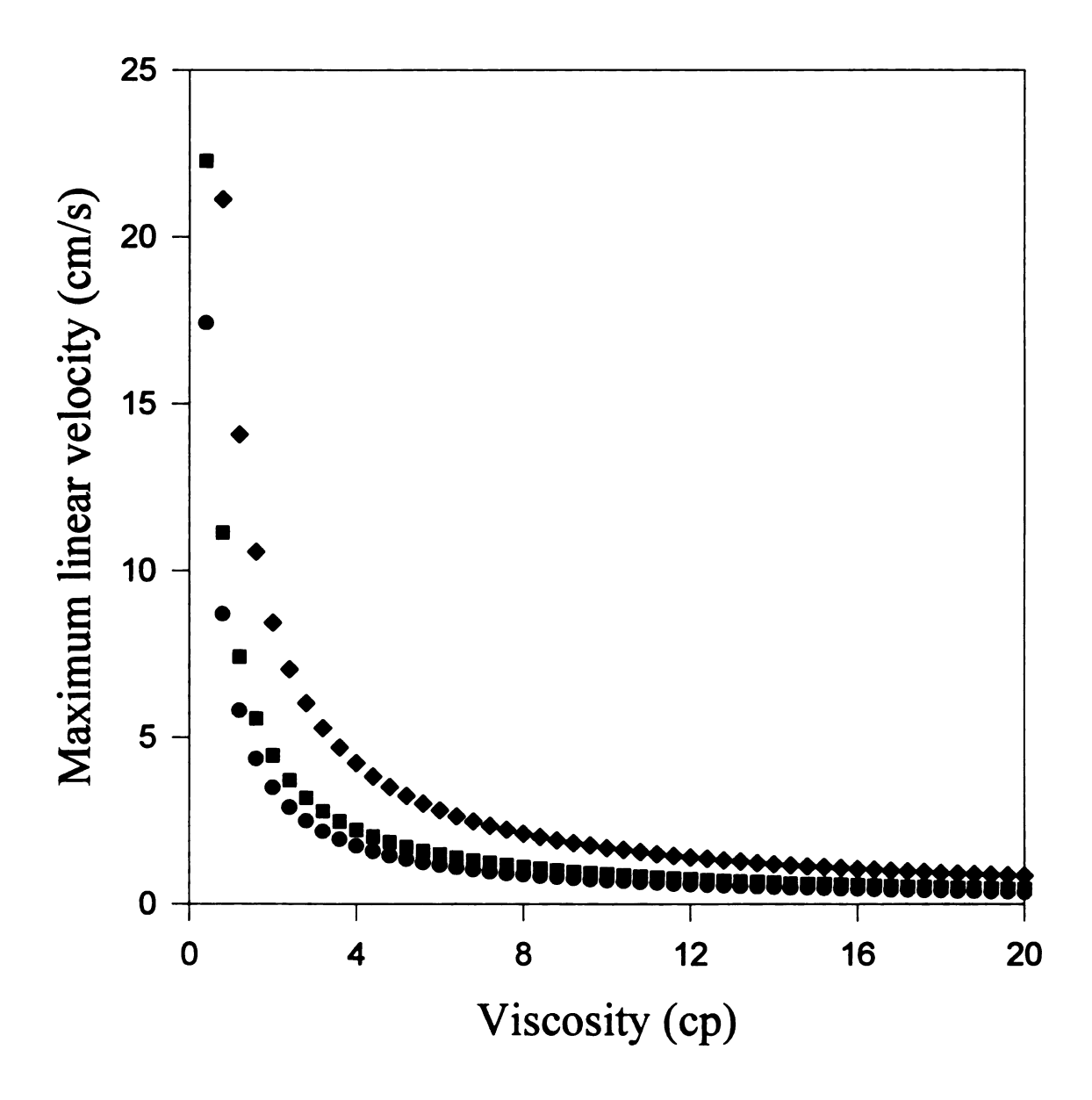


Figure 3.6c. Calculated maximum linear velocity plotted as a function of solution viscosity using both the peristaltic pump and the syringe pump with various syringe sizes. The maximum change in pressure employed for the calculations involving the peristaltic pump (•) was 7.9 bar. The pressure changes employed for the 10cm³ (•), 5 cm³ (•), and 3 cm³ (•) syringes were 7.9, 10.1, and 19.2 bar respectively.

Thus, various pretreatment steps of certain samples may not be possible with conventional peristaltic pumps or syringe pumps.

3.2.4 Reproducibility of Pumping Mechanisms

The reproducibilities of the peristaltic and syringe pumps were investigated in two manners. First, a dye was repeatedly injected into a borate buffered stream at various flow rates and the reproducibility in peak height was measured. We have previously shown⁸ that at a linear velocity of 2 cm s⁻¹, the standard deviation in peak height of the injected dye is approximately 1%. Table 3.2 shows the reproducibility at various pressures obtained by simply increasing the velocity and calculating the pressure drop across the capillary. The linear flow rate was calculated by injecting the phenol red dye into a reactor of 175 cm and measuring its residence time. The residence time was then divided by the reactor length and substituted back into equation 3.1. As shown, the peristaltic pump exhibits excellent reproducibility right up to its pressure output boundary. From a practical standpoint, the syringe pump pressure reproducibility is not as good. This is because the syringe pump seems to require more time to equilibrate after the flow rate is changed. Thus, reproducibility may be sacrificed for speed of analyses using a syringe pump if flow gradients or frequent flow rate changes are employed. When the pump was allowed to equilibrate for about 5 minutes between flow rate changes, the reproducibility approached 1.0% and these data are also shown in table 3.2.

In a second method, we chose to demonstrate pump reproducibility with the widely used enzymatic reaction for the determination of glucose¹¹. Since this reaction can require in excess of 15 minutes to reach steady state at room temperature, it would allow

Table 3.2. Reproducibility of the pressure output using the peristaltic and syringe pumps at varying pressures.

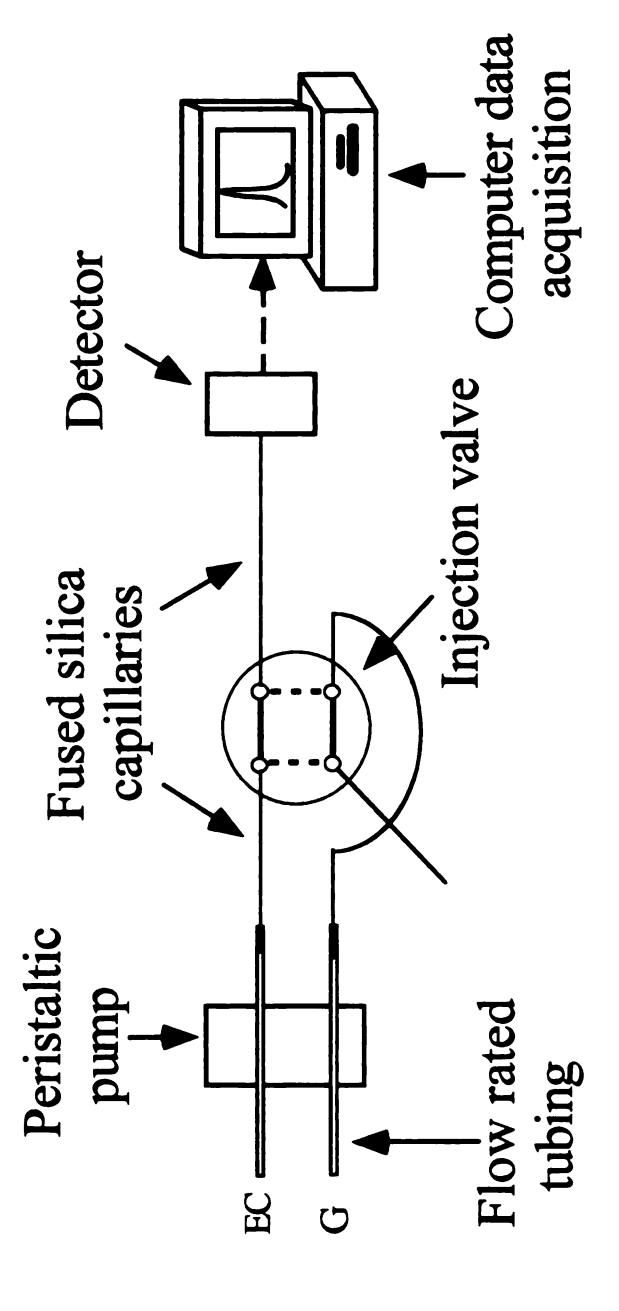
	RSD^d	9.0	1.0	1.2	1.7
Syringe ^a	% RSD°	5.5	0.9	8.9	6.7
	Pressure drop (bar) ^b % RSD ^c	4.5	7.6	13.5	18.2
<u>Peristaltic</u>	% RSD	6.0	1.2	1.3	1.4
	Pressure drop (bar) ^b	1.5	3.8	4.7	6.3

^a Syringe volume = 3.0 cm^3 .

^b Average of 3 injections of dye.

^c Percent relative standard deviation of pressure output when not giving the syringe pump time to equilibrate.

^d Percent relative standard deviation of pressure output after the syringe pump was allowed time to equilibrate.



tubing to the switching valve is about 15-20 cm. The length of the reactor Schematic of manifold employed for the enzyme-catalyzed determination of glucose. The distance of the fused silica capillary from the flow rated was 400 cm. EC = enzyme composite reagent, G = glucose sample. **Figure 3.7.**

for longer reaction periods to be employed. The basic configuration for this determination is shown in figure 3.7. No mixing tee was employed in this study (further studies of mixing efficiencies are reported in chapter 5 where a comparison of the extent of mixing is made between a conventional and capillary FI system). Figure 3.8 shows the data obtained from this determination while employing a 400 cm capillary reactor. Since the reaction is not yet complete when the absorbance measurement is made, each peak represents product formed after a fixed reaction time. The reaction periods for the various glucose standards shown are $1.65 \pm .01 \text{ cm s}^{-1}$. The correlation coefficient between concentration and peak absorbance is 0.996, thus it is clearly evident that the peristaltic pump is capable of delivering reagents from run-to-run in a reproducible fashion.

3.3 CONCLUSIONS

Results of an investigation of pressure in a capillary flow injection (CFI) system have been presented. Three different types of pumps, namely dual piston, peristaltic, and syringe were used to drive reagents through a manifold employing fused silica capillaries (75 μ m i.d.) as the reactor tubing. A comparison of pressure capabilities, baseline noise levels and reproducibility was performed. The maximum stable pressure for the peristaltic pump and syringe pump were 7.6 and 19.2 bar, respectively. The maximum stable pressure for the syringe pump varies with the inner radius of the syringe. The reproducibilities of the peristaltic pump and syringe pump were measured in two manners. First, the reproducibility is reported as the percent relative standard deviation of the ΔP for repetitive injections of a dye into a buffered stream. For the peristaltic pump, the percent relative standard deviation was less than 2.0%, while the syringe pump reproducibility

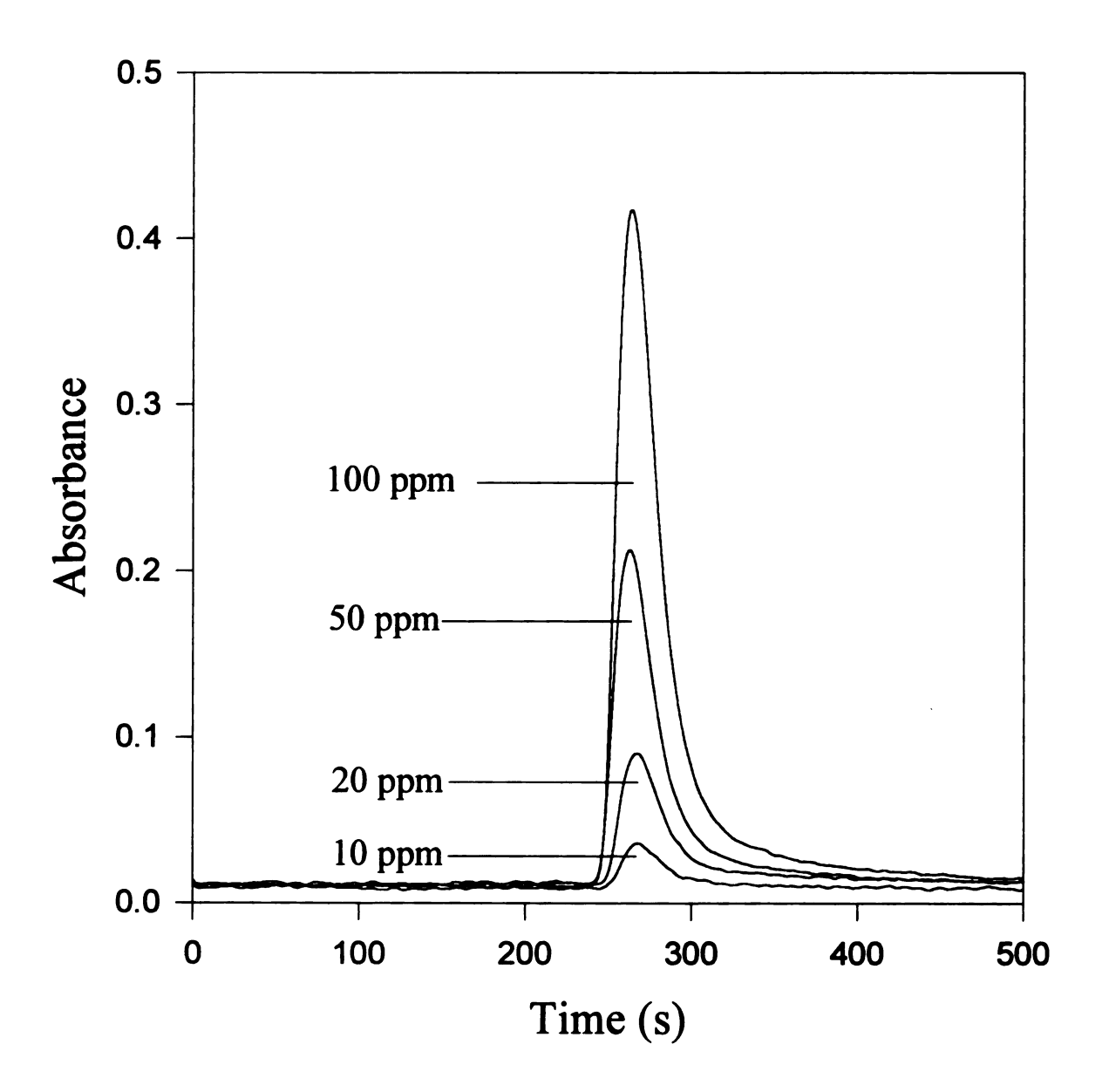


Figure 3.8. Absorbance measurements as a function of glucose concentration. The measurements were made at a wavelength of 540 nm. The correlation coefficient between the peak height and the glucose concentration is 0.996.

was between 6.0% and 10%. The syringe pump reproducibility is poorer because it takes more time to equilibrate upon flow rate changes. Secondly, an enzyme catalyzed reaction was allowed to react for periods of up to 4 minutes with residence times of 242 ± 1 s. The dual piston pump investigated was not capable of delivering the required volumetric flow rates in the μ L min⁻¹ range. Each pump, except for the dual piston pump, showed baseline noise levels of less than 5 milliabsorbance units. Based on these observed values, practical considerations for designing CFI manifolds are also reported.

Although the peristaltic and syringe pumps employed in this study are reproducible, we believe that in order to fully realize the potential benefits of capillary flow injection systems, a definite improvement in pumping technologies will be required. Although the peristaltic pump does seem to be reproducible over its entire range of achievable flow rates, the range itself is limited. For example, using a 100 cm reactor (75 μm i.d.) in order to obtain reproducibility data, the lowest velocity attainable was roughly 1 cm s⁻¹ corresponding to a flow rate of 2.65 μL min⁻¹. The reason the pump could not attain lower flow rates had nothing to do with its stability or reproducibility, but rather because the lowest pump setting was employed. A restrictor would have been used to further reduce the flow rate, but this was deemed unnecessary for this study. As mentioned earlier in this work, there will undoubtedly be a need for pumping mechanisms capable of delivering volumetric flow rates lower than 10 μL min⁻¹ at pressures of greater than 35 bar.

List of References

- 1. Ruzicka, J.; Hansen, E.H.; Anal. Chim. Acta 1984,161, 1.
- 2. Ruzicka, J.; Anal. Chem. 1983, 55, 1040A.
- 3. Ruzicka, J.; Hansen, E.H. Flow Injection Analysis, Wiley, NY, 1988.
- 4. Liu, S.; Dasgupta, P.K. Anal. Chim. Acta 1992, 268, 1.
- 5. Liu, S.; Dasgupta, P.K. Anal. Chim. Acta 1993, 283, 739.
- 6. Mizuno, T; Akiyama, J.; Tsuda, T. Anal. Chem. 1987, 59, 799.
- 7. Dasgupta, P.K.; Liu, S. Anal. Chem. 1994, 66, 1792.
- 8. Spence, D.M.; Sekelsky, A.M.; Crouch, S.R. *Instrum. Sci. and Tech.* 1996, 24, 104.
- 9. Spence, D. M., Crouch, S. R. Quim. Anal., 1996, 15, 296.
- 10. Patton, C.J.; Ph.D. Thesis, Michigan State University, East Lansing, MI, 1982.
- 11. Raba, J.; Mottola, H.A. CRC Crit. Rev. Anal. Chem. 1995, 25, 1.

Chapter 4

Factors Affecting Zone Variance in a Capillary Flow Injection System

Because modern peristaltic pumps appeared to have the necessary stability at low flow rates we decided to investigate the characteristics of capillary FI with conventional peristaltic pumping. Conventional pumping maintains the simplicity that is so characteristic of FI systems and avoids many of the complications introduced by an electroosmotic flow-driven system (e.g., pH and ionic strength requirements, high voltage isolation). The objective of this work was to attempt to identify and characterize the major contributors to the overall zone dispersion in a capillary FI system and to compare these results with those of a conventional FI system. In particular, we were interested in the reduced dispersion that could be achieved in pump-driven capillary systems with internal diameters of less than $100~\mu m$. The limiting sources of peak variance are identified and used to specify improvements to be made in second generation capillary FI systems.

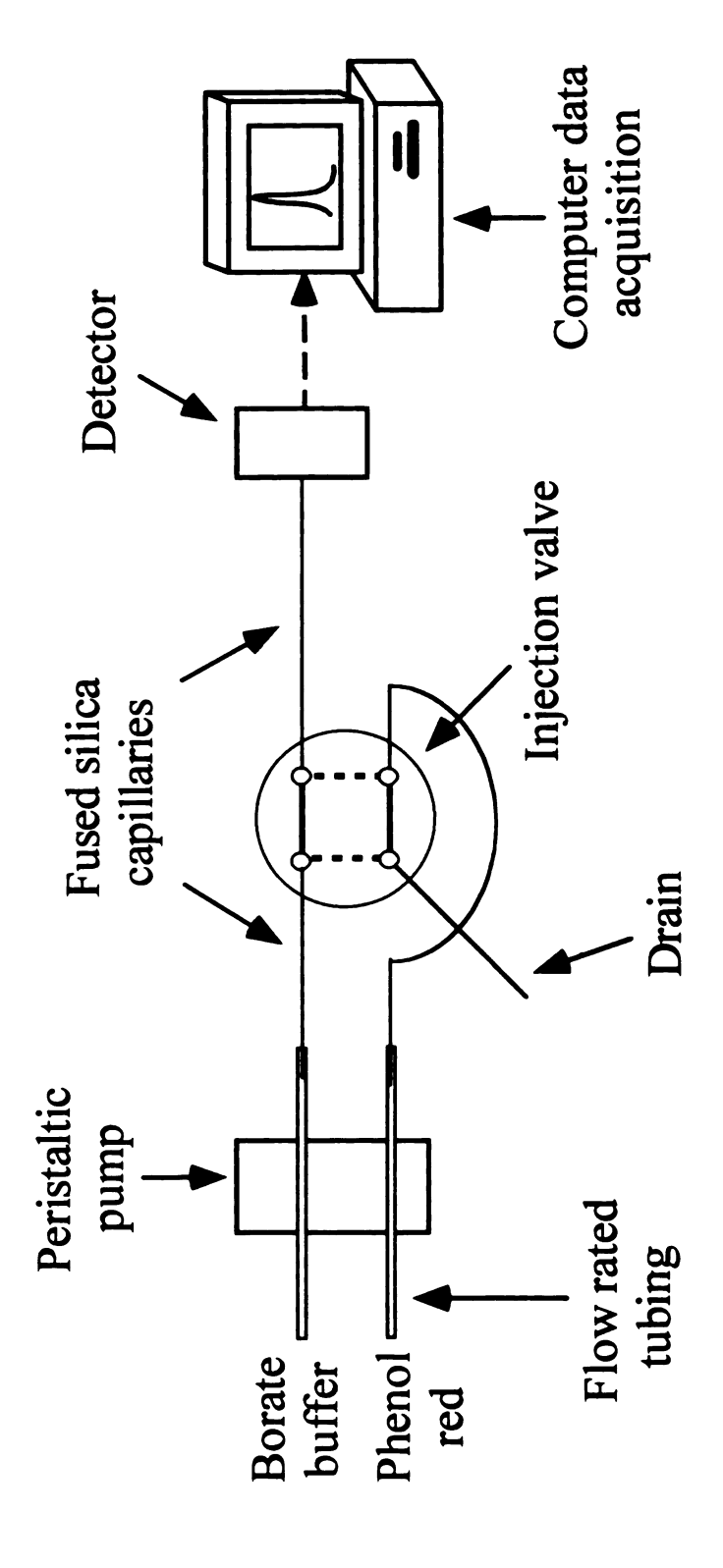
4.1 EXPERIMENTAL SECTION

4.1.1 Pumping Mechanism

The modified peristaltic pump described in chapters 2 and 3 was used in this study. The pump consisted of 16 rollers and used flow rated tubing with an inside diameter of $190 \ \mu m$.

4.1.2 Injection Process

The injector as well as the methods used to adapt the fused silica capillaries to the valve are described in chapter 2. The adaptation of the capillary is shown in figure 2.2 while the method of injection is shown in figures 2.5a-c, respectively. Figure 4.1 shows the manifold used for the dispersion studies. In figure 4.1, the sample and reagent streams are shown flowing to waste and to the detector, respectively. The valve is then switched, as depicted by the dashed lines, using a computer-controlled pneumatic actuator for a preselected period of time. The switching of the valve is fast enough that it does not affect the dispersion process. This was shown by employing different lengths of flow rated tubing between the pump rollers and the capillary and noting that there was no change in the peak height or width of the response signal absorbance. The valve was typically left in the inject mode for periods ranging from 5-20 seconds, which, at a linear velocity of 2.0 \pm 0.1 cm s⁻¹, resulted in typical injection volumes of 300 nL to 1.2 µL for the capillary system and 20 to 80 µL for the conventional flow injection system. When the valve is switched back to its original position, the reactor contains a sample zone which is carried to the detector. To ensure that sample volumes were precise for the variance studies, the peak areas were also determined and are reported.



and flow cell. Fused silica tubing is used at the pump since it can be inserted into the small bore flow rated tubing. Figure 4.1. Manifold used for capillary FI. The PEEK reactor is used since it is easier to adapt to the valve

4.1.3 Tubing

For the capillary FI system, fused silica tubing with an inside diameter of 75 μ m was used to deliver the reagents into the switching valves and to act as the waste line. The reactor tubing, made of polyetheretherketone (PEEK), was 64 μ m i.d. The PEEK tubing, with an outside diameter of 1/16" was used for the reactor since it is much sturdier than the fused silica tubing. In addition, typical HPLC and FI fittings can be used to connect the PEEK tubing to the injector and flow cell. For the conventional FI system, Teflon tubing with an inside diameter of 0.5 mm was employed as the reactor tubing.

4.1.4 Flow Cells

Flow cells were made in-house and ranged in volume from 320 nL up to 2.2 μ L. In order to achieve various volumes, internal sleeves with inside diameters of 0.008" up to 0.021" were used. The design of these flow cells is described in chapter 2.

4.1.5 Reagents

Preparation of the phenol red solutions as well as the borate buffer used as the carrier reagent is described in chapter 2.

4.1.6 Procedures for Dispersion Studies

Characterization of physical dispersion was done by injecting a dye into a buffer solution with no reaction occurring. Dispersion of the phenol red dye was investigated using reactor tubing lengths ranging from 50 cm to 400 cm. Within each system (capillary and conventional), equal-volume injections of the working solution of phenol red were made as indicated by equal areas of the detected peaks. For reactor length effects, approximately 1 µL was injected into the capillary system, while in the conventional

300, and 400 cm, these injection volumes resulted in reactor-to-sample volume ratios of approximately 1.6, 3.2, 6.4, 9.6 and 12.8, respectively, for both systems. Injection and flow cell volume effects on dispersion were also investigated. For injection effects injections were made such that the peak area ranged from 6 to 12 absorbance units • s for both the capillary and conventional systems. For the capillary systems, this corresponds to injection volumes of 330 nL to 700 nL, while in the conventional system the reported areas correspond to injection volumes from 30 μ L to approximately 60 μ L. The linear velocity for both reagent and samples streams was 2.0 ± 0.1 cm s⁻¹ for all studies reported here. Detection of the injected dye was performed using a filter colorimeter² at a wavelength of 540 nm.

The variance values were obtained in triplicate from a 4-parameter fit to an exponentially modified Gaussian³⁻¹⁰ equation, by means of a curve-fitting program (Peakfit, Jandel Scientific). The four parameters returned from the fit are area (a_0) , centroid (a_1) , width (a_2) and distortion (a_3) . The standard error of the fits was typically less than 2%. The variance or second moment, σ^2 of an eluted zone can then be estimated from these parameters as shown in equation 4.1.

$$\sigma^2 = a_2^2 + a_3^2 \quad (4.1)$$

4.2 RESULTS AND DISCUSSION

4.2.1 Studies of Dispersion

Figure 4.2 shows the responses for phenol red as a function of reactor length for the capillary FI system. Some increase in dispersion with reactor length can be seen. The base width of the peak using the 50 cm reactor is ~75 s while that of the 400 cm reactor is

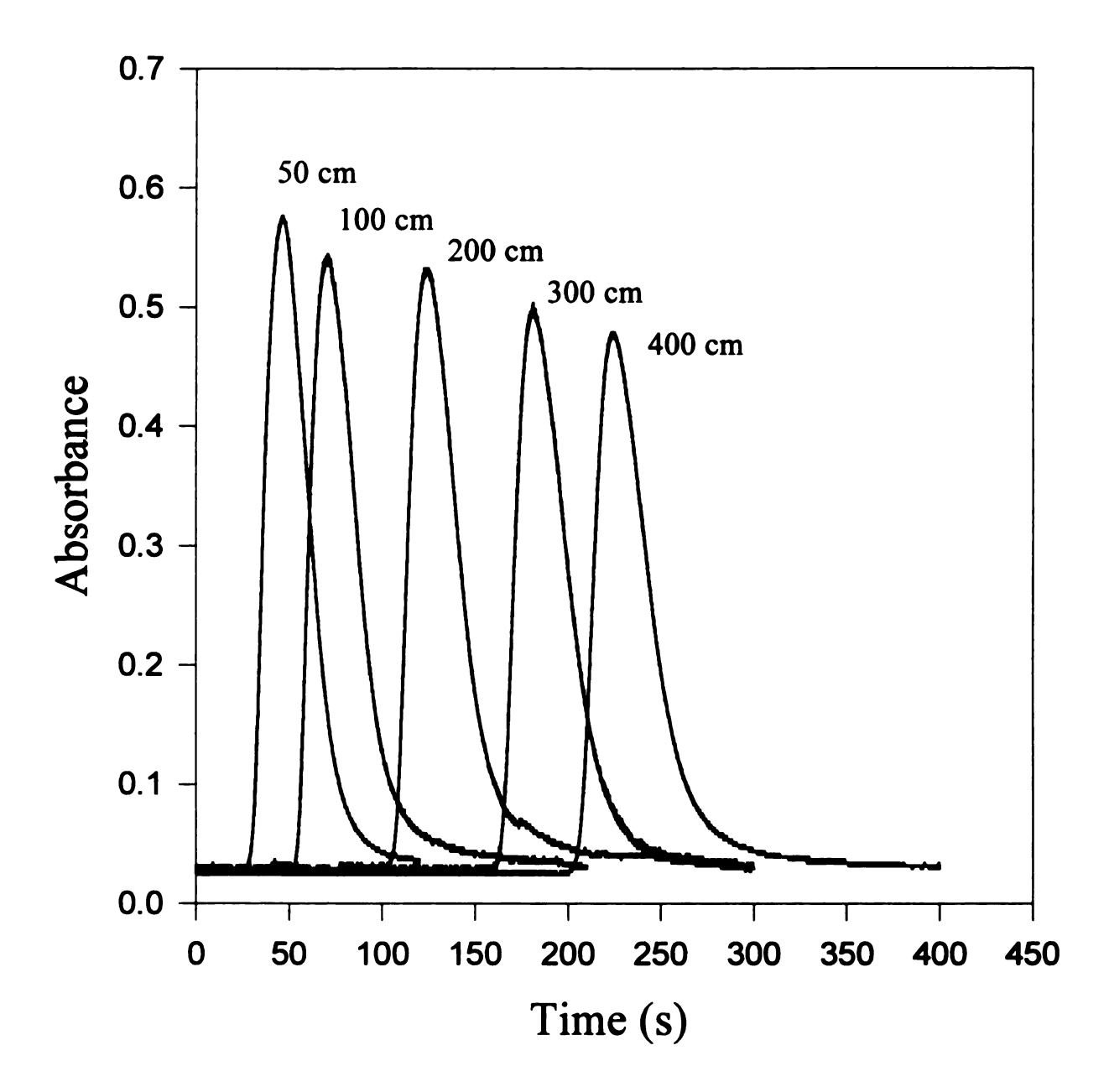


Figure 4.2. Response signals obtained with the capillary FI system by injecting 5 x 10⁻⁵ M solutions of phenol red into buffer flowing at 2 cm s⁻¹ with various lengths (in cm) of 0.064 mm i.d. reactors.

~ 100 s. In addition, the peak height decreases with reactor length by about 15% in going from the 50 cm reactor to the 400 cm reactor. The lower dispersion of the capillary system is apparent when the data in figure 4.2 are compared with those in figure 4.3, which is the same experiment using conventional 0.5 mm i.d. tubing. In figure 4.3, the base width of the 50 cm peak is about 75 s while that of the 400 cm reactor is 150 s. Also, using the conventional 0.5 mm i.d. tubing, the peak height decreases by 40% over the range of reactor lengths used. In order to demonstrate the increased sensitivity of the capillary FI system, the peaks obtained using the 400 cm reactors for both capillary tubing and conventional tubing are compared in figure 4.4. Here, the marked increase in dilution of the sample using the conventional system is evident by the decrease in peak height and the increased width of the peak. The decrease in dispersion of the sample plug in the capillary system can be directly attributed to the decrease in diameter of the tubing, since the amount of dispersion in a system utilizing open tubular columns or reactors should be directly proportional to the square of the tubing radius^{1,11,12}. Thus, a tenfold decrease in tubing radius should result in a 100-fold decrease in sample dispersion. However, since the observed decrease in dispersion is lower than predicted, there must be other factors affecting the overall variance of the peak.

4.2.2 Determination of the Zone Variance

Various studies¹³⁻¹⁵ have shown that the total time variance for a flow injection or chromatography peak can be described as

$$\sigma_{tot}^2 = \sigma_{rc}^2 + \sigma_{ex}^2 \tag{4.2}$$

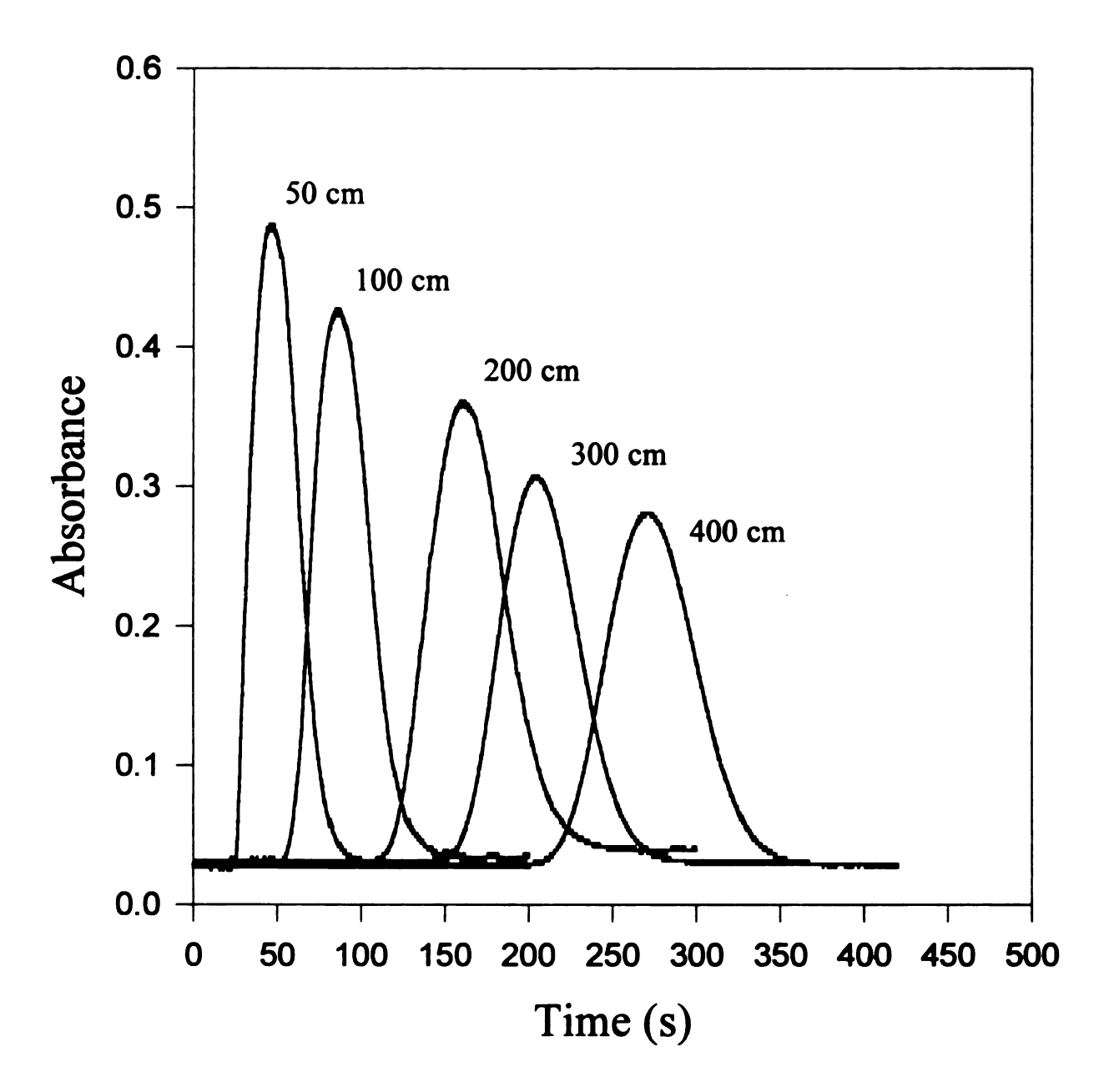


Figure 4.3. Response signals obtained with the conventional FI system by injecting 5 x 10⁻⁵ M solutions of phenol red into buffer at 2 cm s⁻¹ with various lengths (in cm) of 0.50 mm i.d. reactors.

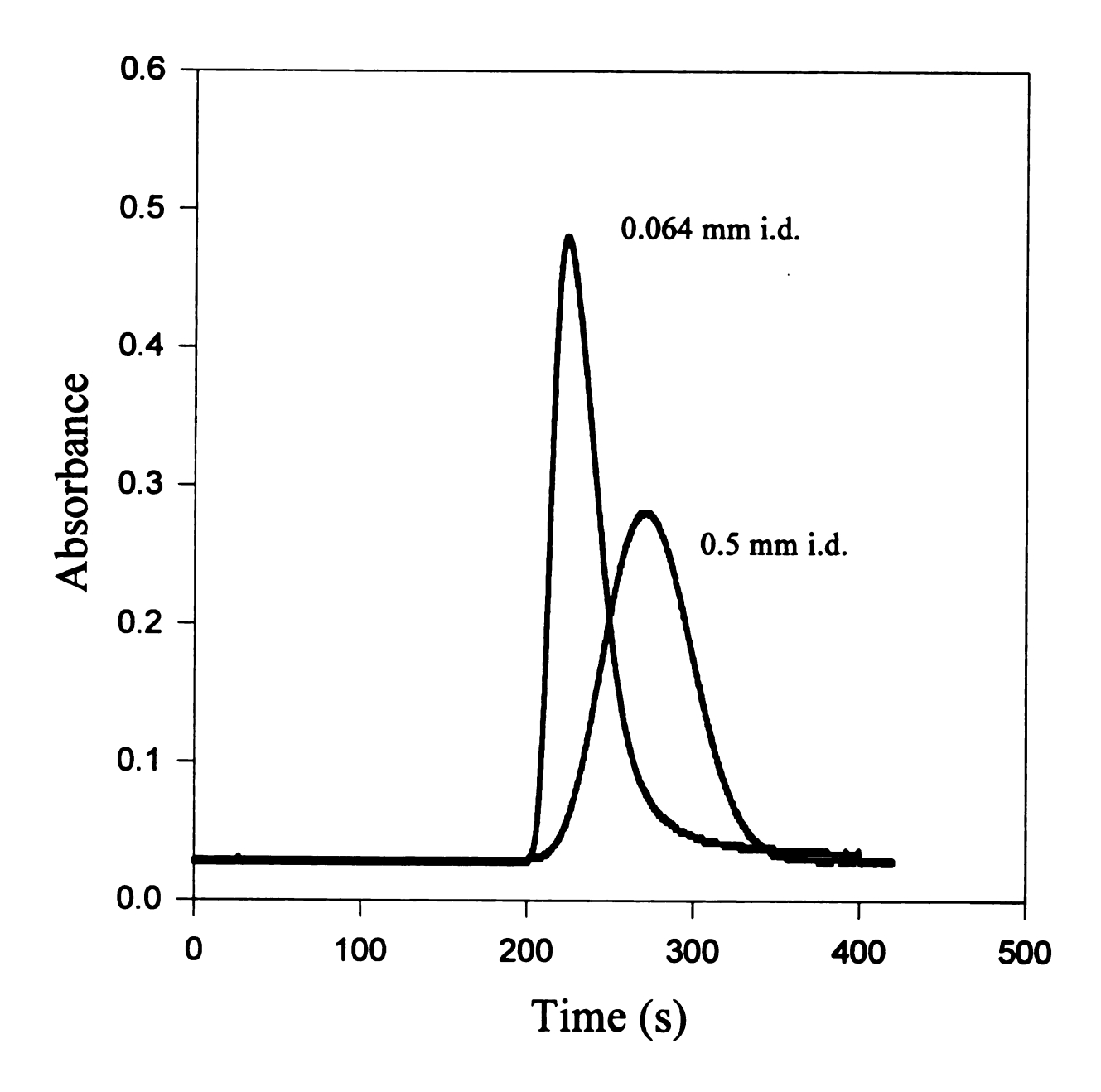


Figure 4.4. Response signals obtained with 400 cm reactors of capillary tubing and conventional tubing. The maximum absorbance obtained with the capillary FI system is nearly twice that with the conventional FI system.

where σ_{tot}^2 is the total time variance, σ_{rc}^2 is the time variance due to the reactor or column itself and σ_{ex}^2 is the time variance due to extra-column effects 16-18 such as injection and detection. This latter variance can be written in more detail as

$$\sigma_{ex}^2 = \sigma_{con}^2 + \sigma_{fc}^2 + \sigma_{inj}^2 \qquad (4.3)$$

where σ_{con}^2 is the time variance due to any connections such as fittings or mixing tees, σ_{fc}^2 is the time variance arising from the flow cell or detection system, and σ_{inj}^2 is the time variance due to the sample volume injected. It was noted in our studies that the variance due to connections, σ_{con}^2 , was negligible in all cases in comparison to variance due to injection and detection processes. Thus, in order to characterize the leading contributors to peak variance in the FI systems, a more thorough study involving injection volumes and flow cell volumes was undertaken. For the capillary system, figure 4.5 shows the effect of injection volume (proportional to peak area) on peak shape, whereas figure 4.6 shows the effect of changing flow cell volumes. These data clearly provide evidence that peak variance is not only a function of reactor length, but it is also a function of injection volume and flow cell volume. In order to determine the amount of variance due to the reactor, injector and detector, one may use estimation methods 19,20 or measurement methods²¹⁻²⁶. Though there are errors associated with both methods²⁷, we chose to use the direct measurement method to estimate the variance from each of the processes shown in equation 4.4.

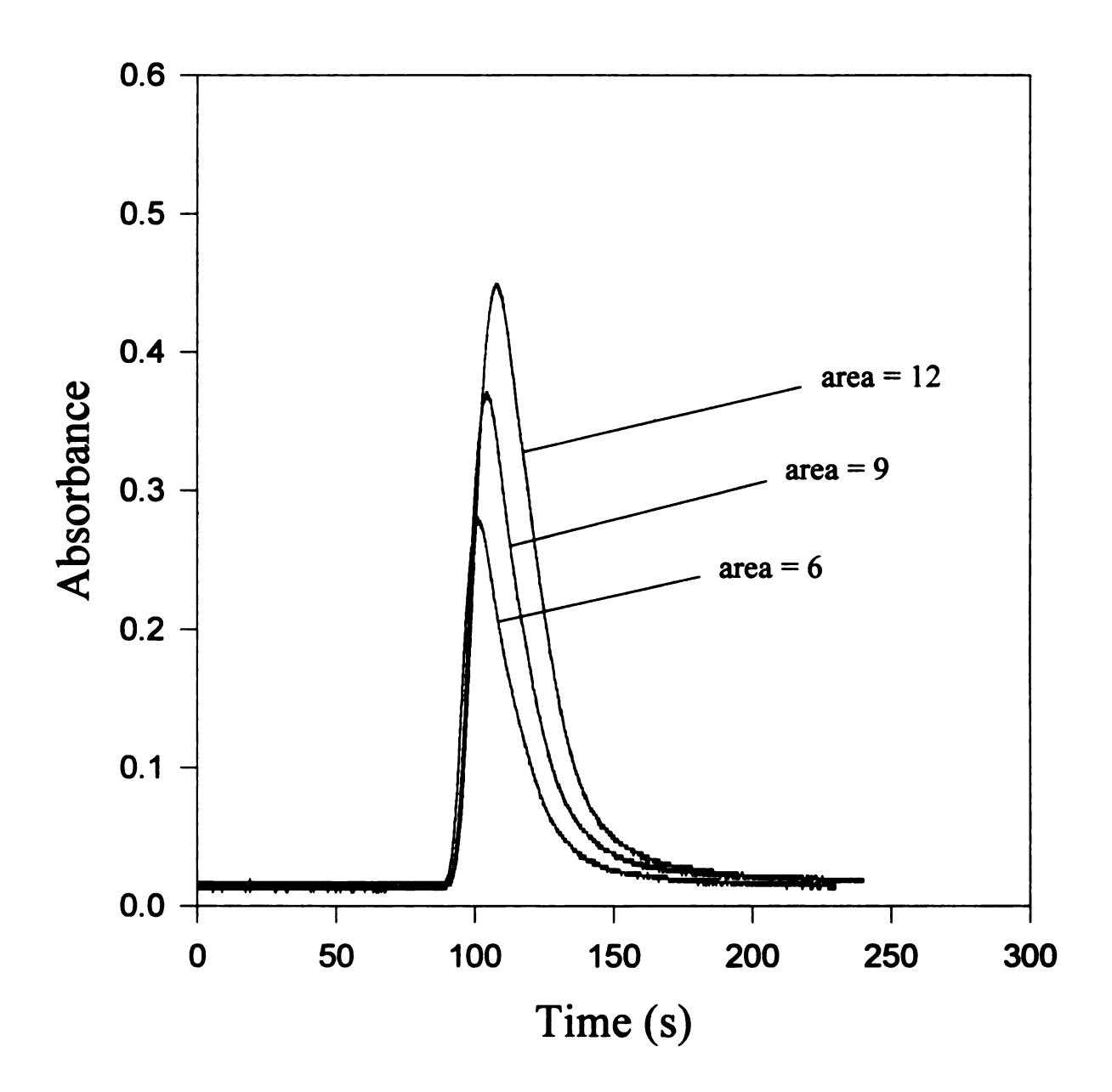


Figure 4.5. Response signals obtained with the capillary FI system as a function of the volume of sample injected (proportional to peak area). The sample volumes represented by the three curves are 720 nL (area = 6), 1.0 μ L (area = 9), and 1.25 μ L (area = 12).

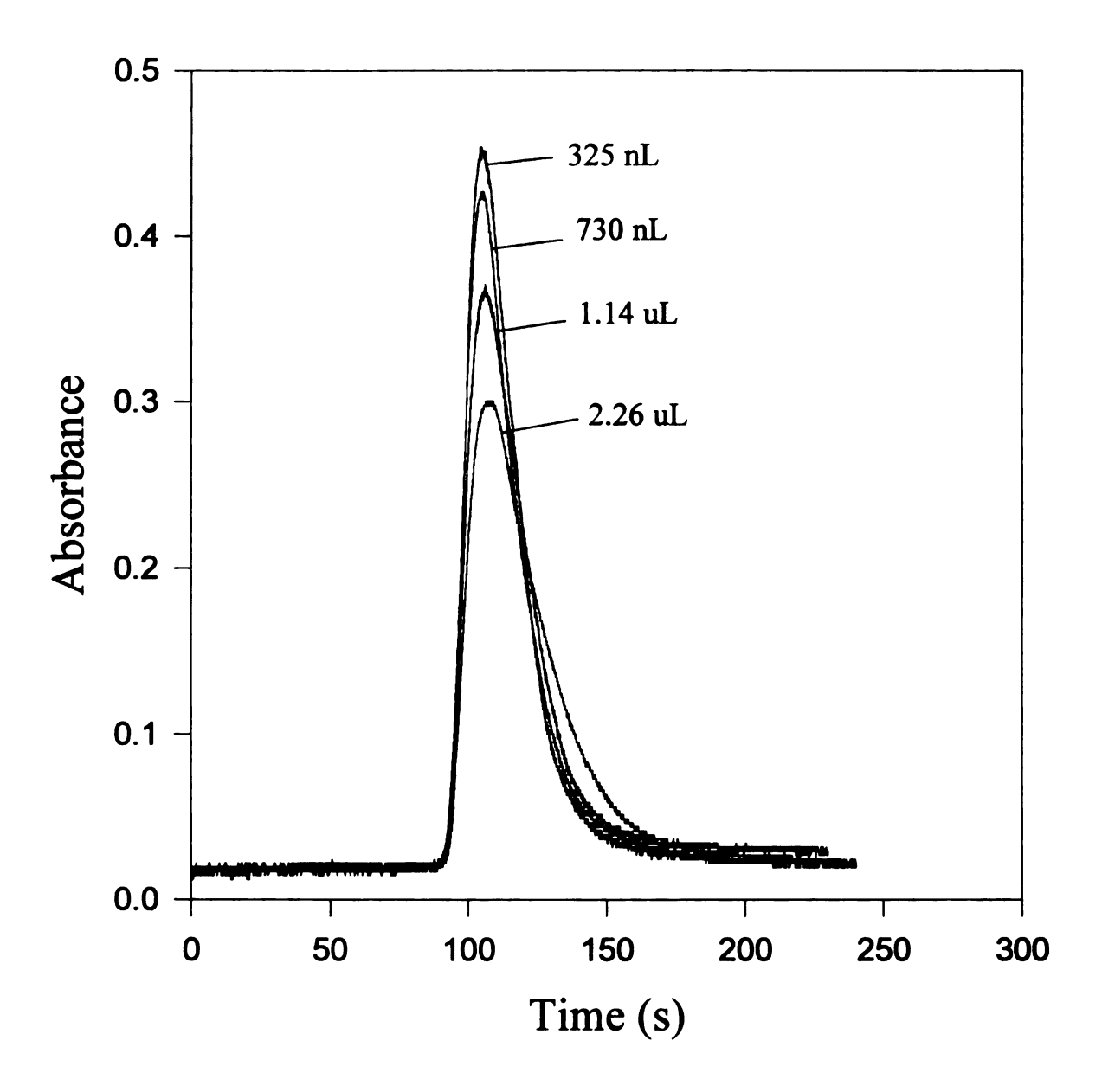


Figure 4.6. Response signals obtained with the capillary FI system as a function of flow cell volume. The flow cell volume was varied by inserting PEEK sleeves of varying i.d., thus, the path length for each volume studied was identical (1 cm). The areas under each curve are equal (± 1%).

To separate these effects, consider the total variance to be given by equations 4.2 and 4.3 with σ_{con}^2 negligible

$$\sigma_{tot}^2 = \sigma_{rc}^2 + \sigma_{inj}^2 + \sigma_{fc}^2 \qquad (4.4)$$

At a constant linear velocity we can assume that, for small changes, zone variance is a linear function of the variance due to reactor length, injection volume or flow cell volume. By extrapolating to zero length or volume, the contribution of each variance source described in equation 4.4 can be determined. The results of such measurements are presented in table 4.1. When zone variance versus reactor length is plotted, for example, the y intercept (reactor length of 0 cm) represents the peak variance due to the volume injected and the flow cell. If the variance is plotted versus peak area, the y-intercept (where the volume injected is 0 μ L) is the variance due to the reactor and flow cell. Likewise, the y-intercept in a plot of variance versus flow cell volume represents the variance due to the reactor and injection processes.

The three intercepts obtained can be arranged as

$$(\sigma_{tot}^2)_1 = \sigma_{inj}^2 + \sigma_{fc}^2 \tag{4.5}$$

$$(\sigma_{tot}^2)_2 = \sigma_{rc}^2 + \sigma_{fc}^2 \tag{4.6}$$

$$(\sigma_{tot}^2)_3 = \sigma_{rc}^2 + \sigma_{inj}^2 \tag{4.7}$$

Equations 4.5-4.7 can be solved simultaneously to give the individual variance contributions as presented in table 4.2, which also compares the major contributors of

Table 4.1. Regression analyses for the capillary and the conventional FI system*

Conventional FI system	L 2	0.9959 0.9995 0.9999
	intercept ^b	166 ± 13 241 ± 6 359 ± 5
	slope	1.39 8.39 23.1
tem	I ² 2	0.9951 0.9993 0.9919
Capillary FI syster	intercept	204 ± 6 195 ± 2 172 ± 6
	slope	0.60 6.39 80.9
	Variance vs.	Reactor length Sample volume Flow cell volume

* uncertainties are standard errors for the intercepts obtained from the regression

* slope is in units of s² cm¹, s² µL¹, and s² µL¹ for the reactor, sample volume and flow cell volume, respectively

^b intercept units are s²

Table 4.2. Major contributors to peak variance in a conventional and a capillary FI system*

Capillary FI	28 ± 2 40 ± 3 32 ± 2
Conventional FI	40 ± 12 6 ± 2 60 ± 17
Percentage of zone variance due to:	injection detection reactor

*uncertainties are standard deviations in the percentages.

peak variance for the capillary system to a conventional system. As can be seen, much of the variance in the capillary FI system is due to extra-column effects. For this reason, results do not show as large an improvement with a decrease in tubing radius as expected. Despite this fact, the efficiency of FI is still enhanced. For example, when using the Fe²⁺/1,10-phenanthroline reaction for the determination of Fe²⁺, we have performed up to 500 injections hr⁻¹ using the capillary FI system as opposed to 360 injections hr⁻¹ when a conventional system is employed. In addition, when using the Fe²⁺/1,10-phenanthroline reaction, absolute detection limits in the femtomole range have been achieved with the capillary FI systems, a value almost 50 times lower than a conventional FI system. The system configuration used in this study was very similar to that shown in figure 4.1. The iron sample was simply injected via the 4-port switching valve into a continuously flowing stream of buffered 1,10-phenanthroline at 6 cm s⁻¹. The reactor length was 30 cm, while the injection volume was approximately 260 nL. Obviously this is a very fast reaction and not much residence time is required to obtain a product response signal.

The reduced amount of dispersion due to the reactor should allow for slower reactions to be now studied in FI. Chapter 3 described the enzyme-catalyzed reaction conversion of glucose to glucose oxidase. By optimizing such a system, it may not be necessary to employ stopped flow methods^{1,28,29} for certain determinations. However, if stopping the flow is required, capillary stopped flow injection will still have advantages such as minimal sample and reagent usage and less generated waste. We have already shown that a multiple line capillary FI system employing mixing tees and multiple valves can be implemented for stopped flow determinations²⁹. Results of this study are shown in chapter 6.

4.3 CONCLUSIONS

Dye dispersion studies have been reported to characterize zone variance in a capillary flow injection system. Variance sources were compared with similar sources in a conventional flow injection system. The inside diameters of the reactors in the capillary and conventional system were 64 µm and 0.5 mm, respectively. In both systems, reactor length, detector flow cell volume, and injection volume are the major contributors to the total zone variance. The individual contributions of each variance source were determined. Results show that in a single line capillary system, the majority of the peak variance is due to extra-column effects. However, in the conventional system, the reactor was found to be the major contributor to the overall zone variance.

Major improvements in this CFI system are still obtainable by reducing the extracolumn effects. By lowering the detection volume, either by new flow cell designs, oncolumn detection, or a capillary Z-cell³⁰, the dispersion should be reduced substantially. If the flow cell volume is reduced, the injection volume can also be reduced simultaneously. Therefore, in a capillary flow injection system, it may be possible to inject volumes in the pL range with minimal dispersion which should dramatically improve sample throughput.

List of References

- 1. Ruzicka, J.; Hansen, E.H. Flow Injection Analysis, Wiley, New York, 1988.
- 2. Patton, C.J. Ph.D. Thesis, Michigan State University, East Lansing, MI, 1982.
- 3. Schmauch, L.J. Anal. Chem. 1959, 31, 225.
- 4. Johnson, H.W.; Stross, F.H. Anal. Chem. 1959, 31, 357.
- 5. Grushka, E. Anal. Chem. 1972, 44, 1733.
- 6. Barber, W.E.; Carr, P.W. Anal. Chem. 1981, 53, 1939.
- 7. Foley, J.P.; Dorsey, J.G. Anal. Chem. 1983, 55, 730.
- 8. Anderson, D.J.; Walters, R.R. J. Chromatogr. Sci. 1984, 22, 353.
- 9. Delley, R. Anal. Chem. 1985, 57, 388.
- 10. Hanggi, D.; Carr, P.W. Anal. Chem. 1985, 57, 2394.
- 11. Taylor, G. Proc. Roy. Soc. (London), 1953, 219A, 186.
- 12. Aris, R. Proc. Roy. Soc. (London), 1956, 235A, 67.
- 13. Evans, C.E.; McGuffin, V.L. Anal. Chem. 1988, 60, 573.
- 14. Evans, C.E. Ph.D. Thesis, Michigan State University, East Lansing, MI, 1990.
- 15. Brooks, S.H., Leff, D.V., Hernandez Torres, M.A., Dorsey, J.G. *Anal. Chem.* **1988**, *60*, 2737.
- 16. Sternberg, J.C. in *Advances in Chromatography*; Giddings, J.C.; Keller, R.A. Eds.; 1966; Vol. 2, pp. 205-270.
- 17. Kirkland, J.J. J. Chromatogr. Sci. 1969, 7, 7.

- 18. Halasz, I.; Walking, P. J. Chromatogr. Sci. 1969, 7, 129.
- 19. Martin, M.; Eon, C.; Guiochon, G. J. Chromatogr. 1975, 108, 229.
- 20. Yang, F.J. J. Chromatogr. Sci. 1982, 20, 241.
- 21. Lauer, H.H.; Rozing, G.P. Chromatographia 1981, 14, 641.
- 22. Freebairn, K.W.; Knox, J.H. Chromatographia 1984, 19, 37.
- 23 Scott, R.P.W.; Simpson, C.F. J. Chromatogr. Sci. 1982, 20, 62.
- 24. Hupe, K.P.; Jonker, R.J.; Rozing, G. J. Chromatogr. 1984, 285, 253.
- 25. Kutner, W.; Debowski, J.; Kemula, W. J. Chromatogr. 1981, 218, 45.
- 26. Kok, W.T.; Brinkman, U.A.T; Frei, R.W.; Hanekamp, H.B.; Nooitgedacht, F.; Poppe, H. J. Chromatogr. 1982, 237, 357.
- 27. Huber, J.F.K.; Rizzi, A. J. Chromatogr. 1987, 384, 337.
- 28. Christian, G.D.; Ruzicka, J. Anal. Chim. Acta 1992, 261, 11.
- 29. Spence, D.M.; Crouch, S.R. Quim. Anal. 1996, 15, 296.
- 30. Moring, S.E.; Reel, R.T.; van Soest, R.E.J. Anal. Chem. 1993, 65, 3454.

Chapter 5

Mixing Efficiencies in Capillary Flow Injection Systems

5.1 INTRODUCTION TO MIXING IN FLOW INJECTION

A controlled amount of dispersion is often a prerequisite for successful performance in flow injection (FI)¹. In fact, the amount of dispersion that arises from convective forces is usually the main source of mixing between reagent zones. Since its inception, practitioners of FI have employed many methods in an attempt to increase the amount of mixing that occurs within the reactor tubing. One simple method of enhancing the mixing efficiency in non-segmented systems consists of manipulating the shape of the tubing itself (such as coiling the tube) in hopes of creating a secondary or bolus flow²⁻⁴ within the tube. A more sophisticated method of improving the extent of mixing within reactor tubing is to employ some form of a packed bed, such as a single bead string reactor (SBSR)⁵. The main goal with a SBSR is to break up the laminar flow profile within the tube which enhances the mixing. However, with most conventional FI manifolds, coiling of the tubing will provide enough secondary flow to enhance the mixing inside a reactor. The inside diameter typical of most FI manifolds (>0.5 mm) is large enough to establish the parabolic laminar flow profile that allows for overlapping of

reagent and sample zones. However, establishing an efficient mixing profile in smaller bore tubing may be more challenging since the dispersion in the reactor is inversely related to the square of the tubing radius as was shown by the Aris-Taylor model in equation 1.1.

The work performed by Dasgupta's group⁶⁻⁸ has mainly focused on electroosmotic flow (EOF) as the pumping mechanism in a FI setup where the inside diameter of the reactor tubing was 75 µm. EOF results in nearly plug flow where most of the interspersion of the reagent and sample zones is probably due to diffusion effects. Our group has also reported on similar capillary flow injection (CFI) systems⁹⁻¹¹ that use peristaltic pumps to induce flow. By using a pumping mechanism that is pressure induced. a laminar flow profile is expected, although its magnitude should be reduced since the surface area to volume ratio is increased as the tubing inside diameter decreases. In fact, results from chapter 4 and elsewhere 12 reveal that the relative amount of zone variance due to the reactor in a conventional system ($\approx 60\%$) was twice that of a CFI system ($\approx 30\%$). This type of data is encouraging from the standpoint that more complex applications (dialysis, extraction, reactions) may now be used in a FI system without a loss in sensitivity due to excessive dispersion. However, it also dictates that more attention must be paid to proper mixing strategies since convective forces alone may not suffice in capillary-based systems. For example, figure 5.1 shows calibration curves for the enzyme catalyzed determination of glucose that was described at the end of chapter 3. The sensitivity of the curve obtained with the conventional FI system is 1.5 times greater than the capillary-based system. Since residence times and manifold-to-injection volume ratios were identical for both systems, the respective peak absorbances are greater with the

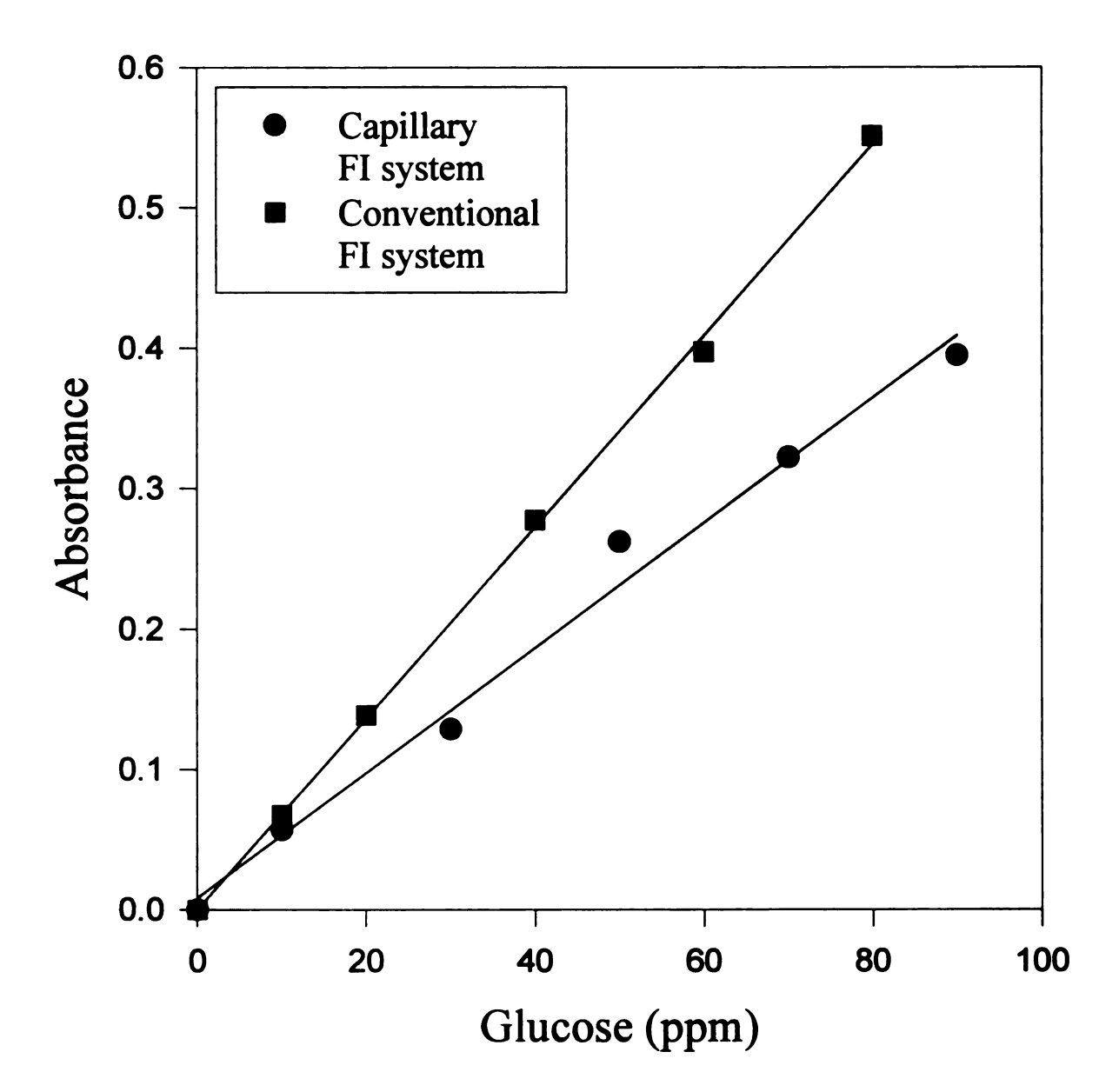


Figure 5.1. Calibration curves for the enzyme-catalyzed determination of glucose. Note the increased slope of the curve using the conventional FI system due to more efficient mixing within the reactor.

conventional system due to the extent of mixing. Figure 4.2 in chapter 4 showed that the measured absorbances were generally greater for similar manifolds in the capillary FI system as compared to a conventional system. Keep in mind, however that these absorbances were for an injected dye (i.e., no reaction was occurring). Thus, the increased absorbance values for the capillary FI system is an indicator of less dispersion and hence, less mixing. In addition to decreased convective forces, secondary flow contributions due to coiling are essentially zero in such small bore tubing. Thus, traditional techniques to enhance mixing will not be beneficial.

The work presented here demonstrates not only the differences in mixing efficiencies due to convective forces, but also the benefits of employing a mixing tee in a CFI system.

5.2 EXPERIMENTAL

5.2.1 Reagents

The preparation of the phenol red solution and the borate buffer were described in chapter 2. For the fast reaction studies, the iron solution (0.5 mM) was prepared by dissolving 0.10 g of Fe(NO₃)₃ (Baker) in 1 L of 0.05 M H₂SO₄. The thiocyanate solution (10 mM) was prepared by dissolving 0.98 g of KSCN (Baker) in 1 L of 0.05 M H₂SO₄.

5.2.2 Apparatus

The manifold employed for the dispersion studies without the mixing tee was identical to the setup shown in figure 4.1. The system used to investigate the dispersion and extent of reaction with a mixing tee is shown in figure 5.2. A peristaltic pump (Ismatec IP-12) was used as the pumping mechanism. Flow rated tubing (Cole Parmer)

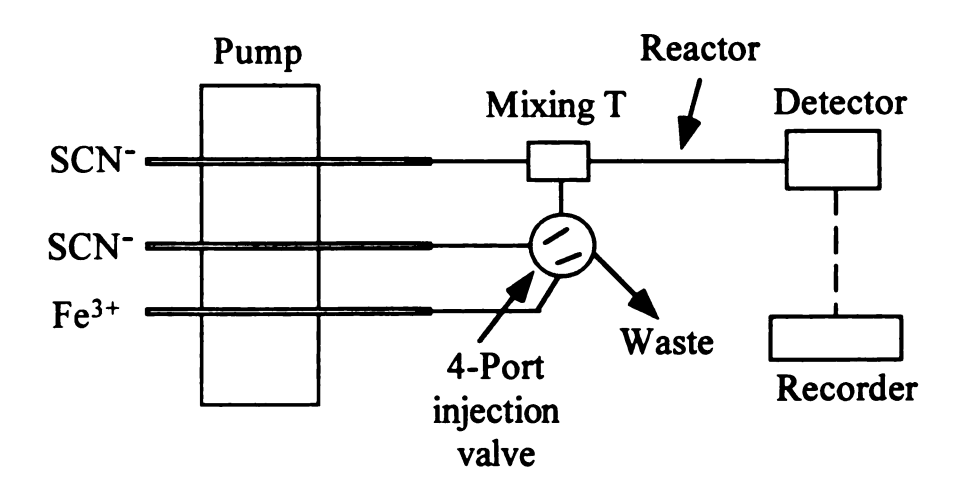


Figure 5.2. Manifold employed for the investigation of mixing using the Fe(SCN)₃ reaction.

with an inside diameter of 190 µm was laid across the pump rollers. The 75 µm i.d. fused silica tubing (Polymicro Technologies) was inserted into the flow rated tubing. The SCN was pumped continuously through the mixing tee (Upchurch Scientific) of 0.029 µL internal volume which is shown in figure 5.3. The SCN was also pumped through one side of a 4-port valve with a 500 nL internal injection loop (Valco). The Fe³⁺ was pumped continuously through the other ports of the valve. The four port valve operates much like the conventional 6-port injection valves. Thus, when switched to the inject mode, the Fe³⁺ is injected into the SCN stream, first traveling through the mixing tee and then proceeding towards the detector. The flow cell was designed and built in-house. Detection was performed using a colorimeter with an interference filter at 480 nm. The pump, switching valve and the flow cell have been described previously in chapter 2 and elsewhere. The mixing tee used in the capillary FI system was a 0.029 µL mixing tee (Upchurch Scientific). A 2.9 µL mixing tee (Upchurch Scientific) was used with the conventional FI All data acquisition was accomplished using a program written with the system. LabWindows/CVI software package and a LabPC+ board (National Instruments).

5.3 **RESULTS**

5.3.1 Dye Dispersion Studies

Ruzicka and Hansen have defined the dispersion coefficient D of an injected sample plug in FI as the ratio of the undiluted sample concentration to the sample concentration after some amount of dispersion has taken place¹. This ratio is shown in equation 5.1. Here, C₀ represents the steady state (undiluted) concentration of the phenol

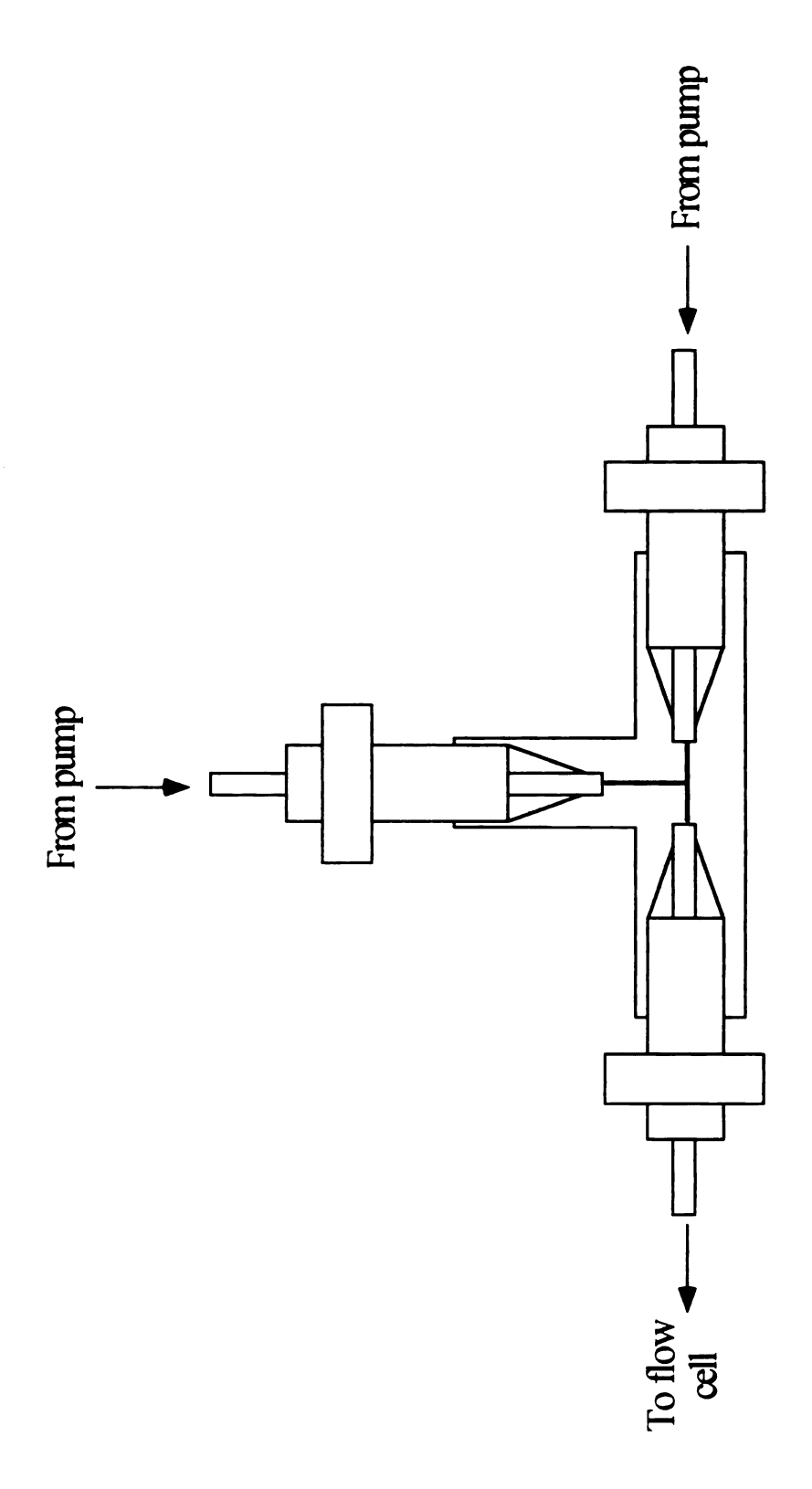


Figure 5.3. Drawing of the 0.029 µL mixing tee.

$$D = \frac{C_0}{C}$$
 (5.1)

red dye while C represents the measured concentration after some form of dispersion or mixing has occurred. According to Beer's law, equation 5.2 shows that C_0 can be replaced by the measured steady state absorbance A_0 of the phenol red with no mixing tee in the manifold which represents the undiluted and unmixed dye concentration. The dye can be considered unmixed because the entire manifold is filled with the dye. Assuming the absorbance is linearly related to the concentration of the dye, the value for C can be replaced by the measured steady state absorbance A of the phenol red dye after being mixed with buffer in the $0.029~\mu L$ mixing tee. In equation 5.2, b represents the effective path length of the flow cell while ϵ represents the molar absorptivity of the phenol red dye. Figure 5.4 is an example of Ruzicka and Hansen's dispersion

$$D = \frac{C_0}{C} = \frac{A_0}{A} = \frac{A_0}{A}$$
 (5.2)

coefficients. The upper trace represents the value for A_0 . This steady state reading thus represents undiluted and unmixed dye. The lower trace, representing the value for A, is the steady state absorbance measurement for the dye after first having been mixed with buffer in the 0.029 μ L mixing tee. The ratio of A_0 to A in this case gives a dispersion

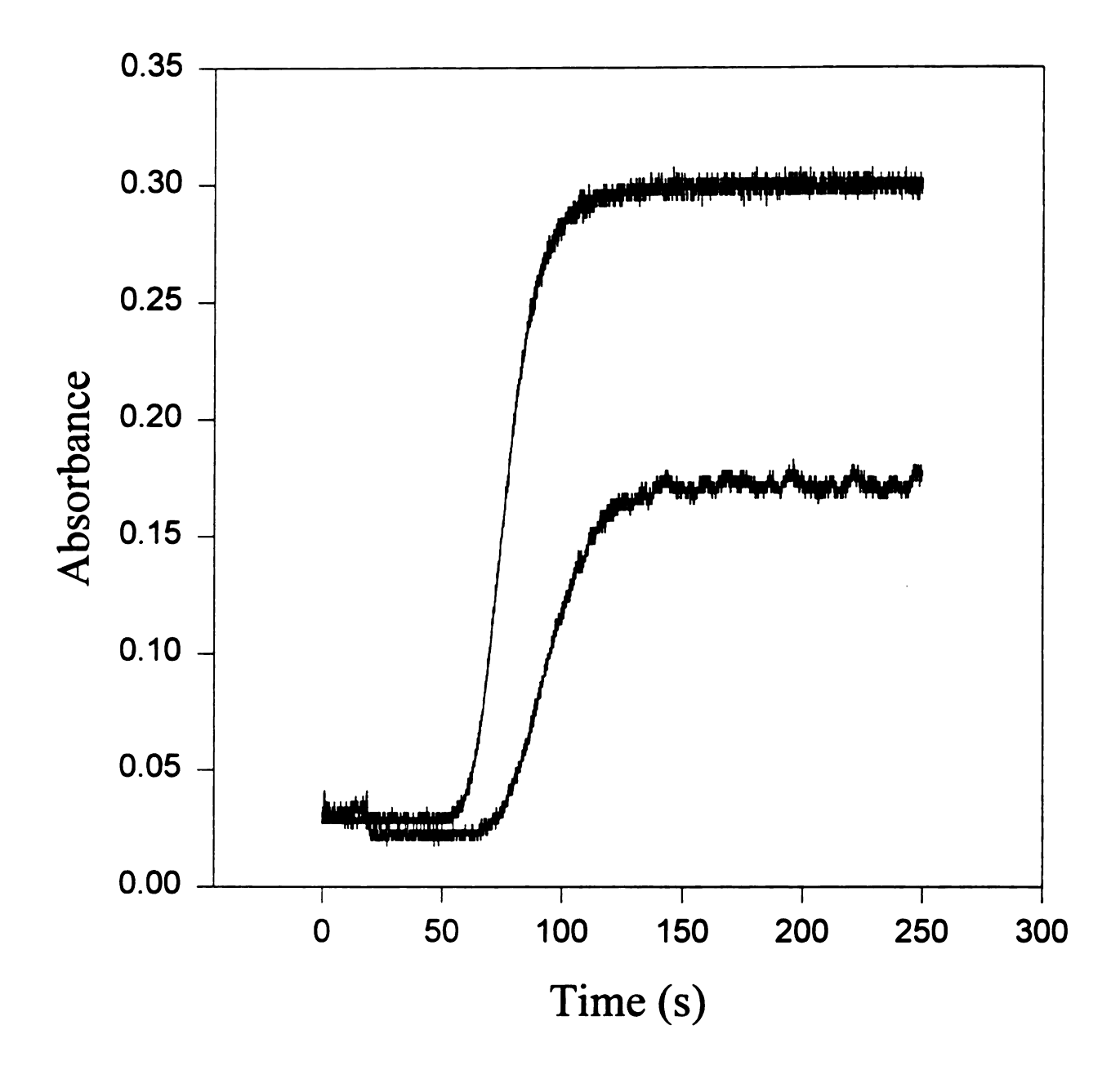


Figure 5.4. Steady state absorbances of phenol red. The upper trace is for the capillary system with no mixing tee. The bottom trace is the response signal after the phenol red was mixed with buffer in the 0.029 µL mixing tee.

coefficient D of approximately 2. In other words, dispersion due to the mixing tee has caused the sample to become diluted to half of its original absorbance or concentration.

For the capillary FI system, the dispersion coefficients were calculated from the steady state response of the phenol red without and with mixing aides using increasing lengths of reactor tubing. These results are shown for capillary FI system in table 5.1. The data in this table reveal important information pertaining to mixers used in such continuous flow systems. Consider the dispersion coefficients for the 25 and 50 cm reactors. Since the overall dispersion coefficient increases with reactor length, this indicates that mixing is not yet complete. If the mixing were complete in the 25 cm reactor, one would not witness any change in the overall dispersion coefficient as the reactor length is increased. If mixing were complete, the stream would be homogeneous and changing the reactor length to 50 cm would result in the same dispersion coefficient.

5.3.2 Investigating the Completeness of Mixing with the Fe(SCN)₃ Reaction

As shown by the calibration curves in figure 5.1, the extent of mixing is greater in a conventional FI system. Therefore, to compare the extent of mixing in the capillary and conventional FI systems, the determination of Fe^{3+} by its complexation with SCN was investigated. Since this reaction is complete within milliseconds, complete mixing can be determined as the point where the area under the response signal is no longer increasing with reactor length. The results of this investigation are shown in figure 5.5. This figure indicates that mixing within the conventional system reaches $\approx 90\%$ of steady state in about 20 seconds (40 cm of reactor at 2 cm s⁻¹ linear velocity). The capillary system

Table 5.1 Dispersion coefficients for the capillary FI system as a function of varying reactor lengths. The linear flow rates were held constant for each reactor at $2.0 \pm .1$ cm s⁻¹

Reactor length (cm)	Dispersion coefficient
25	1.88
50	2.09
75	2.46

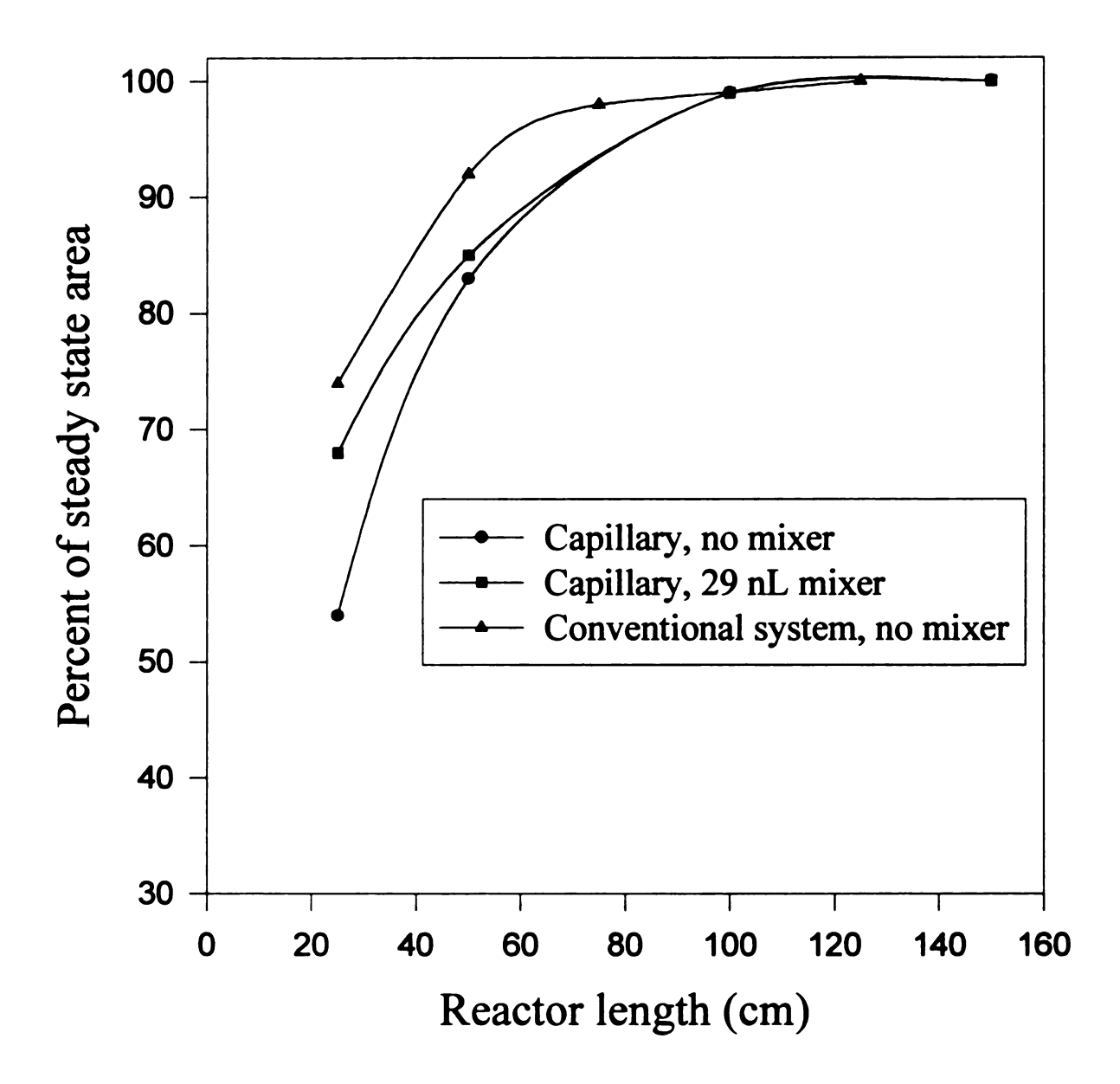


Figure 5.5. Examination of the extent of mixing of a conventional FI system, a capillary FI system and a capillary FI system with a mixing tee. The linear velocities in all three manifolds was held constant at 2.1 ± 0.1 cm s⁻¹.

without a mixing tee requires almost twice the amount of time (75 cm of reactor at 2 cm s⁻¹ linear velocity) in order to reach the same extent of reaction completeness.

The results from these studies were then compared to a capillary system employing a mixing tee. From these results, also shown in figure 5.5, it is evident that the mixing tee is a benefit when measurements are made before approaching a steady state value. For example, when using the 25 cm reactor (about 12-13 s of residence time) with no mixing tee the initial percentage of the steady state area is only 55% as compared to almost 70% with the mixing tee. However, after 25 s of residence time within the reactor tubing, the percentage of the steady state area without and with the mixing tee are 83 and 85%, respectively. We believe this may be an indication that mixing due to diffusion actually plays a very large role in reactors of capillary dimensions. As shown, the extent of mixing in the capillary system was not as great as the conventional FI system, even when a mixing tee was employed.

5.4 CONCLUSIONS

It is a well established fact that increasing the sample volume in a FI system is a powerful method of increasing peak height and improving sensitivity. However, this may not be as powerful in a capillary FI system when a reaction is occurring within the flowing stream. Since the length of the sample zone increases as the sample volume is steadily increased, the reagent and sample zones eventually will reach a point where there is no overlap, and hence no mixing or reaction.

In this work, we have shown that the mixing in a conventional FI system is greater than with a capillary system of similar reactor length and flow rate. However, through the use of proper mixing aids, the chances for efficient reagent and sample zone overlap will be increased. Although the use of traditional methods of enhancing mixing such as coiling are of little benefit in a capillary-based system, in the future it may be possible to employ the use of packed beds to increase the mixing efficiency. Although this may cause a problem with high pressure, there are now available syringe pumps capable of delivering pressures over 5,000 psi at flow rates as low as $1 \mu L min^{-1}$, as was described in chapter 3.

List of References

- 1. Ruzicka, J.; Hansen, E.H. Flow Injection Analysis, Wiley, New York, 1988.
- 2. Snyder, L.R. Anal. Chim. Acta 1980, 114, 3.
- 3. Tijssen, R. Anal. Chim. Acta 1980, 114, 71.
- 4. Hofmann, K.; Halasz, I. J. Chromatogr. 1979, 173, 211.
- 5. Reijn, J.M.; Van Der Linden, W.E.; Poppe, H. Anal. Chim. Acta 1981, 123, 229.
- 6. Liu, S.; Dasgupta, P.K. Anal. Chim. Acta 1992, 268, 1.
- 7. Liu, S.; Dasgupta, P.K. Anal. Chim. Acta 1993, 283, 747.
- 8. Dasgupta, P.K.; Liu, S. Anal. Chem. 1994, 66, 1792.
- 9. Spence, D.M.; Sekelsky, A.M.; Crouch, S.R. *Instrum. Sci. Technol.* 1996, 24, 104.
- 10. Spence, D. M., Crouch, S. R. Quim. Anal., 1996, 15, 296.
- 11. Spence, D.M.; Crouch, S.R. Anal. Chim. Acta, submitted for publication.
- 12. Spence, D.M.; Crouch, S.R. Anal. Chem. 1997, 69, 165.

Chapter 6

Capillary Flow Injection for Stopped Flow Kinetic Determinations

In proceedings¹ from the Fifth International Conference on Flow Analysis in Spain in the summer of 1995, leaders in the field of flow injection (FI) offered what they feel will be the most beneficial improvements of the technique. Our group²⁻⁵ and others⁶⁻⁹ definitely believe that the miniaturization of FI will improve the overall performance and allow for an expansion of its applications.

The goal of this chapter is to present some of the realized and potential advantages of capillary FI for kinetic methods of analysis, particularly when compared to conventional FI and air-segmented continuous flow (ASCF) analysis. In addition, our initial studies have brought to light several possible problems that can be encountered with capillary FI systems. In the research reported here, we have used the stopped-flow FI technique¹⁰ and applied it to a capillary FI system for a determination of ascorbic acid. We have chosen to use a simple reaction for ascorbic acid determinations based on the reduction of toluidine blue¹¹. Although it was not our goal to perform an in-depth study of stopped-flow capillary FI, we show here some preliminary data gathered with our system. We also discuss some of the other benefits and possible drawbacks that we have observed with capillary FI systems.

6.1 EXPERIMENTAL

6.1.1 Instrumentation

The peristaltic pump (Ismatec), the 4-port injections valve (Upchurch Scientific), and the flow cell used in this study have been described in detail in chapter 2 and elsewhere². The capillary FI system was easy to assemble since most of the fittings, tees, and connectors were for standard 1/16" o.d. tubing and are commercially available. The flow cell used in the stopped-flow experiments was the variable volume type, also described in chapter 2, with a path length of 1 cm and internal volume of 500 nL. The additional 6-port valve used in the stopped-flow experiment was also from Upchurch Scientific. A mixing tee (Upchurch Scientific) with an internal volume of 560 nL was employed to help mix the sample and reagents. The 4-port valve was pneumatically actuated and controlled by means of software on a 486 computer. Data were also acquired using the same computer with a program written with the LabWindows/CVI (National Instruments) software package.

6.1.2 Reagents

All reagents were prepared using distilled water (DW). No special filtering of the solutions was required. We have found that the capillary FI system rarely clogs as long as the system is flushed with water after use. The toluidine blue reagent (Aldrich) was prepared as a 3.3 mM stock solution by dissolving 1.021 g in 1L of DW. This stock solution was then diluted with DW to give a 0.33 mM solution for the FI experiments. Ascorbic acid solutions (30-230 μ M) were made by appropriate dilution of a 3.0 mM stock solution in 0.2 M HCl. All reagents were temperature controlled at 24.6 \pm 0.2 °C.

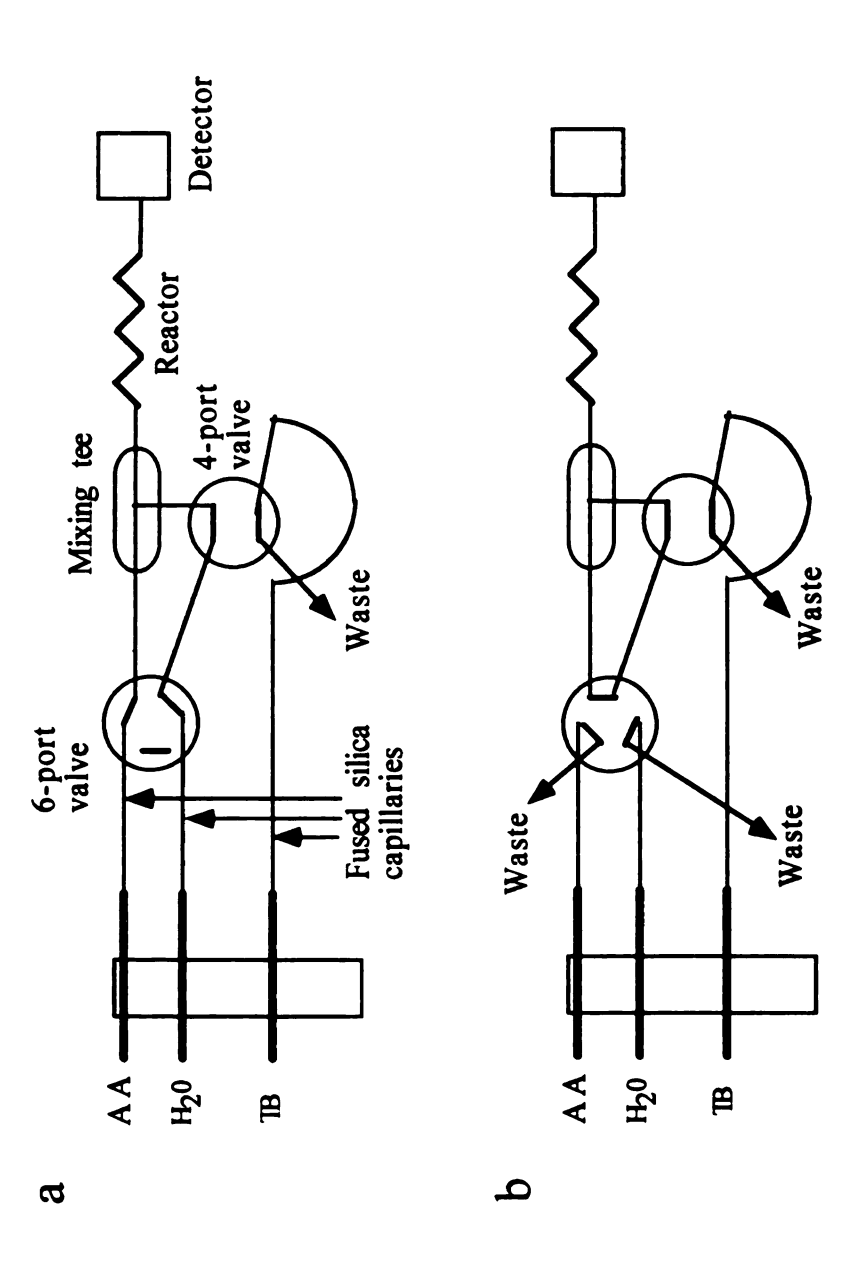
6.1.3 Procedure

The manifold shown in figure 6.1 was used for the stopped-flow kinetic studies. Figure 6.1a represents the manifold in the non-inject mode, before the flow is stopped. When injection of toluidine blue is required, the 4-port valve is switched and dye is introduced into the mixing tee until the valve is switched back to its original position. The ascorbic acid sample is continuously pumped through the mixing tee. Once injected, the dye mixes with the ascorbic acid before it is pumped to the flow cell whereupon the flow is stopped by means of the 6-port valve. Figure 6.1b shows the configuration for stopping the flow. After the flow was stopped, the reaction was monitored for 240 seconds with a filter colorimeter at 660 nm wavelength.

6.2 RESULTS AND DISCUSSION

6.2.1 Stopped Flow Considerations

The 6-port valve used in the stopped-flow capillary FI apparatus is essential. Figure 6.2 shows two sample determinations by the stopped-flow method using a conventional manifold, one of the samples being a blank. Here, the reaction mixture is being trapped in the flow cell by simply turning off the peristaltic pump. Figure 6.3 shows the same determination using the stopped-flow technique with the capillary manifold. It is evident that simply turning off the pump does not cause complete cessation of the flow, undoubtedly because of the smaller volume and high amount of back pressure experienced within the capillary FI system. In figure 6.4, the 6-port valve has been used to disconnect the pump from the reaction coil and flow cell as depicted in figure 6.1b. Since the flow is now abruptly stopped, the reaction can be followed with minimal flow contributions.



amount of time, a zone of toluidine blue is introduced into the reaction tubing. In figure 6.1b, Manifolds used for stopped-flow kinetic determination of ascorbic acid. In figure 6.1a, the blue, TB) through the flow cell. When the 4-port valve is switched for a pre-selected the 6-port injection valve is switched, thus disconnecting the pump from the reagent pump delivers the sample (ascorbic acid, AA) and reagents (water and toluidine and sample coils.

Figure 6.1.

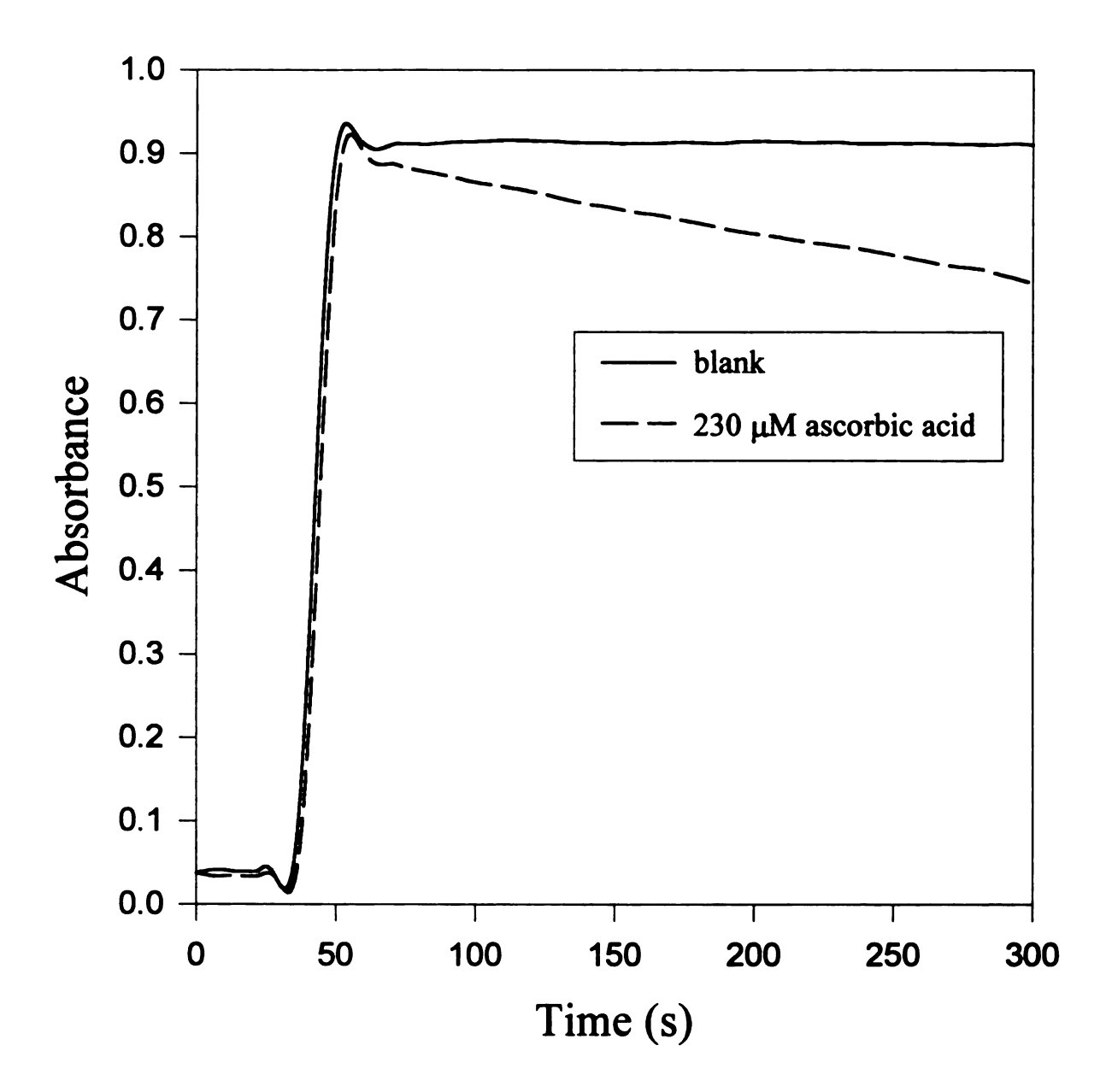


Figure 6.2. Stopped-flow kinetic determination of 230 µM ascorbic acid using a conventional FI manifold. The inside diameter of the reaction tubing was 0.5 mm. In order to stop the flow, the peristaltic pump is simply turned off near the toluidine blue peak maximum.

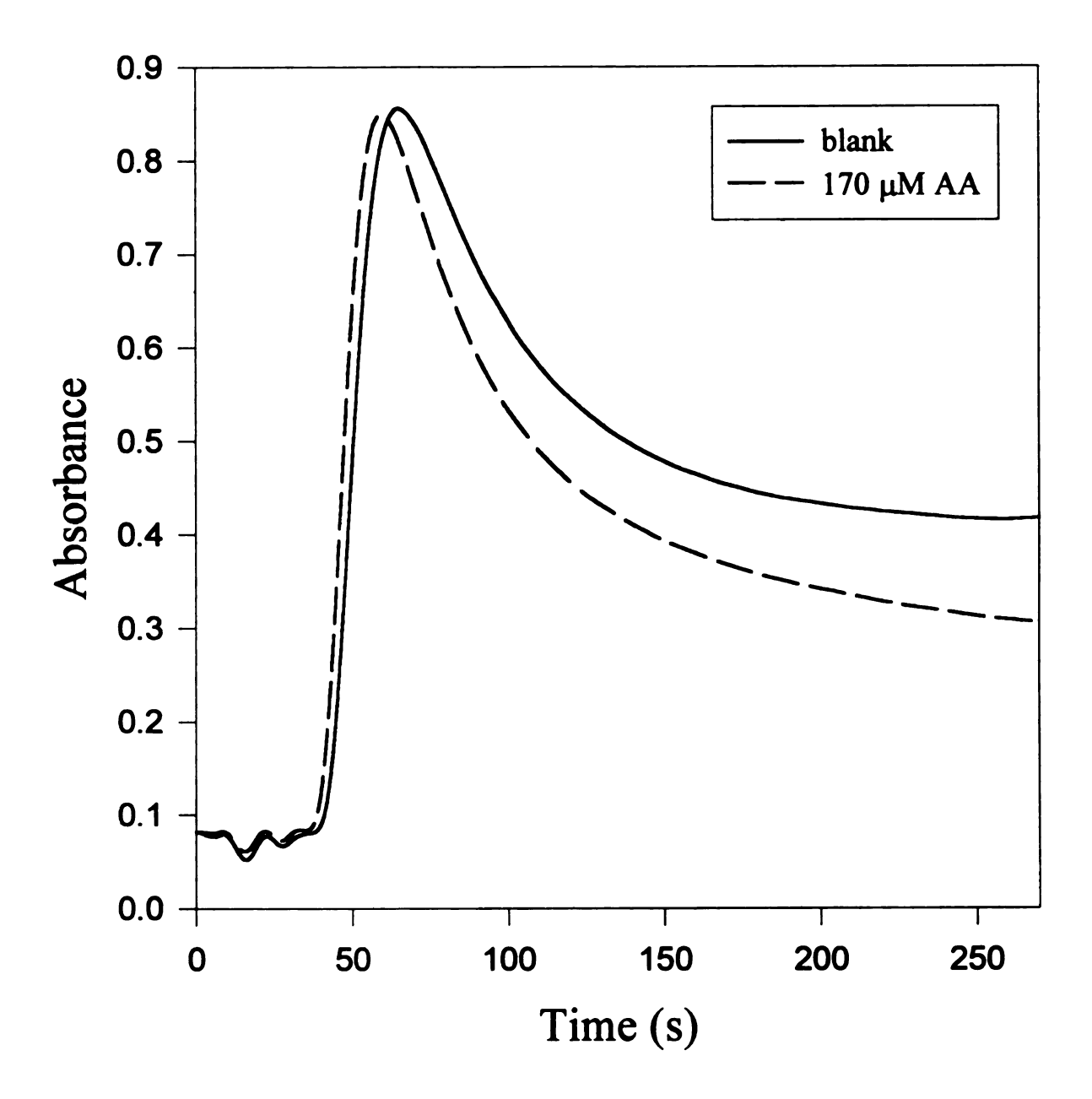


Figure 6.3. Stopped-flow kinetic determination of ascorbic acid using a capillary FI manifold. The inside diameter of the reaction tubing was 0.064 mm. Again, the flow is stopped by turning off the peristaltic pump. However, the sample zone continues to flow through the cell.

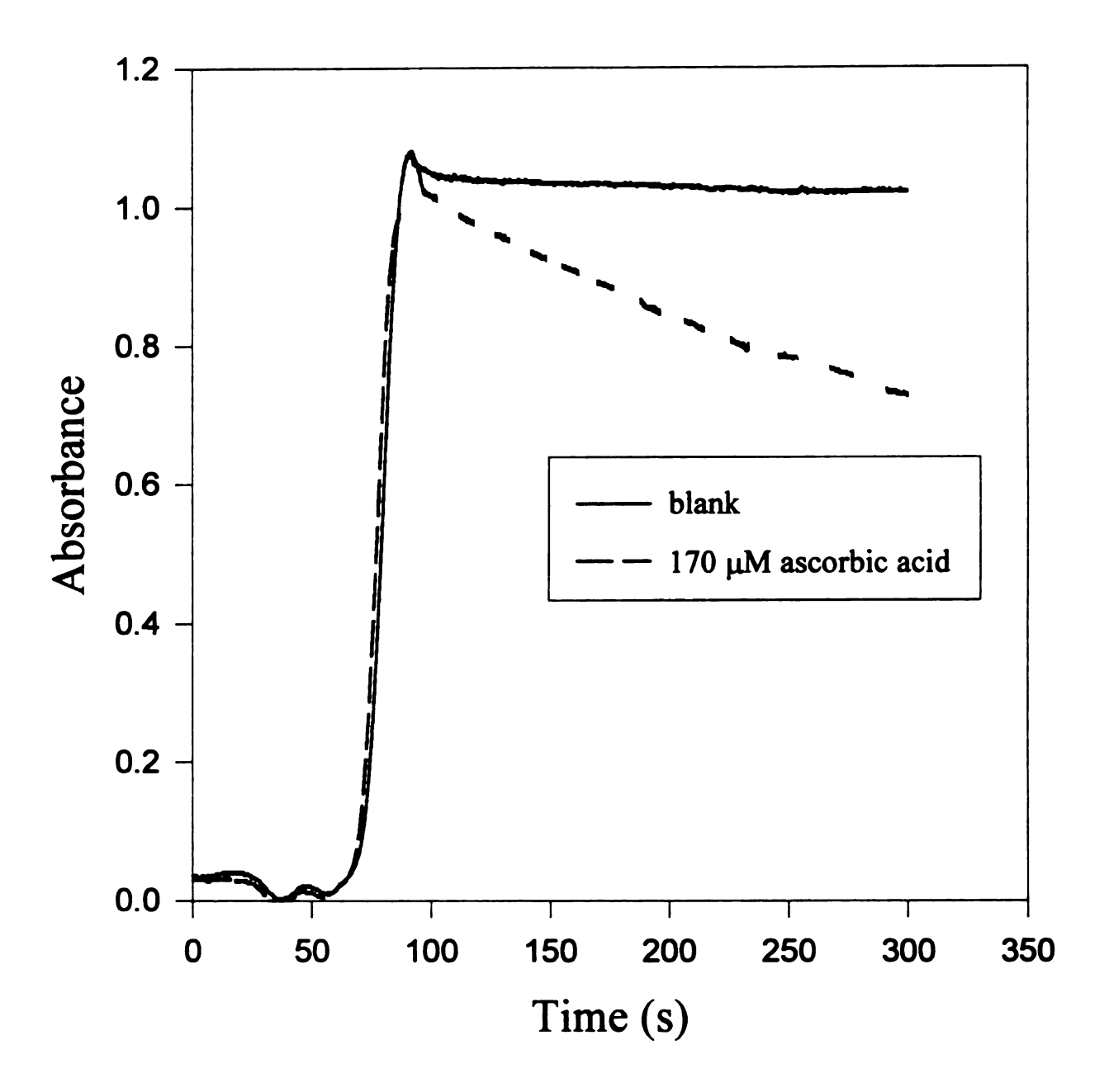


Figure 6.4. Stopped-flow kinetic determination of ascorbic acid using the same system used to collect the data in figure 6.3. Now the flow is being stopped by switching the 6-port valve as shown in figure 6.1b.

There are certain advantages and disadvantages that a capillary FI system has when compared to a conventional FI system when operating in the stopped-flow mode. An advantage is the much smaller reagent and sample volumes used for capillary FI. These small volumes mean lower analysis costs and lower production of waste materials. The total volume of reagents used to obtain the data in figure 6.4 was 20 µL while the volume needed to obtain the data shown in figure 6.2 (the conventional FI system) was 600 μL, a 30-fold increase. A disadvantage of capillary techniques is that mixing may not be as efficient because of lower dispersion. However, we have found that significant reaction occurs without including the mixing tee in the manifold shown in figure 6.1. For example, the data used to construct the calibration curve in figure 6.5 were obtained without the use of a mixing tee. In figure 6.5, the initial rate of change of absorbance during the first 10 seconds after stopping the flow is plotted versus the ascorbic acid concentration. Similar results were obtained with the mixing tee in the manifold. The non-zero intercept is probably due to a very small flow of the sample plug after switching the valves.

6.2.2 Benefits of a Capillary FI System

Patton and Crouch¹² have compared conventional FI with ASCF methods and concluded that FI has advantages where the chemistry and sample manipulations are relatively simple and the reactions are fairly rapid. In other situations, the dispersion that occurs in FI methods can lead to a lack of sensitivity or an inability to detect a product at all. Dispersion can also severely limit the sampling frequency of FI methods involving complicated chemistry or slow reactions. ASCF also outperforms FI in the area of kinetic

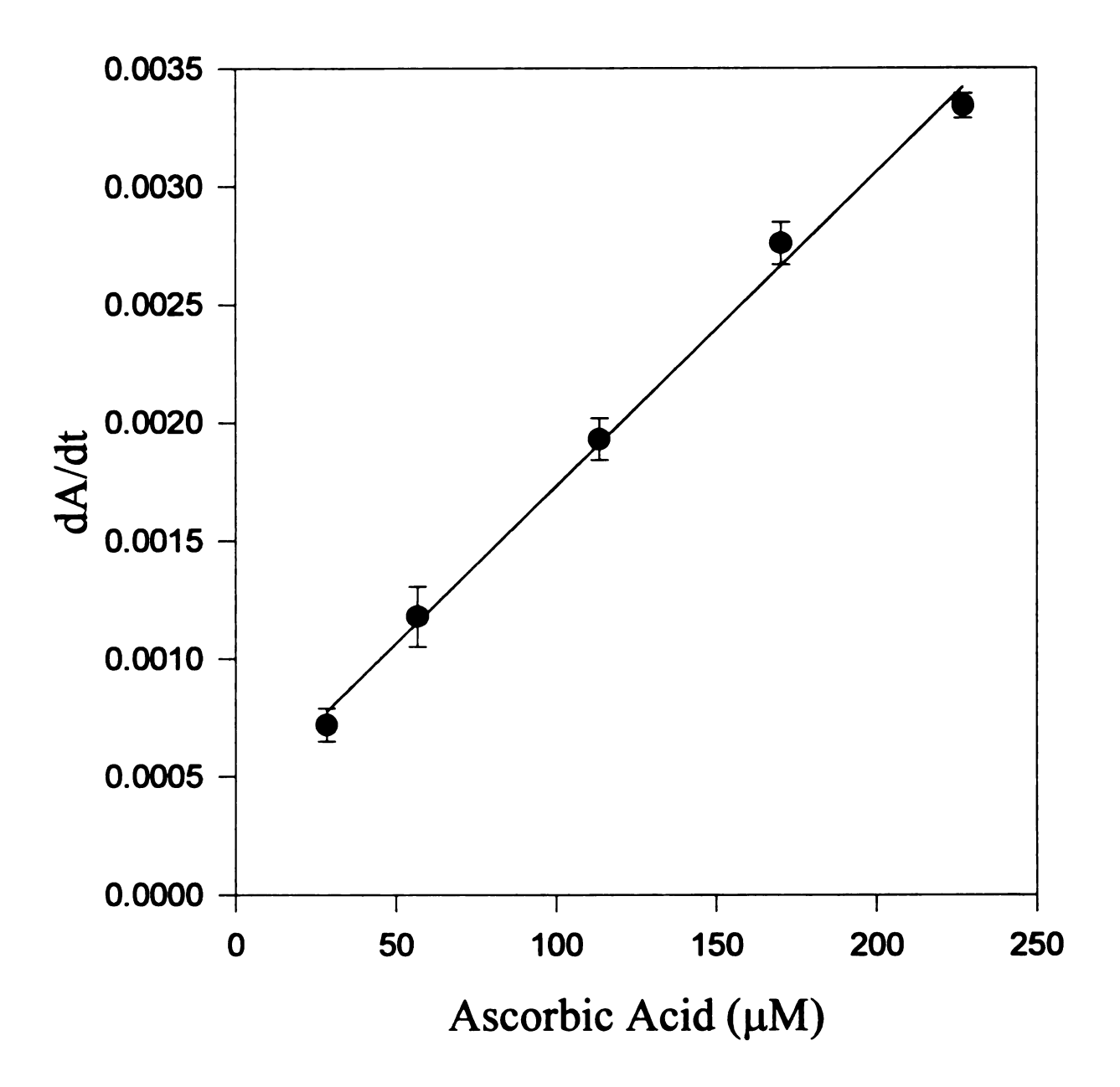


Figure 6.5. Calibration curve obtained by running ascorbic acid samples ranging in concentration from 30-230 μ M. The correlation coefficient for the determination is 0.9957. The non-zero intercept is most likely caused by some slight continued movement of the sample zone through the cell after stopping the flow.

determinations and in automated kinetic studies. In FI, the physical dispersion and the reaction kinetics are often difficult to deconvolute so as to obtain results that are indicative only of the chemical reaction. In ASCF, the air bubbles act as physical barriers to dispersion and, as a result, kinetic information can be more readily extracted.

The aforementioned reasons provide excellent motivation for the development of a capillary FI system. In conventional FI, dispersion can be limited by reducing the flow rate and the distance traveled in the manifold¹³. Using tubes of smaller diameter also reduces dispersion, which is usually considered to be proportional to the square of the tubing radius. The inside diameter of a typical capillary used in our initial studies of capillary FI (60 μm) was about 10 times less than that used in a conventional FI system (0.5 mm). The dispersion should thus be reduced by a factor of approximately 100 in the capillary FI system. However, factors such as injection variance and detector variance may contribute to the overall peak variance in a capillary system. These factors have been compared and contrasted with a conventional flow injection system as shown in chapter 4 and elsewhere⁴. It was found that the reactor only contributed ≈ 35 % of the total peak variance, while in a conventional system this value was ≈ 65 %. Thus, on-column detection schemes in capillary FI system should be beneficial. For example, employing detection at more than one point along the capillary will allow for multiple measurements to be made in time without the added dispersion contributions from multiple passes through a single flow cell.

Another area in kinetics where less dispersion of the sample should be of benefit is in fundamental kinetic studies aimed at determining reaction orders and rate constants.

Since knowing the concentrations is imperative in determining rate constants, ASCF techniques are usually preferred over FI systems. Therefore, if one begins a reaction with a known reagent or sample concentration, the determination of the rate constant is straightforward since the concentration remains unchanged by dispersive effects as it traverses the reaction coil. In an unsegmented system, rate constant determinations are difficult since concentrations change, due to dispersive processes, as the flow proceeds through the tubing. However, the data in figures 4.2 and 4.3 in chapter 4 shows the sample's peak absorbance is still about 88 % of its steady state value in a capillary FI even though the residence time is increased from 25 s to 200 s. In fact, data from figure 4.2 show that residence times of up to 50 s result in minimal dispersion of the sample zone. This should allow for kinetic data to be examined with some knowledge of the initial concentration(s) of reagent(s) involved.

6.3 CONCLUSIONS

This work demonstrates some of the advantages of a capillary system as compared to a conventional FI system. However, the results also reveal some added obstacles that are normally not encountered when employing a conventional FI system. As may be expected, there is still a great deal of work to be performed in order to fully characterize and adapt many of the "macro-scale" techniques to the micro-scale level. It is anticipated that many of the current kinetic techniques using FI as a tool will be enhanced. For example, Hsieh and Crouch¹⁴ have shown that because of dispersion, flow reversals and flow recycling are difficult to employ for kinetic methods with conventional FI. A system using capillaries for the reagent coils may make flow reversals or recycling more practical

for kinetic methods with unsegmented streams. A capillary system also would allow for on-column detection schemes¹⁵ which should enhance determinations even further, since there would be no dispersion introduced by a flow cell and any connections or unions.

Finally, kinetic determinations which use immobilized enzymes should benefit from systems using microbore tubing. As discussed by Ruzicka and Hansen¹³, the surface areato-volume ratio is greatly increased by the use of capillary tubing. This feature should help increase reaction rates since the concentration of the enzyme should always be in excess of the sample. This is especially true since many reactions involving immobilized media are diffusion limited. With small bore tubes, diffusion time would be lower since the sample does not have as far to diffuse before reaching the immobilized enzyme, antibody, or antigen. These concepts are discussed further and in more detail in chapter 8.

Capillary FI has been presented as a possible new tool for kinetic determinations. Although there are certain precautions that the user must consider, we believe that capillary FI will broaden the realm of kinetic determinations that can be performed with continuous flow analyzers. Initial studies and considerations lead us to believe that FI in microbore capillaries will be readily incorporated into the family of continuous flow techniques.

List of References

- 1. Proceedings from the Sixth International Conference on Flow Analysis, *Anal. Chim. Acta* 1995, 308, 1.
- 2. Spence, D.M.; Sekelsky, A.M.; Crouch, S.R. *Instrum. Sci. Technol.* 1996, 24, 104.
- 3. Spence, D. M., Crouch, S. R. Quim. Anal. 1996, 15, 296.
- 4. Spence, D.M.; Crouch, S.R. Anal. Chem. 1997, 69, 165.
- 5. Spence, D.M.; Crouch, S.R. Anal. Chim. Acta, submitted for publication.
- 6. Liu, S.; Dasgupta, P.K. Anal. Chim. Acta 1992, 268, 1.
- 7. Liu, S; Dasgupta, P.K. Anal. Chim. Acta 1993, 283, 739.
- 8. Dasgupta, P.K.; Liu, S. Anal. Chem. 1994, 66, 1792.
- 9. Daykin, R.N.C.; Haswell, S.J. Anal. Chim. Acta 1995, 313, 155.
- 10. Christian, G.D.; Ruzicka, J. Anal. Chim. Acta 1992, 261, 11.
- 11. Safavi, A; Fotouhi, L. Talanta 1994, 41, 1225.
- 12. Patton, C.J.; Crouch, S.R. Anal. Chim. Acta 1986, 179, 189.
- 13. Ruzicka, J.; Hansen, E.H. Flow Injection Analysis, Wiley, New York, 1988.
- 14. Hsieh, Y.S.; Crouch, S.R. Anal. Chim. Acta 1995, 304, 333.
- 15. Albin, M; Grossman, P.D.; Moring, S.E. Anal. Chem. 1993, 65, 489A.

Chapter 7

Simulating Flow Injection Response Signals using a Non-Linear Partial Least Squares Regression Algorithm

The magnitude of success for a particular research project or experiment can often be measured by the number of other researchers and teachers that find it useful in their own endeavors. It has therefore often been the goal of our research group not only to perform meaningful research, but also to spread this knowledge to others in a meaningful and easily understood manner. Of course this knowledge is often presented orally (through talks or private transactions) or in written form (such as publications or poster presentations). However, many agree that the best way for a new method, technique or topic to be understood is to perform the actual experiment. In some cases, where the materials needed to perform the experiment are readily available, inexpensive, and safe, or where the technique described is neither labor intensive nor complex, reproducing the results is not difficult. However, there are times when the required materials are expensive, not commercially available, and dangerous to handle. Performing the experiment may also require substantial user expertise. Thus, incorporating this newly found knowledge into one's own repertoire may not be as easy as reading the original publication or following a set of instructions in a lab manual. This chapter describes some of our initial attempts to use a non-linear partial least squares (NLPLS) regression algorithm¹⁻³ to simulate response signals obtained with a capillary flow injection system. Although some initial success has been observed with the current method of simulating these signals, further work is needed to successfully complete the study. These future studies are also discussed in this chapter.

7.1 EXPERIMENTAL

7.1.1 Apparatus

The setup employed for obtaining the experimental data used in the NLPLS regression is described in chapter 4 and shown in figure 4.1. The system used a peristaltic pump (Ismatec, model IP-12) to induce flow. The injections were performed using the 4-port switching valve with time-based injections as described in chapter 2. The switching valve was used in order to obtain several different injection volumes to be used in the calibration set. The tubing employed was fused silica capillary (Polymicro Technologies) with an inside diameter of 75 μ m and an outside diameter of 365 μ m. The detector flow cell, described in chapter 2, was the variable volume type with an internal volume of 560 nL and a path length of approximately 1 cm. The detector was designed in-house and utilized an interference filter at 540 nm.

7.1.2 Reagents

Two reagents were used in this study and both have been described previously. Preparation of the phenol red dye solution was described in chapter 2. The resultant working solutions ranged in concentration from 5 x 10⁻⁵ M to 1 x 10⁻³ M. All of the solutions were prepared in a pH 9.5 borate buffer that is also described in chapter 2.

7.1.3 Programs used for Data Acquisition and Simulation

All experimental data were acquired with a program written with the LabWindows CVI (National Instruments) software package. The multivariate calibration and simulation were performed using the PLS_Toolbox within the Matlab software package (Eigenvector Technologies).

7.1.4 Procedures for Obtaining Calibration Data

Collecting the experimental data for calibration of the NLPLS regression involved the variation of four parameters vital to the shape of response signals obtained in flow injection (FI). Reactor length, sample concentration, volume injected, and flow rate were all systematically varied in order obtain response signals that would have a wide range of areas, widths, and residence times. Reactor lengths of 75, 150, 200, and 400 cm were employed in conjunction with the concentration ranges described in section 7.1.2. Injections of the dye ranged in volume from 0.5 to 2.0 µL while the flow rates were varied from 1.5 to 4.0 µL min⁻¹.

Once the data were obtained, the peak area, centroid, width, and distortion were determined by fitting the signal to an exponentially modified Gaussian (EMG) function^{4,5} shown below in equation 7.1. An example of a response signal with the EMG parameters

$$y = \frac{a_0}{2a_1} \exp\left(\frac{a_2^2}{2a_1^2} + \frac{a_1 - 1}{a_1}\right) \left[1 + \operatorname{erf}\left(\frac{\sqrt{2}}{2}\right) \left(\frac{x - a_1}{a_2} - \frac{a_2}{a_1}\right)\right]$$
(7.1)

(area, a_0 ; centroid, a_1 ; width, a_2 ; distortion, a_3) is shown in figure 7.1. It should be noted that the parameters listed in equation 7.1 are actually labels used by Peakfit. Although the true area is given by a_0 , the actual centroid (a_1) , width (a_2) and distortion (a_3) are given by

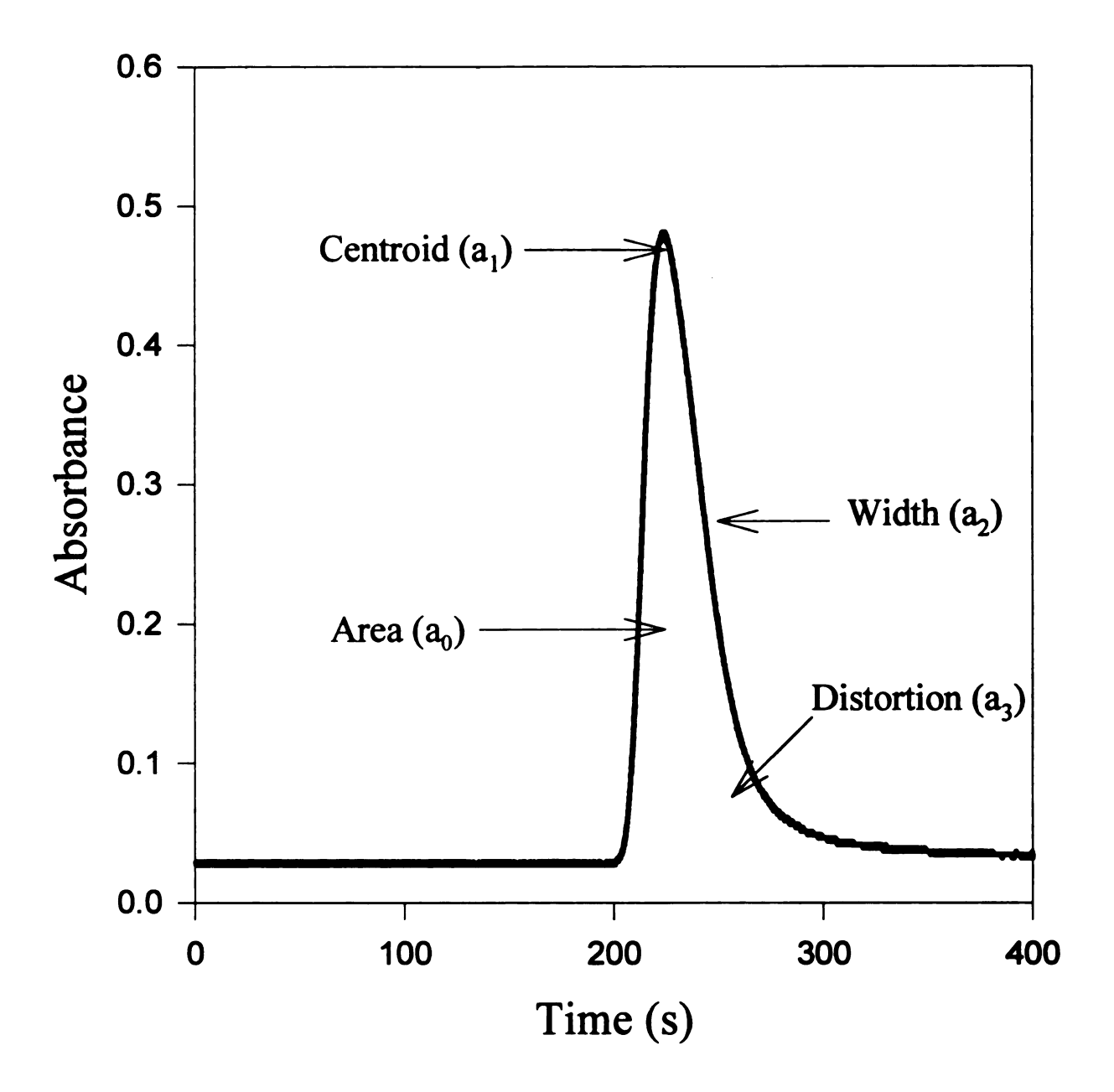


Figure 7.1. Response signal in the form of an exponentially modified Gaussian (EMG) equation. The EMG is described using the area, centroid, width and distortion. These terms are shown in equations 7.1 and 7.2a-c and described in section 7.1.4.

112

$$a_1 = t_G + \tau$$
 7.2a
 $a_2 = (\sigma_G^2 + \tau^2)$ 7.2b

7.2c

the relationships shown in equations 7.2 a-c. In equations 7.2a-c, t_G is the retention time of the peak, σ_G is the standard deviation of the peak, and τ is an exponential modifier⁵.

 $a_3 = 2\tau^3$

7.1.5 Performing the NLPLS Regression

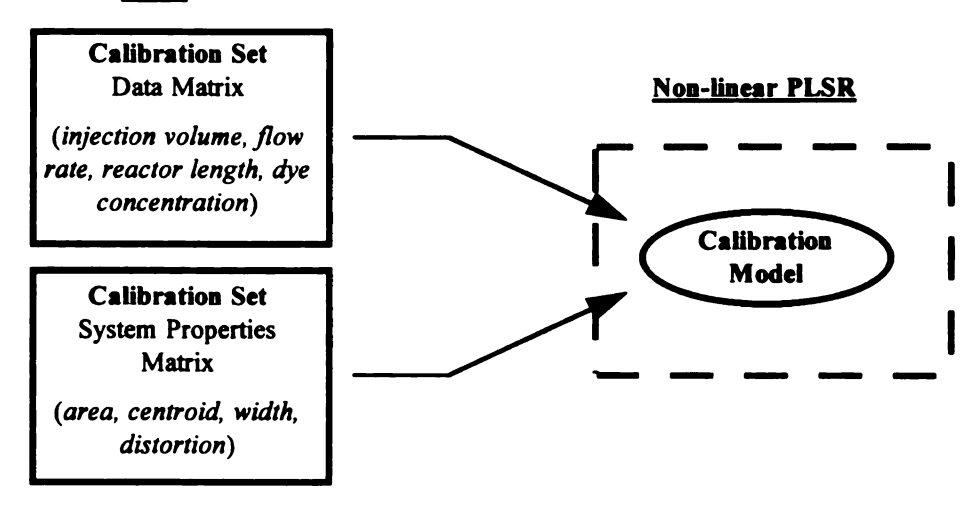
A detailed explanation of how the NLPLS algorithm occurs is described elsewhere⁶. Here, a very simple discussion will attempt to give the reader an introduction as to how the algorithm proceeds. Figure 7.2 is a very efficient way of graphically explaining the multivariate calibration technique⁷. In this figure, the calibration technique is broken down into two steps, namely generating the calibration model and performing the regression.

In the generation of the calibration model, each individual response signal is entered as a reactor length, concentration, injection volume and flow rate. Also entered into the calibration model along with these real time parameters is the area, centroid, width and distortion of each signal. This calibration model is then used in step two where the actual regression occurs.

In step two, the users will enter an unknown data matrix. In other words, the user is now entering in a set of real time parameters that will be used in the simulation. After these parameters have been entered, the regression is performed and the model then returns the system properties matrix. This generated matrix is nothing more than the area,

Step I: Generating the Calibration Model

Input



Step II: Performing the Regression

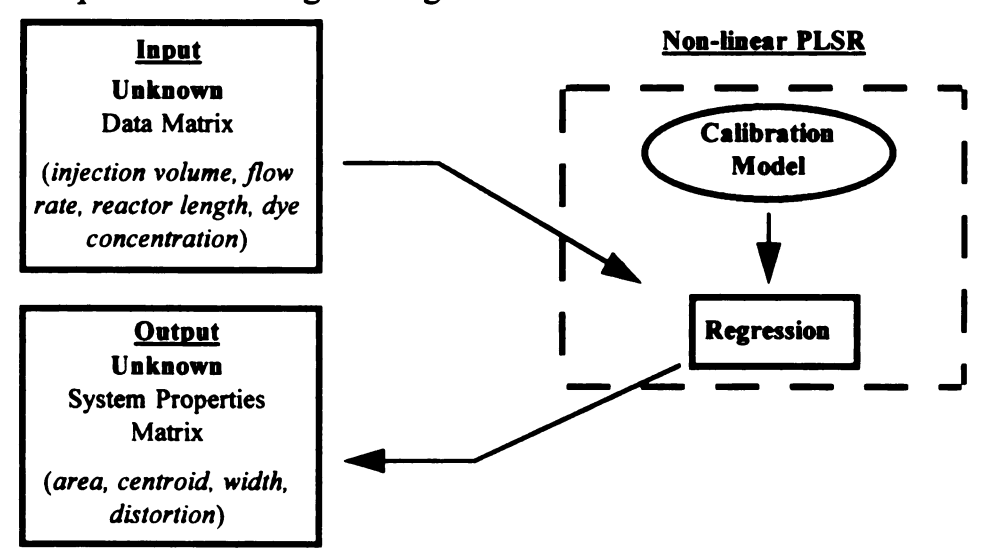


Figure 7.2. Multivariate calibration as a "black box". The calibration model is generated from the data matrix and system properties matrix. The regression is then performed and the unknown system properties matrix (the simulated data) is returned.

centroid, width and distortion as predicted from the regression. These values are then placed back into equation 7.1 to generate the predicted response signal.

7.2 RESULTS AND DISCUSSION

7.2.1 Comparison of Simulated vs. Experimentally Obtained Data

The results from the peak fitting to the EMG function revealed that the areas for the various response signals ranged from 1 to 30 absorbance units • s. Based on the inability of the regression model to return a value for the area that resembled that of the experimentally obtained data, it was hypothesized that either the range of prediction was too large or that not enough response signals were included in the calibration set that possessed areas above 10. Therefore, the range of areas used was reduced to include only those response signals whose areas were between 1 and 11. Upon this reduction of the calibration set, the areas predicted by the calibration set versus the actual areas was plotted and is shown in figure 7.3a. The majority of the areas are within 15% of the experimentally obtained area values. Figures 7.3b, 7.3c, and 7.3d show plots of predicted values from the calibration versus the actual values used in the calibration set for the peak centroid, width, and distortion, respectively. As shown, these correlation plots are much better than the area correlation plot shown in figure 7.3a.

It is important to keep in mind that figures 7.3a to 7.3d simply represent the error in the prediction between values obtained from the NLPLS regression and experimental input values. It would be similar to performing a simple least squares fit of a linear calibration curve and then asking the regression to return a y value from the best fit curve for a corresponding x value. The true test of the simulation is to enter in four random

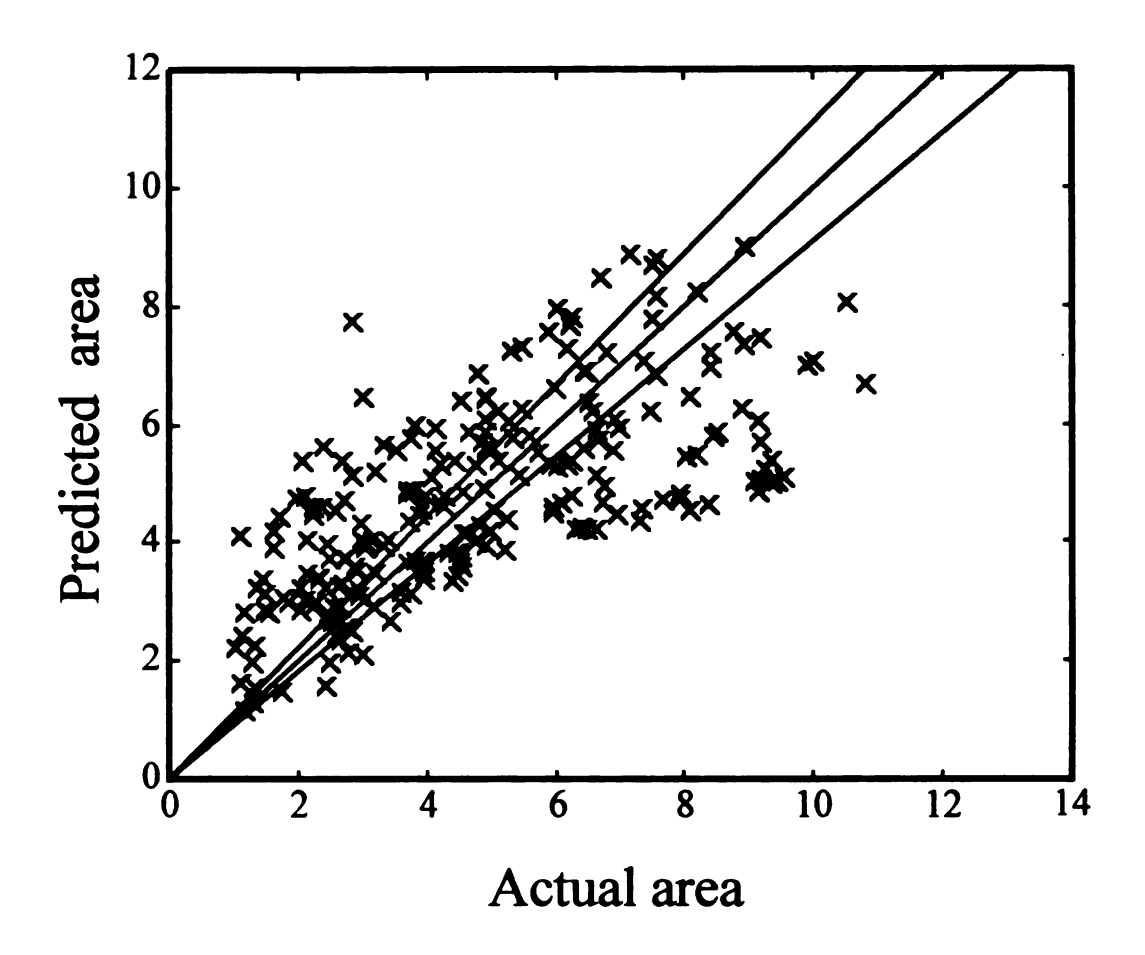


Figure 7.3a. Predicted areas from the NLPLS algorithm versus the actual areas used in the calibration model. The correlation coefficient is 0.473. The lines within the plot represent \pm 10% error.

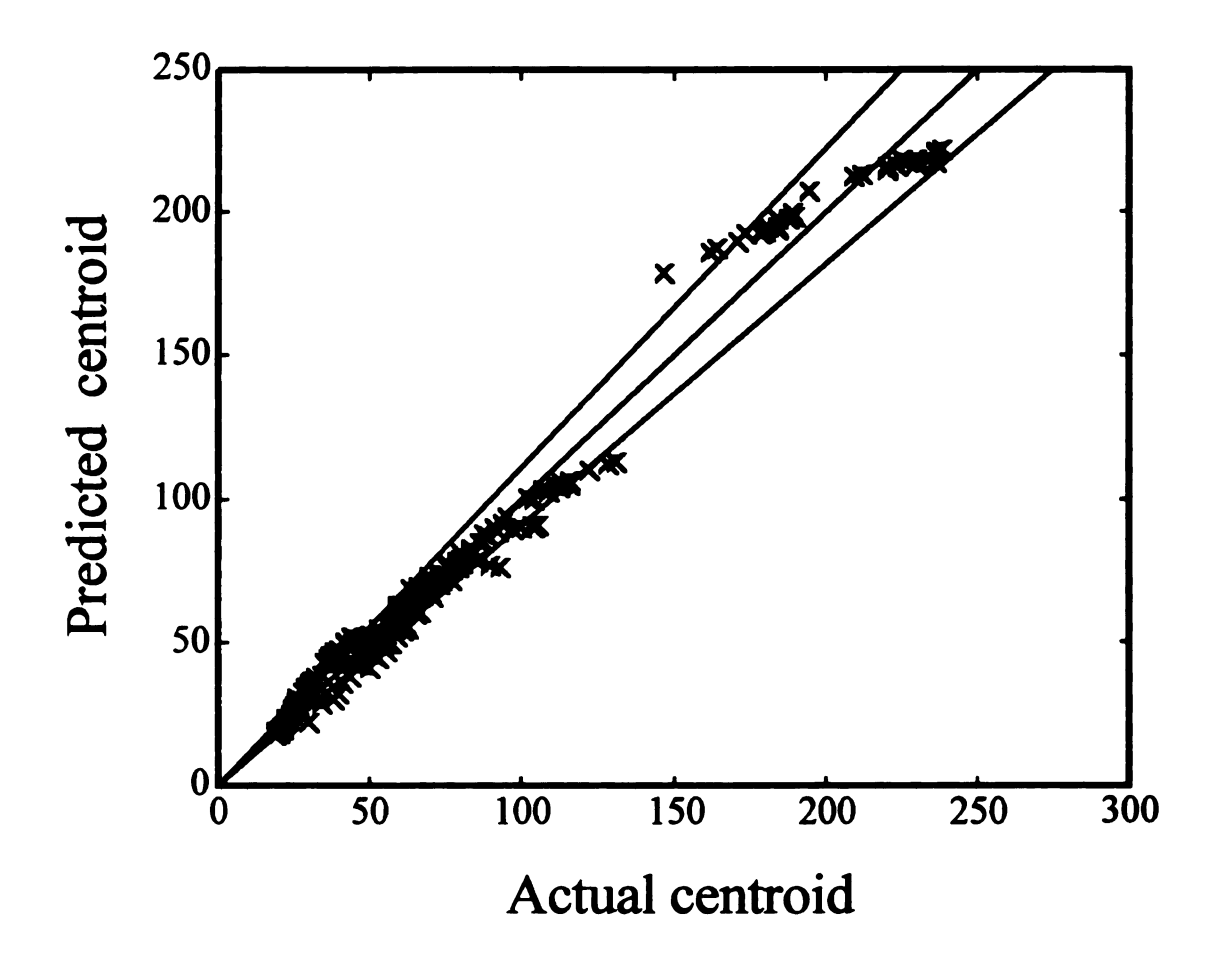


Figure 7.3b. Predicted centroids from the NLPLS algorithm versus the actual centroids used in the calibration model. The correlation coefficient is 0.983. The lines within the plot represent \pm 10% error.

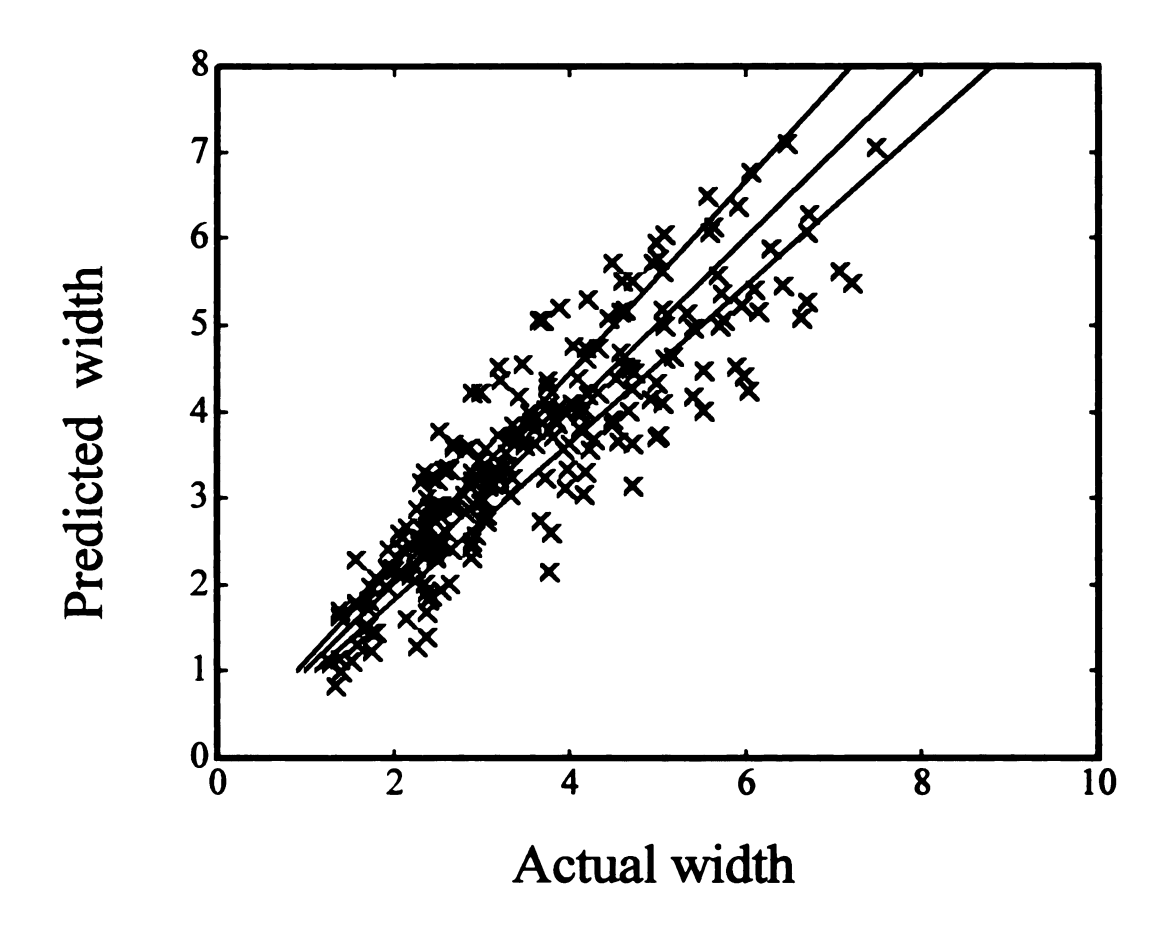


Figure 7.3c. Predicted widths from the NLPLS algorithm versus the actual widths used in the calibration model. The correlation coefficient is 0.770. The lines within the plot represent \pm 10% error.

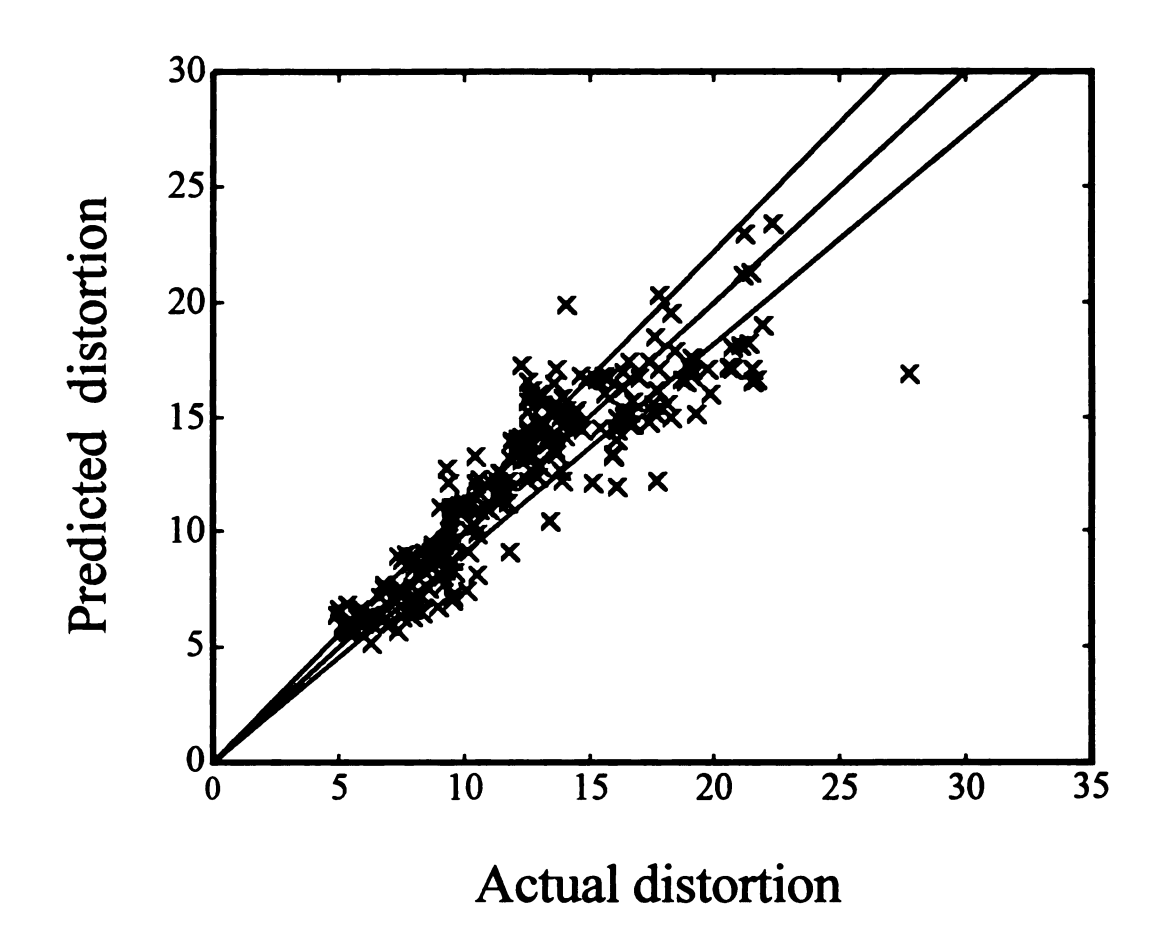


Figure 7.3d. Predicted distortions from the NLPLS algorithm versus the actual distortions used in the calibration model. The correlation coefficient is 0.786. The lines within the plot represent \pm 10% error.

values for the reactor length, dye concentration, volume of the dye injected and the flow rate and then compare the simulated data with that obtained experimentally in real time. Thus, figure 7.4 shows the simulated response curves obtained as a function of varying the reactor length. Comparing this data with that in figure 4.2 (Chapter 4) indicates that the simulation is predicting correctly such trends as peak height, width, and residence time^{8,9}. Some possible reasons for the differences in the overall peak absorbances for the two figures may be based on different amounts of sample volume injected, inner radius of the reactor tubing, and a different internal volume of the flow cell employed while obtaining the two sets of data. From a qualitative standpoint, the trend of increasing peak width with increasing reactor length is being correctly followed.

The simulation also is successful at correctly reproducing trends concerning concentration and volume injected. Figure 7.5 shows the simulated response signals as a function of increasing concentration. As expected the area increases with concentration and shows a linear relationship ($r^2 = 0.996$). However, if the dye sample with concentration of 6 x 10⁻⁴ M is included in the linear regression of the data shown in figure 7.5, the $r^2 = 0.948$. This again demonstrates some of the range problems we encountered during this simulation process. Figure 7.6 shows the simulated response signals as a function of volume injected. The range of injected volumes was 0.5 μ L up to 2.0 μ L. Again, the trend is correct in displaying an increased area versus volume injected ($r^2 = 0.978$).

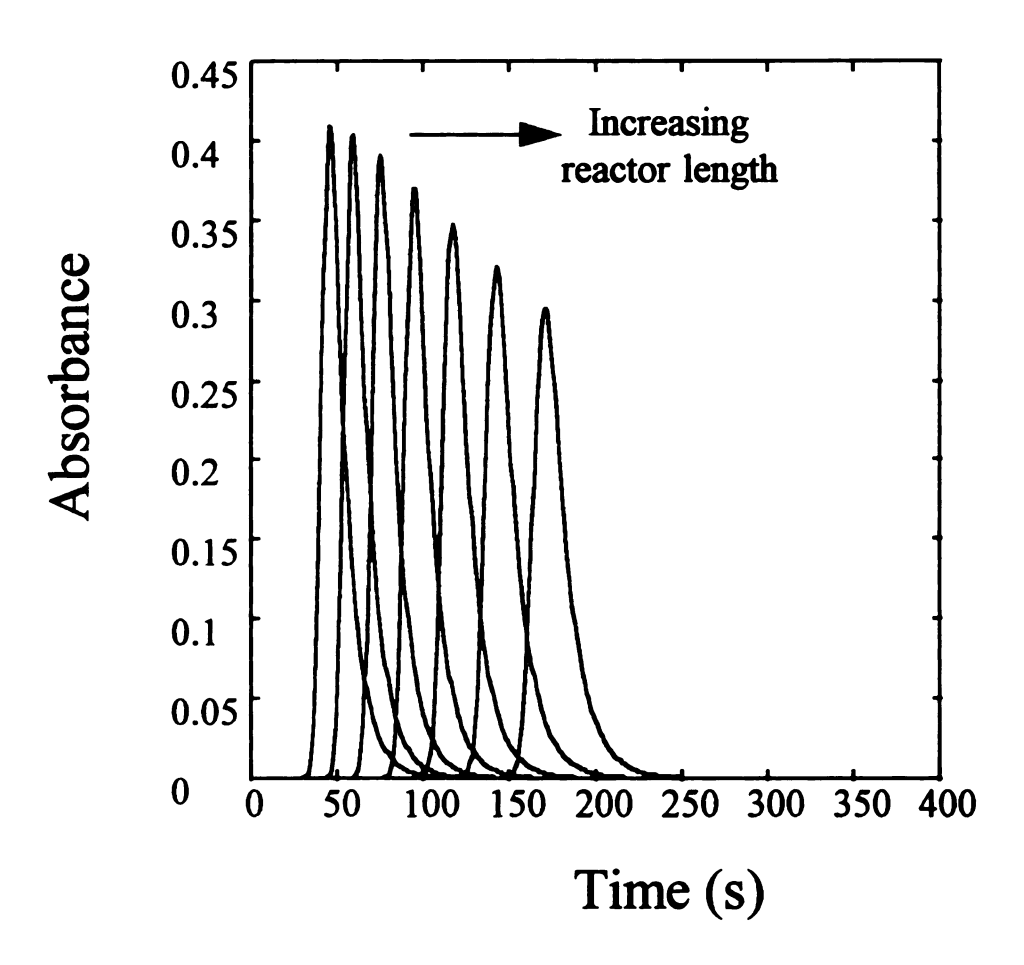


Figure 7.4. Simulated response signals as a function of increasing reactor length. The reactor lengths were varied from 100 cm to 350 cm; concentration of the dye = 5×10^{-4} ; volume injected = $2.0 \mu L$; flow rate = 3 cm s^{-1} .

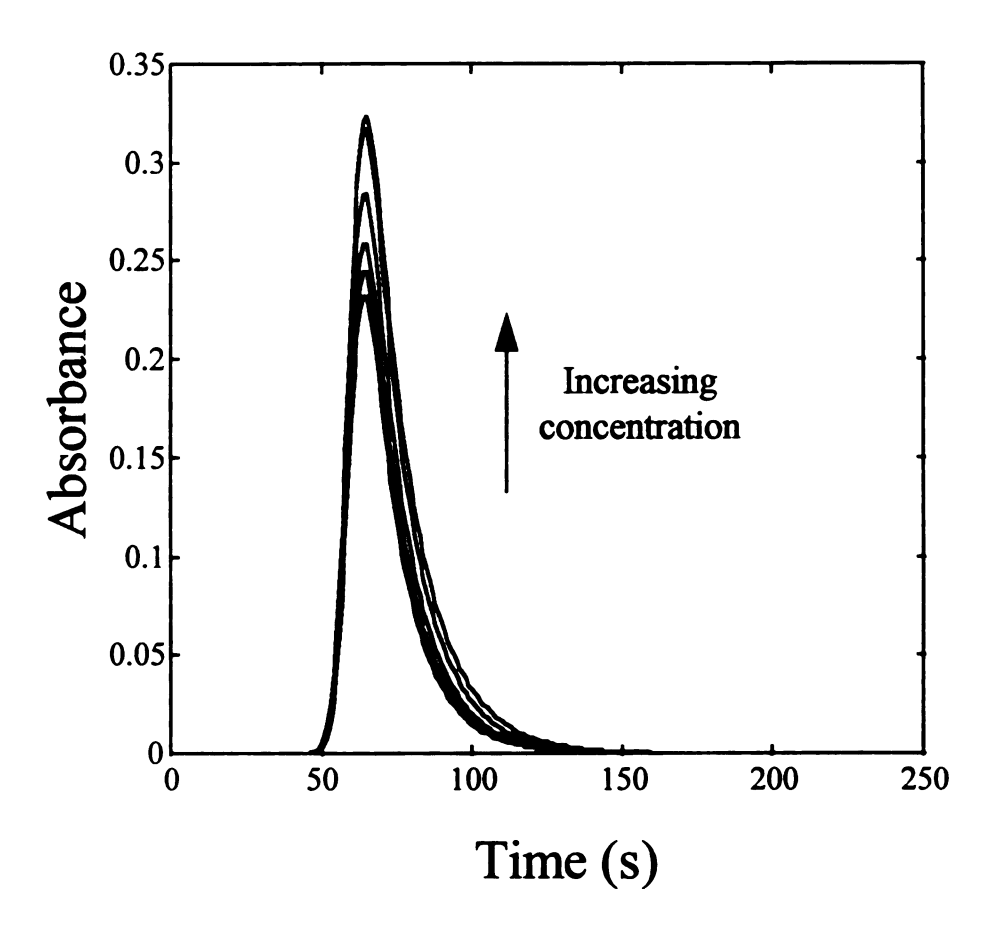


Figure 7.5. Response signals as a function of dye concentration. Reactor length = 125 cm; concentrations ranged from 1 x 10⁻⁵ M to 6 x 10⁻⁴ M; volume injected = 1.8 μL; flow rate = 2.4 cm min⁻¹. The linear regression statistics are discussed within the text.

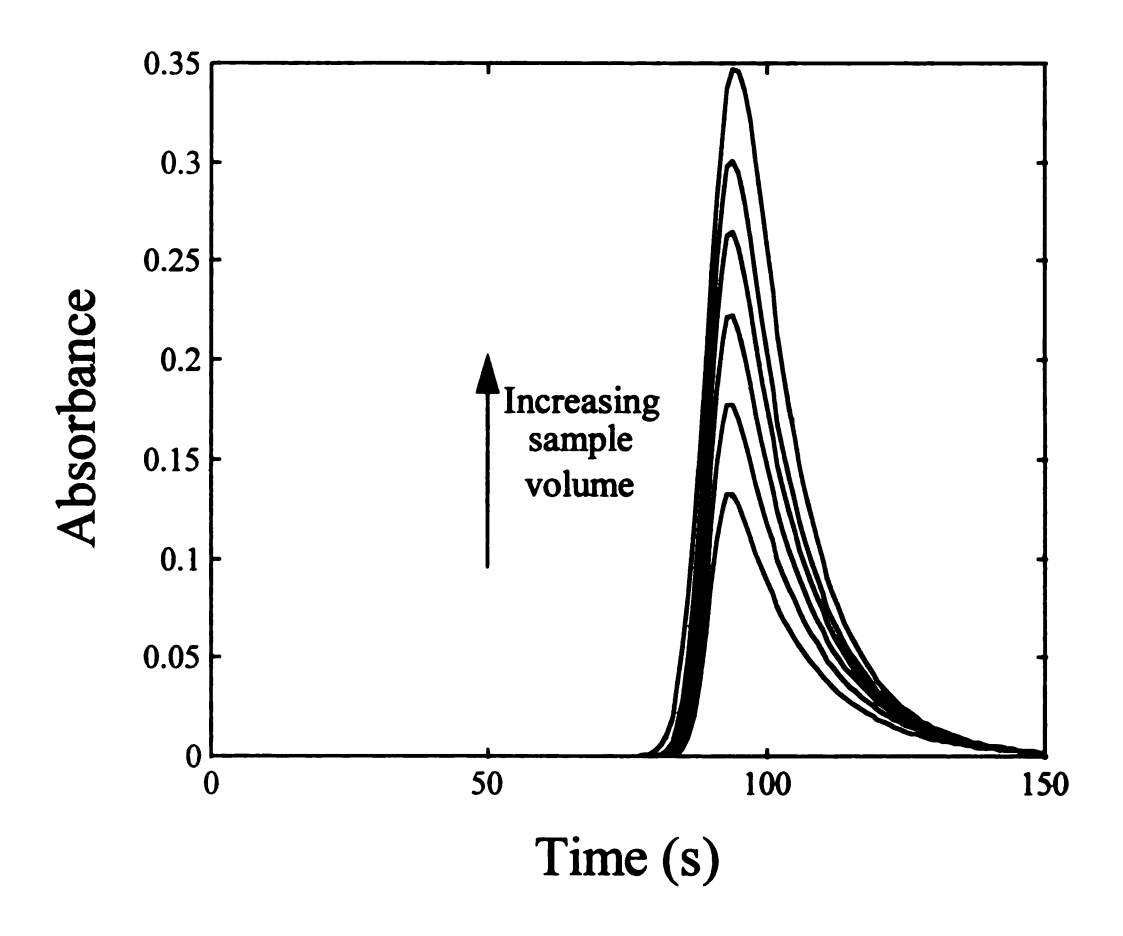


Figure 7.6. Simulated response signals as a function of increasing sample volume . Reactor length = 150 cm; concentration of the dye = 5 x 10^4 M. sample volumes were varied from 0.5 μ L to 2.0 μ L; flow rate = 2 cm s⁻¹. The correlation coefficient between peak height and sample volume was 0.978.

7.2.2 Errors in the Simulation

Although figures 7.4-7.6 show successes with the current simulation, there are times when a certain set of unknown data matrices produce simulated response signals that are not physically correct. With regard to the simulated data shown in figures 7.4-7.6, it only returns frivolous results when unknown parameters are entered by the user that lie outside of the range of the calibration model, but this is to be expected. This can be likened to running a series of standards in a simple Beer's law plot and then attempting to determine an unknown that lies outside of these boundaries. Some error is expected since the user did not previously calibrate using this type of sample. Regression techniques, particularly nonlinear, should never be used outside the calibration range.

However, there are cases where the model does not return results typically expected in FI. For example, figure 7.7 shows a series of response signals as a function of increasing flow rate. In flow injection applications, it is well established that the magnitude of dispersion increases with increasing flow rate. Therefore, one would expect the peak heights in figure 7.7 to be decreasing as the flow rate increases. As shown, just the opposite trend is observed. Initially, the model appears to be incorrect. However, it is important to note that with EMG profiles, the peak distortion plays a large role in determining peak shape. Therefore, in may be that flow rate affects the distortion more than the width, thus the peak height actually increases. Further studies concerning these questions will be required.

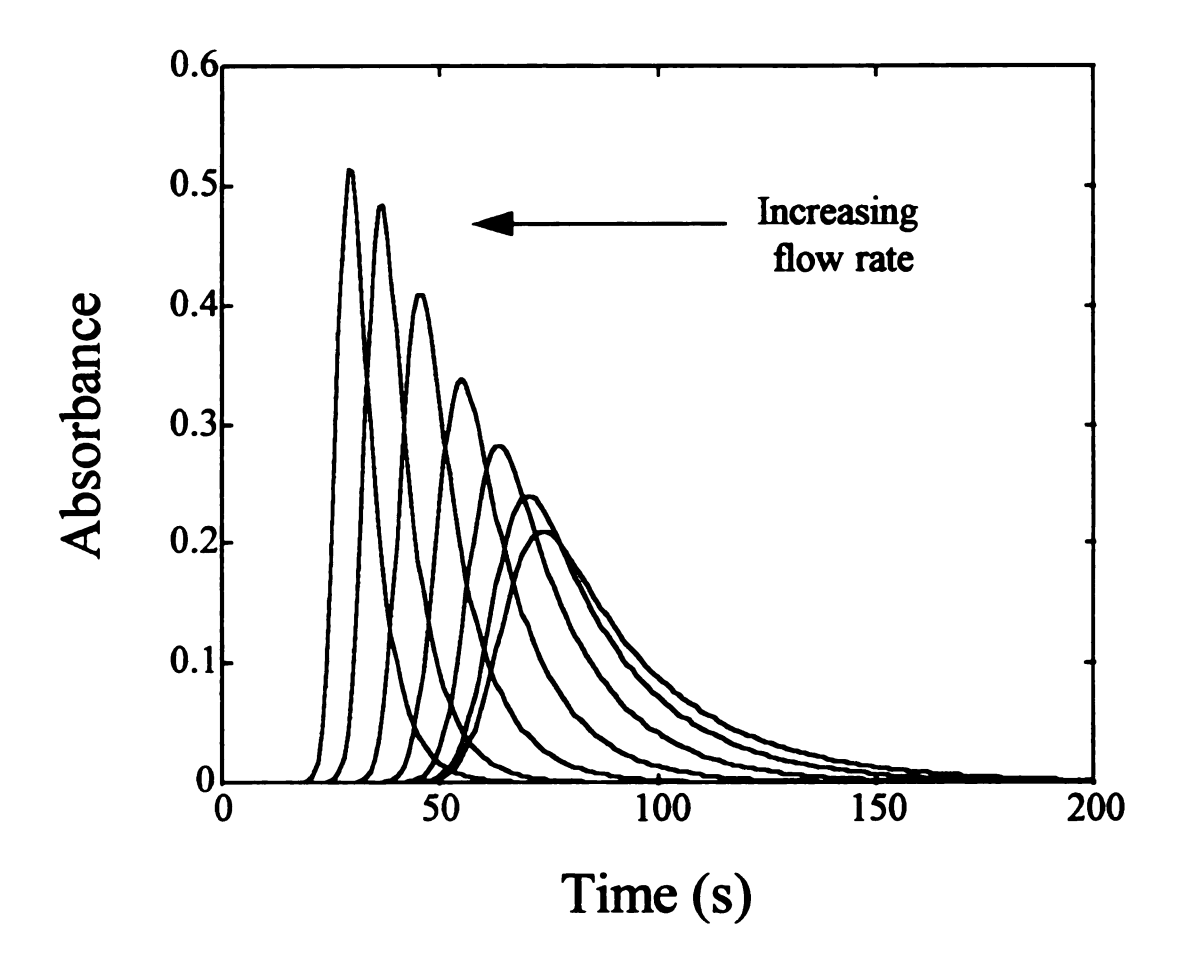


Figure 7.7. Simulated response signals as a function of increasing flow rate. Reactor length = 100 cm; concentration of the dye = 5×10^{-4} . sample volume injected = $2.0 \mu L$; flow rates were varied from 1 cm s⁻¹ up to 4 cm s⁻¹.

7.3 CONCLUSIONS

Although there are definitely some aspects of the model that need improvement, we feel that some of the early successes of this project warrant future investigation. Improvements in the methods of obtaining the data for the calibration model may lead to improvements in the regression output. For example, the injections are currently performed using the time-based methods described in chapter 2. Although this method has proven to be reproducible at a constant pump setting, it is not as reproducible when the pump speed is often changed. In this experiment, the pump speeds are changed often in order to generate the numerous flow rates and injection volumes used in the calibration model. By incorporating fixed loop injection methods and implementing a pump that is capable of achieving higher flow rates at longer reactor lengths, the model may be able to be extended. It is also anticipated that incorporating more reactor lengths and concentrations may also lead to better results, since these types of multivariate techniques generally improve in performance as the amount of data in the calibrating set increases.

List of References

- 1. Geladi, P.; Kowalski, B.R. Anal. Chim. Acta 1986, 185, 1.
- 2. Wold, S.; Kettaneh-Wold, N.; Skagerberg, B. Chem. and Intell.Lab. Systems 1989, 7, 53.
- 3. Sharaf, M.A.; Illman, D.L.; Kowalski, B.R. *Chemometrics*, Wiley, New York, 1986.
- 4. Evans, C.E. Ph.D. Thesis, Michigan State University, East Lansing, MI, 1990.
- 5. Brooks, S.H.; Leff, D.V.; Hernandez Torres, M.A.; Dorsey, J.G. *Anal. Chem.* 1988, 60, 2737.
- 6. Cullen, T.F. Ph.D. Thesis in progress, Michigan State University, East Lansing, MI.
- 7. Cullen, T.F.; Crouch, S.R. Mikrochim. Acta, in press.
- 8. Ruzicka, J.; Hansen, E.H. Flow Injection Analysis, Wiley, New York, 1988.
- 9. Spence, D.M.; Crouch, S.R. Anal. Chem. 1997, 69, 165.

Chapter 8

Future Prospects of Capillary Flow Injection

Miniaturized techniques have many advantages over their conventional counterparts. One aspect that will undoubtedly be mentioned is the reduced amount of sample needed and also the minimized waste that is generated. However, users of such miniaturized techniques, especially those who employ miniaturized analytical instrumentation, will quickly point out that the increase in efficiency and overall performance of a scaled-down technique is the major reason for operating on such a scale.

The work presented in the preceding seven chapters has hopefully laid a solid foundation for future experiments with flow injection (FI) in the capillary format. Although there is definitely much work needed with regard to instrumentation and further fundamental studies before capillary FI will be as common as the present day FI systems, there is already evidence that a microscale FI system will be more beneficial in many areas than the current status quo. In spite of the fact that capillary FI is still in its "first generation" stage, it already shows many advantages over its conventional counterpart. For example, it was shown in chapter 4 that the efficiency of the capillary technique is much higher than the conventional FI systems. In chapters 4 and 6, the stopped-flow

method showed that reaction can occur in the capillaries despite a decrease in the overall amount of mixing due to a decrease in convective dispersion.

With the above advantages in mind, it is very exciting to think about how much more the capillary FI systems will be improved in their second generation manifolds and beyond. In addition, with these improvements will come future applications, some of which will surely be improvements over current FI systems. Others will be new extensions of FI that the current systems are simply not capable of performing. The remainder of this chapter will take the reader into the near future of capillary FI and attempt to explain some upcoming work that will expand the usefulness of the already practical and growing analytical technique, flow injection.

8.1 INSTRUMENTATION IMPROVEMENTS

Throughout the course of this project, commercially available equipment has expanded a great deal in the area of miniaturized instrumentation. Though some of this equipment at this point is rather expensive, the work performed to date concerning capillary FI dictates that this new equipment, which is more sophisticated than current FI equipment, be implemented for further improvement of capillary FI.

8.1.1 Pumping Mechanisms

Chapter 3 contains evidence that the simple peristaltic pumps used in everyday FI may not suffice for future applications where multireagent manifolds are required or high pressures may be encountered. Thus, stable, pulse-free, high pressure syringe pumps may be needed. These pumps are commercially available (Eldex, Isco) and are capable of flow

rates ranging from 0.01 µL min⁻¹ up to 10 mL min⁻¹. These same pumps are capable of reaching pressures as high as 10,000 psi (≈680 bar). Unfortunately, at this point, these pumps are about 2-3 times more expensive than a good peristaltic pump.

Electroosmotic flow (EOF)¹⁻⁶ may also be a possible choice for future applications involving capillary FI. EOF is capable of producing steady flow in the sub μL min⁻¹ range and should also minimize dispersion due to convective forces. However, EOF as a pumping mechanism does possess many disadvantages. For example, EOF is not very reproducible, even when the capillary is properly pretreated. In addition, the generation of EOF requires the presence of ionic species. Thus, not all mediums (e.g., organic solutions) can be used in a EOF-driven capillary system.

8.1.2 Injection Methods

Though the time-based injection method initially described in chapter 2, and used as the injection process throughout much of this project, proved trustworthy and reproducible, it still has possible drawbacks. Since the injection method is based on time and the flow rate of the sample, any change in the flow rate will cause an erroneous or even an unknown amount of sample to be injected. This method of injection also proved to be a problem when the peristaltic pump was operating near its pressure limit. For these reasons, future capillary FI manifolds should attempt to incorporate low volume injectors with fixed internal loops. Although these valves are slightly more expensive and changes in volume injected may only be accomplished by inserting a new internal rotor, their reproducibility is unmatched by time-based methods. The injected volumes are also more

trustworthy, for any slight change in flow rate will not affect the amount of sample that enters the reaction coil(s).

8.1.3 Improved Detection Methods

The variance studies shown in chapter 4 provided much insight on how to further improve the current capillary FI system. In chapter 4, the variance from the detector in a capillary system was roughly 40% of the total system variance. By using an on-column detection scheme or one of the now commercially available capillary Z-cells^{7,8}, the amount of variance due to the flow cell should be reduced. These Z-cells (LC Packings) provide a path length of up to 3 mm and internal volumes as low as 65 nL. The variance due to connectors should also decrease since tubing of different inside diameters will not be required to adapt the reactor capillary to the flow cell. The improved efficiency employing one of these new methods should definitely be noticeable since exponential tailing resulting from connections should be decreased.

The advent of performing FI on a micromachined fused silica chip⁹⁻¹⁴ may also lead to improvements in detection. Since there are no connectors and no fused silica capillaries to bend into the Z pattern as with the flow cells described in the previous paragraph, longer path lengths may be possible while still maintaining a low internal volume flow cell. However, chip-based methods will need to overcome a few obstacles before they become the norm in miniaturized FI. For example, in FI, system manifolds are routinely changed in order to accommodate a new reagent or sample line. These types of changes using manifolds fabricated on chips will be neither practical nor inexpensive. In addition, there is not much volumetric difference in reagent and sample consumption for a manifold

fabricated onto a silicon substrate and one which employs fused silica capillaries with inside diameters of $< 75 \, \mu m$. Nevertheless, micromachined substrates will probably have a place at least in the near future of capillary FI and capillary electrophoresis.

8.2 IMPROVED KINETIC METHODS OF ANALYSIS

As pointed out in the introduction and in chapter 6, FI has been used as a tool for determinations by kinetic methods of analysis. Stopped-flow and flow reversal methods have all met with some success in the FI mode. Other methods using immobilized media such as enzymes and antibodies for catalysis have also been popular in conjunction with FI. These types of kinetic analyses should all find improvement in a miniaturized scale.

8.2.1 Flow Reversal Enhancements

Flow reversal FI and flow recycling FI¹⁵⁻¹⁷ methods, where a single sample or a series of samples make multiple passes by a single detector, are techniques that have met with success in air-segmented continuous flow systems¹⁸ and moderate success in FI. A major drawback of flow reversal/flow recycle FI is the excessive dispersion that is introduced upon each reversal, not only by the reactor, but also by the continuing pass of the sample through the flow cell and all of its associated connections. By performing flow reversals in a capillary with a decreased inside diameter, the amount of dispersion due to convection inside the reactor will be reduced as shown in chapter 4. In addition, by employing an on-column detection scheme, one may be able to avoid the excessive dispersion gained by multiple passes of the sample through the flow cell.

8.2.2 Determinations Involving Immobilized Media

Reactions that use such biological catalysts as antibodies and enzymes should also benefit from a miniaturized FI manifold, especially when these catalysts are immobilized onto the walls of the reactor tubing. Typically, these types of immobilized media rely on diffusion of analytes (e.g., the antigen) to the walls where they then meet the immobilized catalyst (e.g., the antibody). The time t in seconds needed for an analyte with a diffusion coefficient D_m of 10^{-5} cm² s⁻¹ to migrate across an open tube of diameter d can be calculated from equation 8.1. Therefore, if one were to reduce this diameter by a factor of 10, the time needed for this diffusion would be decreased by a factor of 100. Obviously, this would be a tremendous benefit for these types of

$$t = \frac{d^2}{2D_m} \tag{8.1}$$

determinations. In addition, the surface area-to-volume ratio is increased in capillary systems, thus increasing the number of possible sites for catalysis. Typically, cumbersome methods such as roughing the inner wall with hydrofluoric acid are required. Thus, the preparation time of these methods will be reduced in capillary FI.

8.3 AUTOMATED CALIBRATION IN STOPPED FLOW CAPILLARY FLOW INJECTION USING ON-COLUMN DETECTION

Another possible application that may benefit from FI in the capillary format is stopped-flow FI^{19,20}. As described in chapter 6, stopped-flow FI techniques are used so that a reaction or chemical procedure may proceed without the added dispersion due to

flow-induced convection. However, a drawback of the stopped-flow technique is the low sample throughput since only one zone can be measured at any given time. Even sample stacking (injecting numerous sample zones into the tubing before starting flow towards the detector), a practice common in flow reversal techniques, is not feasible in stopped-flow FI. By performing the stopped-flow technique in fused silica capillaries and using oncolumn detection, it may be possible to improve some of the throughput features or efficiency of the technique.

Consider the reduction of toluidine blue described in chapter 6. Once toluidine blue is injected into the ascorbic acid stream, the laminar flow profile begins to form. The tailing edge of this parabolic flow profile is actually a concentration gradient. Thus, if multiple detectors or some form of imaging the portion of the column containing the toluidine blue zone were employed, it would be possible to monitor the changes in absorbance in time. If, for example, the zone were monitored at x number of different points along the toluidine blue zone, one would be able to determine x values of dA/dt. Using the molar absorptivity of the dye, the concentration at each point along the stopped zone can be calculated. Thus, the resultant data set would be a calibration set of concentration versus dA/dt. In this manner, the entire calibration curve could be constructed from just one injection.

All of the methods described in this chapter have the same goal; to enhance the overall performance of FI. Some of the techniques described not only in this chapter, but also in this dissertation have the goal of improving the current status of FI. However,

through these improvements, the FI technique will hopefully be used in conjunction with other exciting venues.

List of References

- 1. Tavares, M.F.M. *Ph.D. Thesis*, Michigan State University, East Lansing, MI, 1993.
- 2. Lee, C.S.; Blanchard, W.C.; Wu, C.T. Anal. Chem. 1990, 62, 1550.
- 3. Lee, C.S.; McManigill, D.; Wu, C.T. Anal. Chem. 1991, 63, 1519.
- 4. Hayes, M.A.; Ewing, A.G. Anal. Chem. 1992, 64, 512.
- 5. Hayes, M.A.; Kheterpal, I.; Ewing, A.G. Anal. Chem. 1993, 65, 27.
- 6. Hayes, M.A.; Kheterpal, I.; Ewing, A.G. Anal. Chem. 1993, 65, 2010.
- 7. Moring, S.E.; Reel, R.T.; van Soest, R.E.J. Anal. Chem. 1993, 65, 3454.
- 8. Albin, M; Grossman, P.D.; Moring, S.E. Anal. Chem. 1993, 65, 489A.
- 9. Harrison, D.J.; Manz, A; Fan, Z.; Ludi, H.; Widmer, H.M. Anal. Chem. 1992, 64, 1926.
- 10. Seiler, K.; Harrison, D.J.; Manz, A. Anal. Chem. 1993, 65, 1481.
- 11. Jacobson, S.C.; Hergenroder, R.; Koutny, L.B.; Warmack, R.J.; Ramsey, J.M. Anal. Chem. 1994, 66, 1107.
- 12. Jacobson, S.C.; Hergenroder, R.; Koutny, L.B.; Ramsey, J.M. *Anal. Chem.* **1994**, *66*, 1114.
- 13. Li, P.C.H.; Harrison, J.D. Anal. Chem. 1997, 69, 1564.
- 14. Kovacs, G.T.A., Petersen, K.; Albin, M. Anal. Chem. 1996, 68, 407A.
- 15. Wade, A.P.; Oate, P.B.; Betteridge, D. Anal. Chem. 1987, 87, 1236.

- 16. Clark, G.D.; Zable, J.; Ruzicka, J.; Christian, G.D. Talanta, 1991, 38, 119.
- 17. Townsend, E.B.; Crouch, S.R. Trends Anal. Chem. 1992, 11, 90.
- 18. Hsieh, Y.S.; Crouch, S.R. Anal. Chim. Acta 1995, 304, 333.
- 19. Christian, G.D.; Ruzicka, J. Anal. Chim. Acta 1992, 261, 11.
- 20. Spence, D.M.; Crouch, S.R. Quim. Anal. 1996, 15, 296.

